THE UNIVERSITY OF MICHIGAN

COLLEGE OF ENGINEERING
Department of Electrical Engineering
Space Physics Research Laboratory

Engineering Report No. 2

ENGINEERING DESIGN OF A PITOT-STATIC PROBE PAYLOAD

G. F. Rupert

ORA Project 05776

under contract with:

NATIONAL AERONAUTICS AND SPACE ADMINISTRATION
GODDARD SPACE FLIGHT CENTER
CONTRACT NO. NAS5-3335
GREENBELT, MARYLAND

administered through:

OFFICE OF RESEARCH ADMINISTRATION ANN ARBOR

April 1967

TABLE OF CONTENTS

TABLE OF CONTENTS (Concluded)

LIST OF TABLES

LIST OF FIGURES

LIST OF FIGURES (Continued)

LIST OF FIGURES (Continued)

LIST OF FIGURES (Concluded)

ABSTRACT

The engineering aspects of the Pitot-Static Probe experiment are presented with emphasis on the design and fabrication of the special instrumentation and circuits that were developed to make implementation of the technique possible.

The fabrication of the mechanical system, testing procedures, and a prelude of launch operations are included. Future considerations towards system improvements and greater measurement accuracy conclude the report.

LIST OF FIGURES (Concluded)

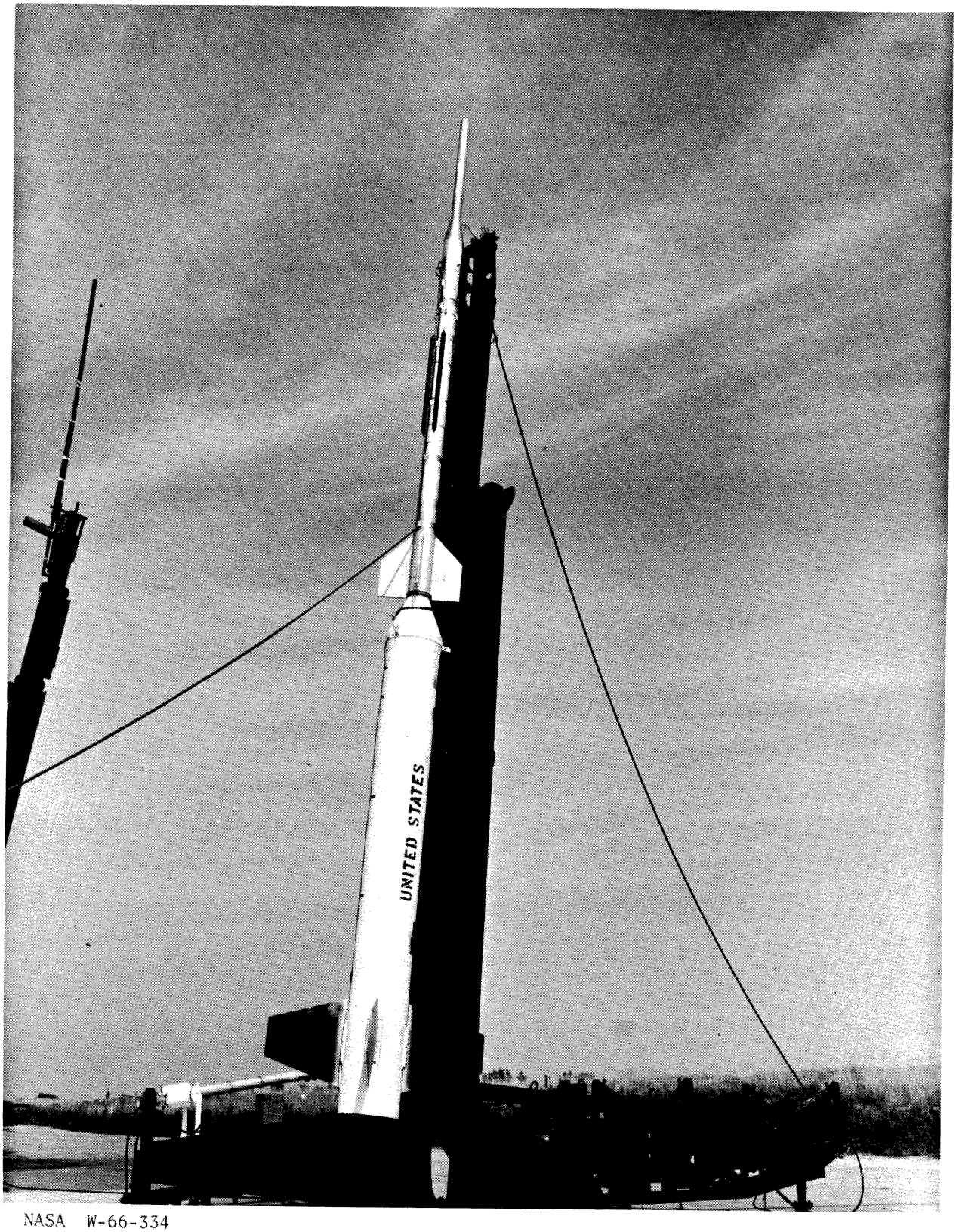

NASA W-66-334

Fig. 1. Pitot-Static Probe rocket before launch.

1. INTRODUCTION

1.1 HISTORY

The Pitot-Static Probe is a fully operational system capable of determining atmospheric density, pressure, and temperature in the altitude range between 30 km and 120 km. Basically, the technique involves making two direct pressure measurements on a rocket surface, one the pitot or impact pressure, the other being the static or ambient pressure (hence the term Pitot-Static Probe). The measured pressures are then used to mathematically derive the other parameters.

Since the program's inception in early 1960, several launchings have been successfully carried out at various locations (see Appendix 8.2).

Initial development of the probe (following work by Ainsworth, Fox, and LaGow[1]) began with the support of the AFCRL Geophysics Research Directorate whereby a prototype nose cone was developed to investigate the feasibility of the experiment. Earlier work by this laboratory resulted in the development of the Densatron,[2,3] a radioactive ionization pressure gage, two of which were subsequently used as the pressure transducers in the prototype nose cone. Other instrumentation needed to support the experiment were also developed and provisions were made for installing DOVAP[4] instrumentation in the nose cone.

A test launching of the prototype nose cone aboard a Nike-Cajun Rocket (AA6.340) was conducted in October, 1960, at Ft. Churchill, Manitoba, Canada. The flight objectives were realized and further work, with the support of NASA, Goddard Space Flight Center, towards the development of a practical system was initiated.

1.2 DESIGN OBJECTIVES

Besides making the basic measurements, primary objectives in the Pitot-Static Probe design were to provide an experiment capable of being launched anywhere with minimum ground support equipment required and without loss of data accuracy. Every effort has been directed towards building a reliable system that requires little field maintenance. The payload design also included provisions for gathering engineering data that would increase knowledge of the measurement and facilitate system improvement. Wherever possible, flexibility was included in the design to allow periodic updating of the instrument that would reflect the latest developments in the technique or instrumentation.

2. SYSTEM DESIGN

2.1 DESCRIPTION

The Pitot-Static Probe experiment is launched aboard a two-stage Nike-Apache rocket which is capable of reaching an altitude of approximately 140 km using the Pitot-Static configuration (Fig. 2). The nose cone serves as the actual measurement probe as well as housing the instrumentation. The pitot or impact gage orifice is located in the 3.5-in. diameter hemispherical nose tip. Ten equally spaced holes 5/15-in. in diameter located approximately 32 in. behind the tip are the inputs to the ambient pressure chamber. Useful pressure data are gathered only on the upleg portion of the flight. A typical flight profile is shown in Fig. 3.

From the standpoint of useful data, the ambient pressure measurement begins almost immediately after Apache burn-out at an altitude of 20 km and continues to 85 km, while the impact measurement starts near 50 km and terminates near 120 km.

During the measurement period, a number of support functions, which are described below, are necessary to complete the experiment.

2.11 Tracking

Primary tracking information is obtained by DOVAP,[4] a continuous wave-tracking system which utilizes the doppler frequency shift to measure rocket velocity. The velocity profile may then be integrated over the entire flight path to yield the trajectory.

A type UDT/B DOVAP* transponder is included as an integral part of the payload, and either a multistation DOVAP system consisting of a transmitter and at least three receiving stations or a Single Station (SSD), which utilizes interferometer techniques, may be used with the Pitot-Static Probe experiment. A detailed analysis and description of the systems may be found in the references and will not be repeated here.[4,5,6] The SSD system offers a particular advantage to the experiment in that the ground support equipment is sufficiently portable to allow its use at remote locations thus maintaining the flexibility of the experiment with respect to possible launch sites.

---

*ITT Labs.

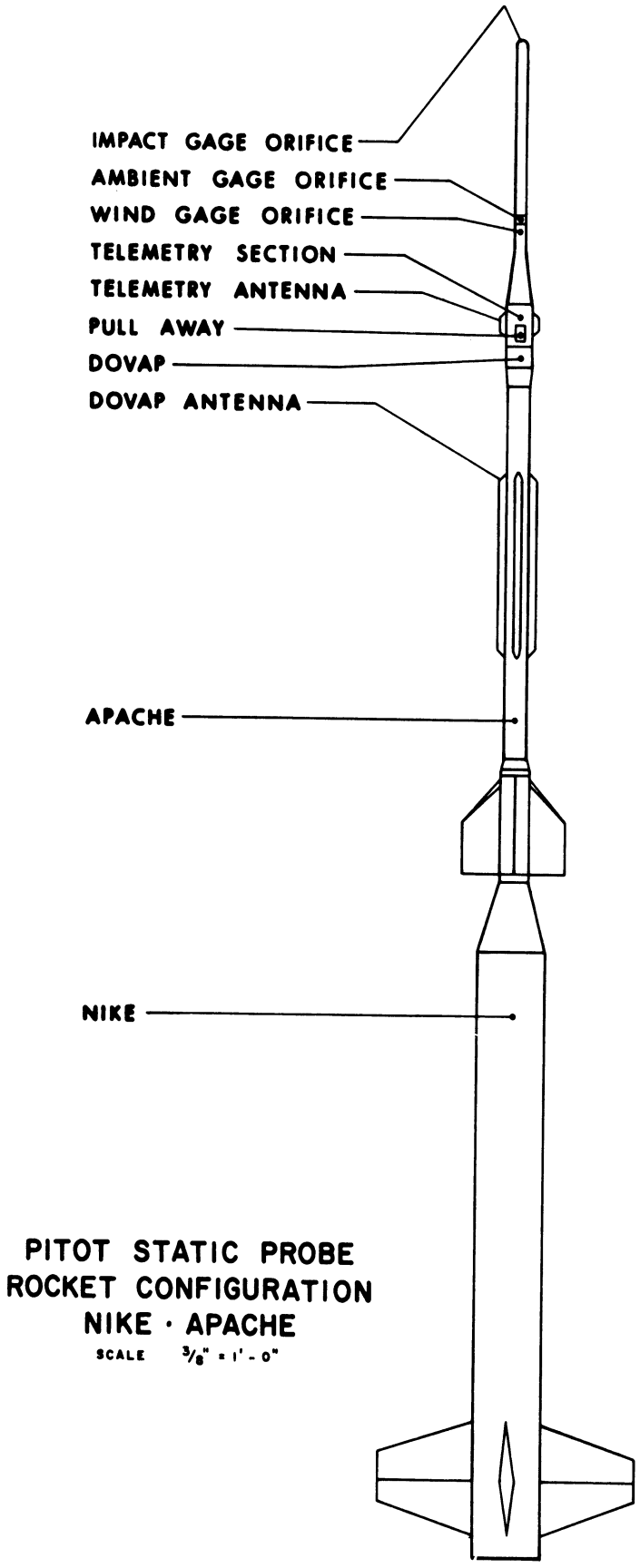
IMPACT GAGE ORIFICE
AMBIENT GAGE ORIFICE
WIND GAGE ORIFICE
TELEMETRY SECTION
TELEMETRY ANTENNA
PULL AWAY
DOVAP
DOVAP ANTENNA
APACHE
NIKE
PITOT STATIC PROBE
ROCKET CONFIGURATION
NIKE · APACHE
SCALE 3/8" = 1'-0"

Fig. 2.

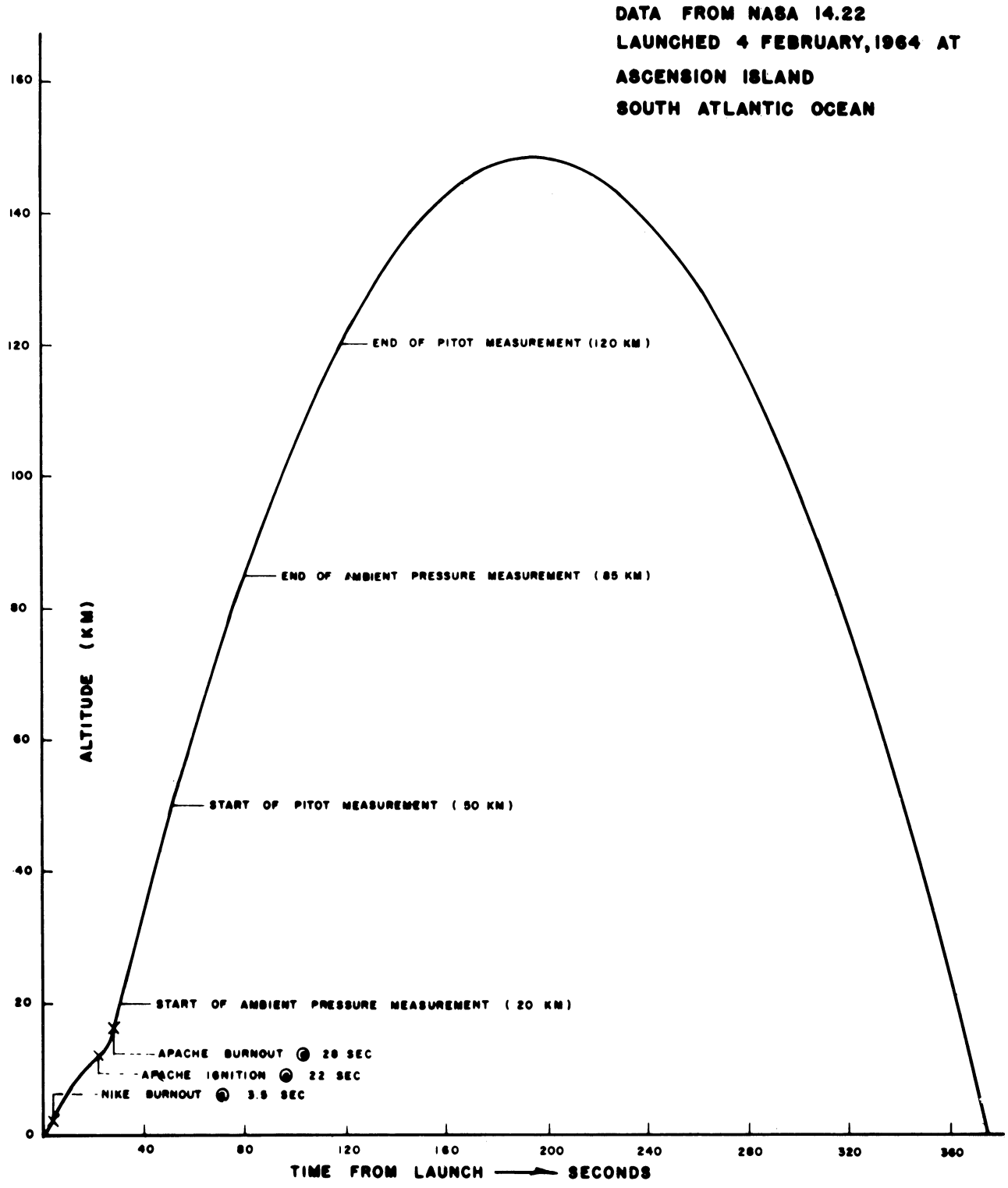

TYPICAL FLIGHT PROFILE
FOR THE
PITOTSTATIC PROBE EXPERIMENT

Fig. 3

2.12 Aspect

The rocket angle of attack figures prominently in the data reduction of the primary probe measurement and is, therefore, considered a requisite of the experiment. An Adcole Digital Solar Aspect System is built into the payload. The system is composed of a model 235 shift register and a model 135B aspect sensor that also includes an earth telescope which senses the presence of earth with a 1° field of view (see Appendix 8.3).

The sun angle is determined by sunlight passing through a slit in a quartz block which is screened by a grey coded reticle that allows or inhibits illumination of six photocells. This information is processed in the form of "ones" or "zeros" corresponding to an illumination or nonilluminated condition and then stored in a shift register for telemeter read-out. The angle of incidence of the sun with respect to the vehicle axis determines which cells are illuminated, and 2^7 or 128 unique combinations of "ones" or "zeros" represent 1° resolution over a 128° field of view.

A serial read-out of the coded information is used for telemeter. The presence of an earth cell output causes a dc shift in the record that is easily distinquishable. The accuracy of sun data can be read to $\pm 0.25°$ at transition.

As a supplement to earth cell data, magnetometers are also used in the aspect measurement. Magnetic sensors mounted in the rocket determine the vehicle's position with respect to the earth's magnetic field vector.

2.2 DENSATRON SYSTEM

The Densatron (Fig. 4), which is capable of measuring pressures found in the region between 30 km to 120 km, is the foundation from which the Pitot-Static Probe experiment evolved. A radioactive ionization gage (Fig. 6A), that produces currents in proportion to neutral particle density, is combined with a multirange differential dc operational amplifier to form the Densatron System. A schematic diagram of the system is shown in Fig. 5. A detailed description of the ionization gage can be found in the references and will not be repeated here.[2,7] Basically, the gage measures gas density which may then be interpreted in terms of pressure when the gas temperature is known. Figure 6B show a typical gage pressure-current characteristic.

The electronic circuits used in the Densatron are composed entirely of solid-state components except for the amplifier input stage, where electrometer tubes are required to obtain the high input impedance necessary to measure low currents.

A thermistor mounted in the ionization chamber measures the gage wall temperature which, it is assumed, is also the gas temperature that must be known for data reduction. A second thermistor measures the temperature of the electronics section.

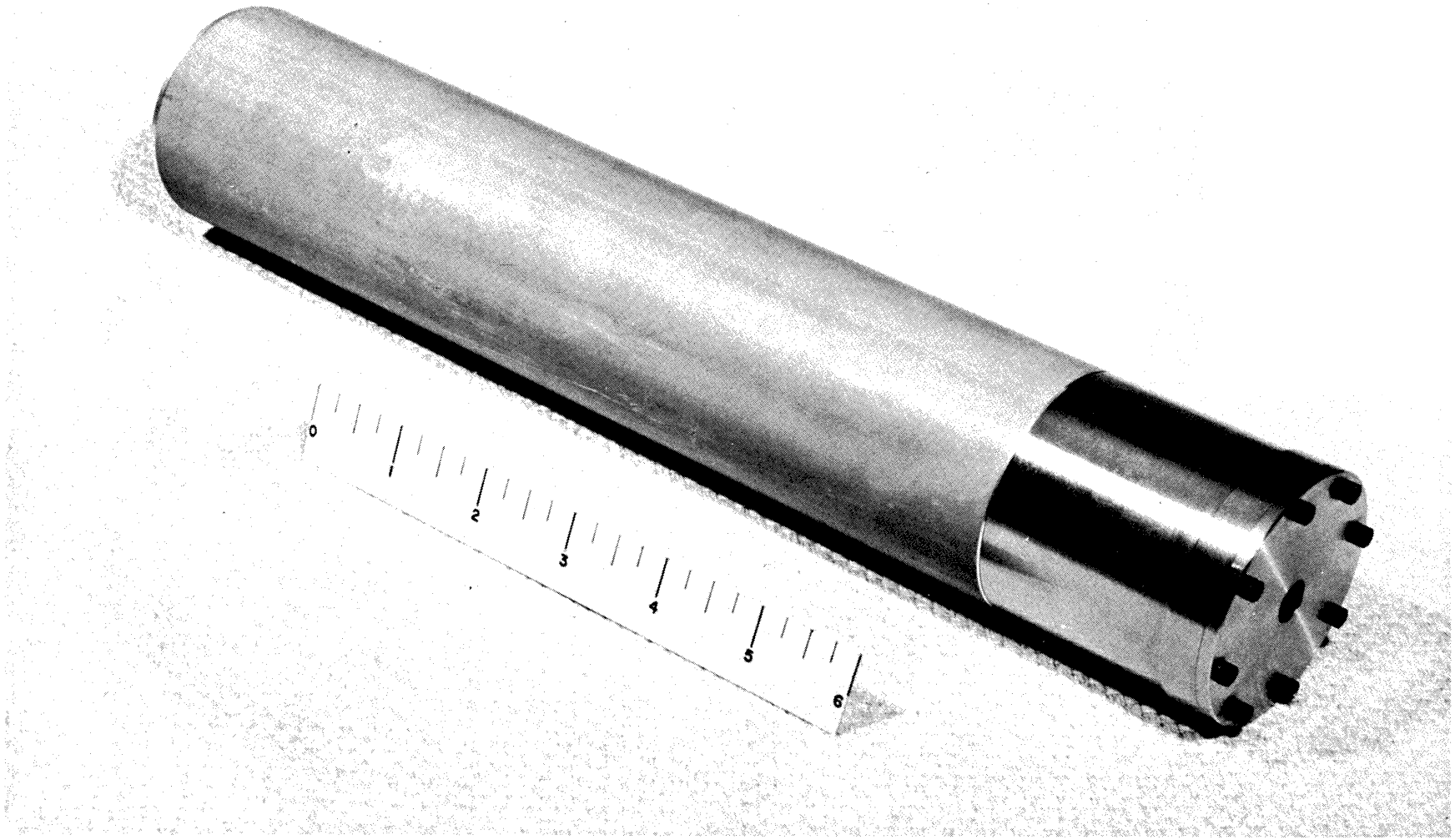

Fig. 4. The Densatron.

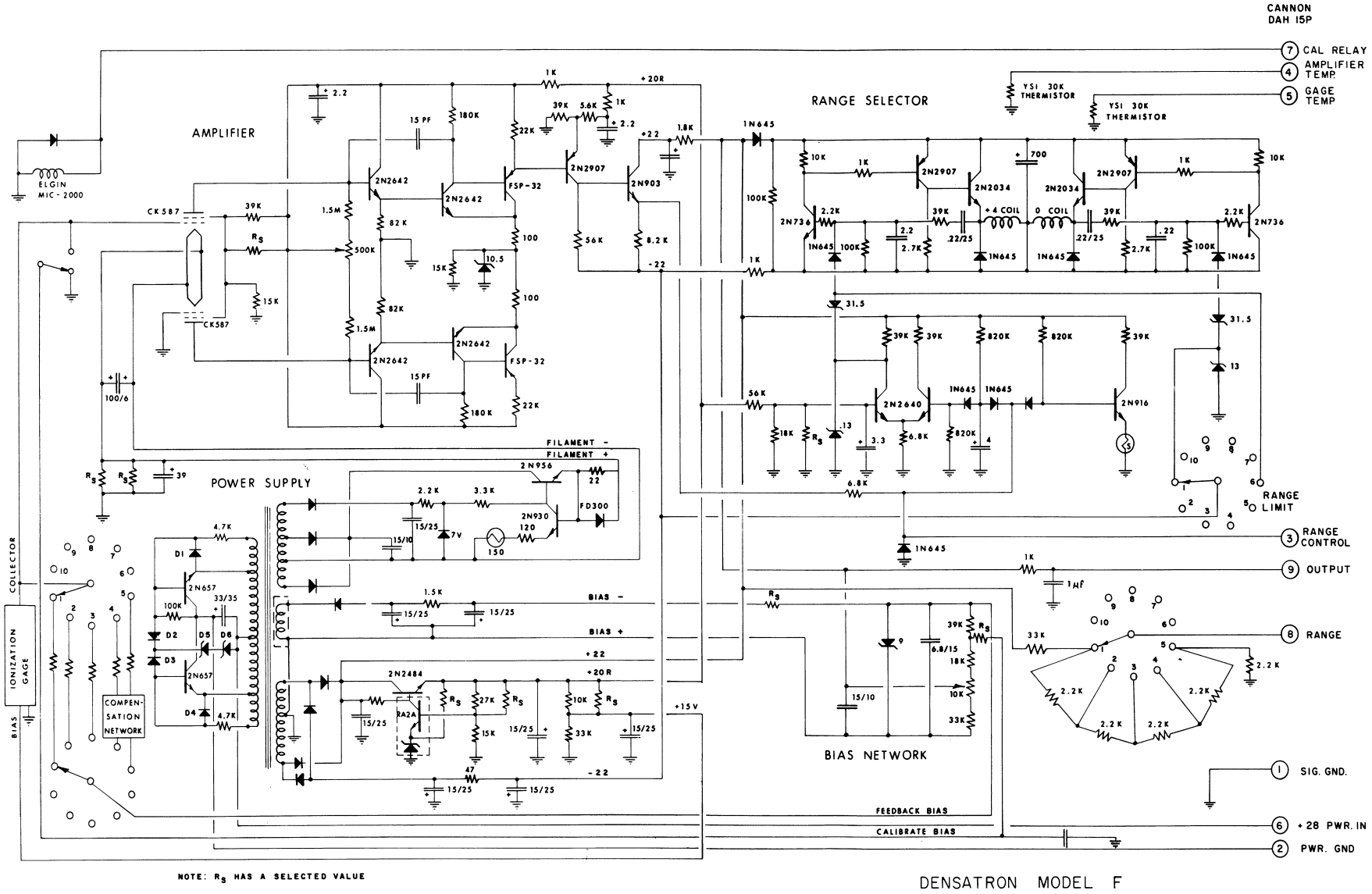

NOTE: R_S HAS A SELECTED VALUE

DENSATRON MODEL F

Fig. 5

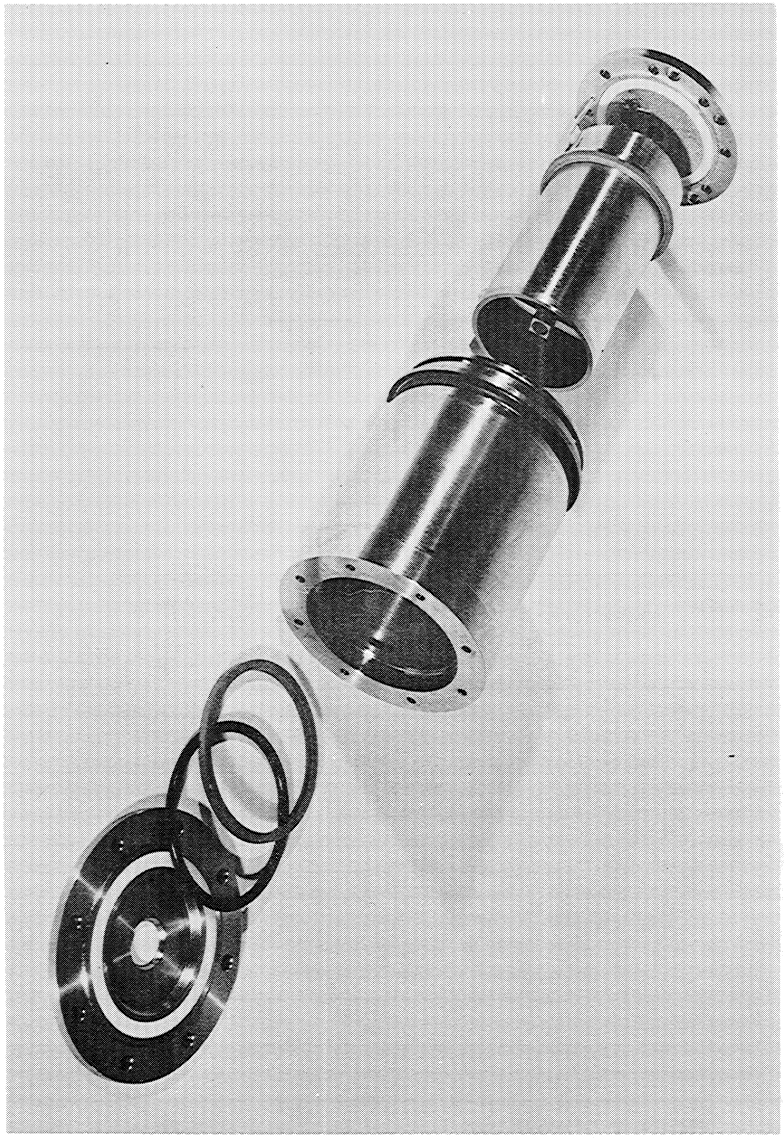

Fig. 6A. Tritium source ionization gage.

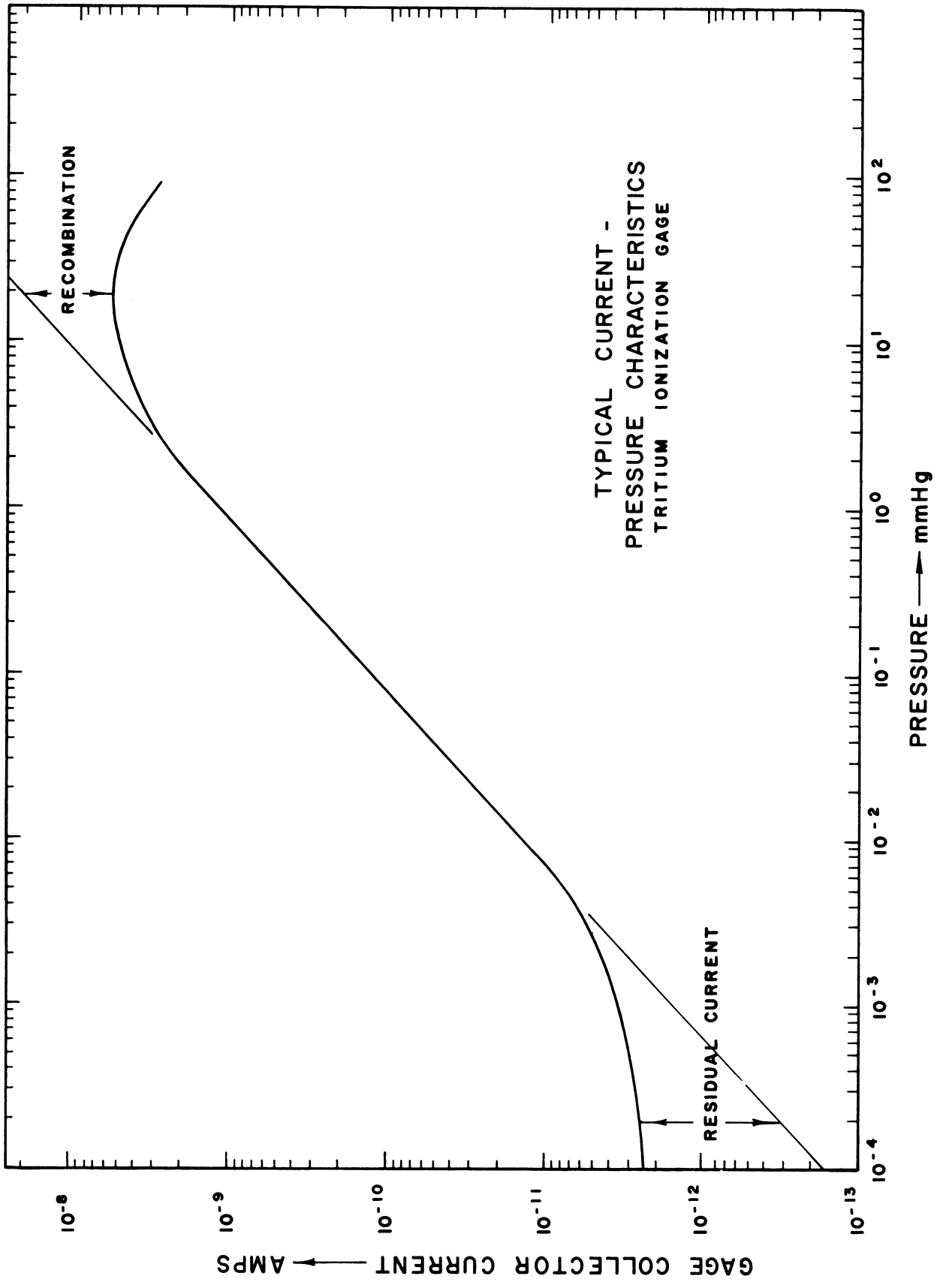
TYPICAL CURRENT -
PRESSURE CHARACTERISTICS
TRITIUM IONIZATION GAGE
RECOMBINATION
RESIDUAL CURRENT
GAGE COLLECTOR CURRENT ⟵ AMPS
PRESSURE ⟶ mmHg
10⁻⁸
10⁻⁹
10⁻¹⁰
10⁻¹¹
10⁻¹²
10⁻¹³
10⁻⁴
10⁻³
10⁻²
10⁻¹
10⁰
10¹
10²

Fig. 6B

Development of the system occurred over a period of years by various personnel of the Space Physics Research Laboratory. Further development of the system is currently in progress to extend the measurement range, and improve the accuracy and response of the instrument.

A description of the various components of the system follows.

2.21 Amplifier

The amplifier block diagram is presented in Fig. 7. Using standard operational amplifier theory,[8] an analysis of the amplifier circuit reveals an output voltage which is linearly related to the input current according to the relation

$$i_{gage} = \frac{E_B - E_{out}}{R_f} \tag{1}$$

where R_f is the feedback resistance of the amplifier and E_B is a dc bias voltage (usually about 6 v) added to the feedback loop. By rearranging terms, the output characteristic then becomes,

$$E_{out} = E_B - i_{gage} R_f \tag{2}$$

From this relation, it can be seen that, given a constant E_B, the sensitivity of the amplifier is dependant upon R_f.

Since any particular gage pressure-current characteristic (Fig. 6B) will encompass many orders of magnitude, the resolution and accuracy of the measurement is increased considerably by changing the sensitivity of the amplifier in different pressure ranges. This is accomplished by having a number of different Hi-megohm resistors (R_f) available, and employing a selector circuit to insert the proper resistor into the feedback loop. A bidirectional Ledex stepping motor, that drives a specially constructed Ledex wafer switch, provides the necessary mechanical configuration. The selector circuit senses the amplifier output voltage and provides switching pulses to the Ledex motor that will either increase the sensitivity as the output increases beyond 5 v, or decrease the sensitivity as the output approaches 0 v.

Five current ranges, each covering approximately one order of magnitude from 10^{-12} amperes are generally used in the Densatron. A voltage divider circuit wired to an additional wafer switch on the Ledex indicates the switch position; hence the range of the amplifier.

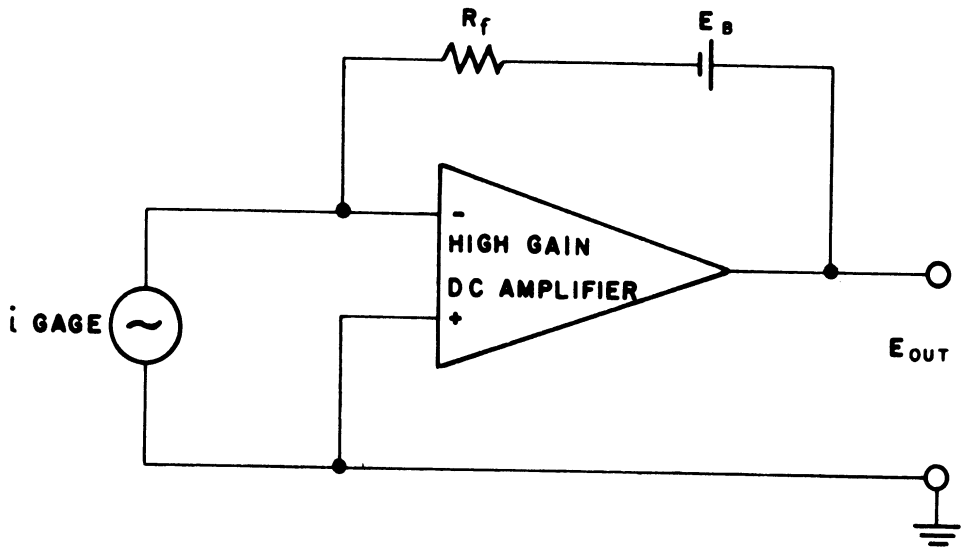

Fig. 7

2.22 Range Selector Circuit

The range switching circuit is a form of voltage comparator that provides output pulses when predetermined voltages are sensed at the input. The amplifier output is coupled to the inputs of the sensing circuits through an isolation resistance (R6 in Fig. 8) that allows external control of the switching circuit irrespective of the amplifier output level. The operation of the circuit can then be tested before flight. Three functions are possible with the range control input. The amplifier may be either up-ranged or down-ranged by applying, respectively, a signal above a positive 5 v or a signal below 0 v. Sometimes, it is desirable to hold the amplifier in a particular range which may be done conveniently by applying any low-source impedance voltage lying between the switching points.

Switching action is controlled in either direction by the sensing amplifiers which command the appropriate drive amplifier to operate. The drive amplifiers are identical and are a form of monostable flip-flop which are used to "dump" the charge from a 450 MFD capacitor through the Ledex coil. The capacitor provides a source of low impedance, high pulse energy needed to switch the Ledex. The pulse width may be adjusted through the monostable for best performance and efficiency. The input stage to the monostable is "gated" off during capacitor recharge, so that no switching can occur until sufficient energy is available in the capacitor to reliably switch the Ledex. By keeping the peak charging current to 100 ma or less, a maximum repetition rate of one switch every 3 sec is obtained. Under the conditions stated, the Ledex usually requires a 20 msec pulse that causes the capacitor to discharge to about 10 v.

2.23 Power Supply

The many supply and bias voltages required to operate the Densatron are derived from a dc-to-dc convertor included as part of the instrument. A single, 1 w power source between 25 and 35 v will operate the unit.

The circuit (see Fig. 5), is a standard square core oscillator operating at approximately 6 kc. Primary regulation is accomplished by zener regulators D5 and D6 and commutating diodes D2 and D3, which clamp the amplitude of the square wave at a level determined by the voltage drop across the diodes and the regulators. The isolation and drift characteristics are improved in the amplifier, by using secondary regulation for the electrometer tube filament supply, and also the positive supply to the rest of the amplifier.

2.3 INSTRUMENTATION SECTION

The operational characteristics of the experiment are primarily defined in the instrumentation section. All of the supplementary circuitry and instru-

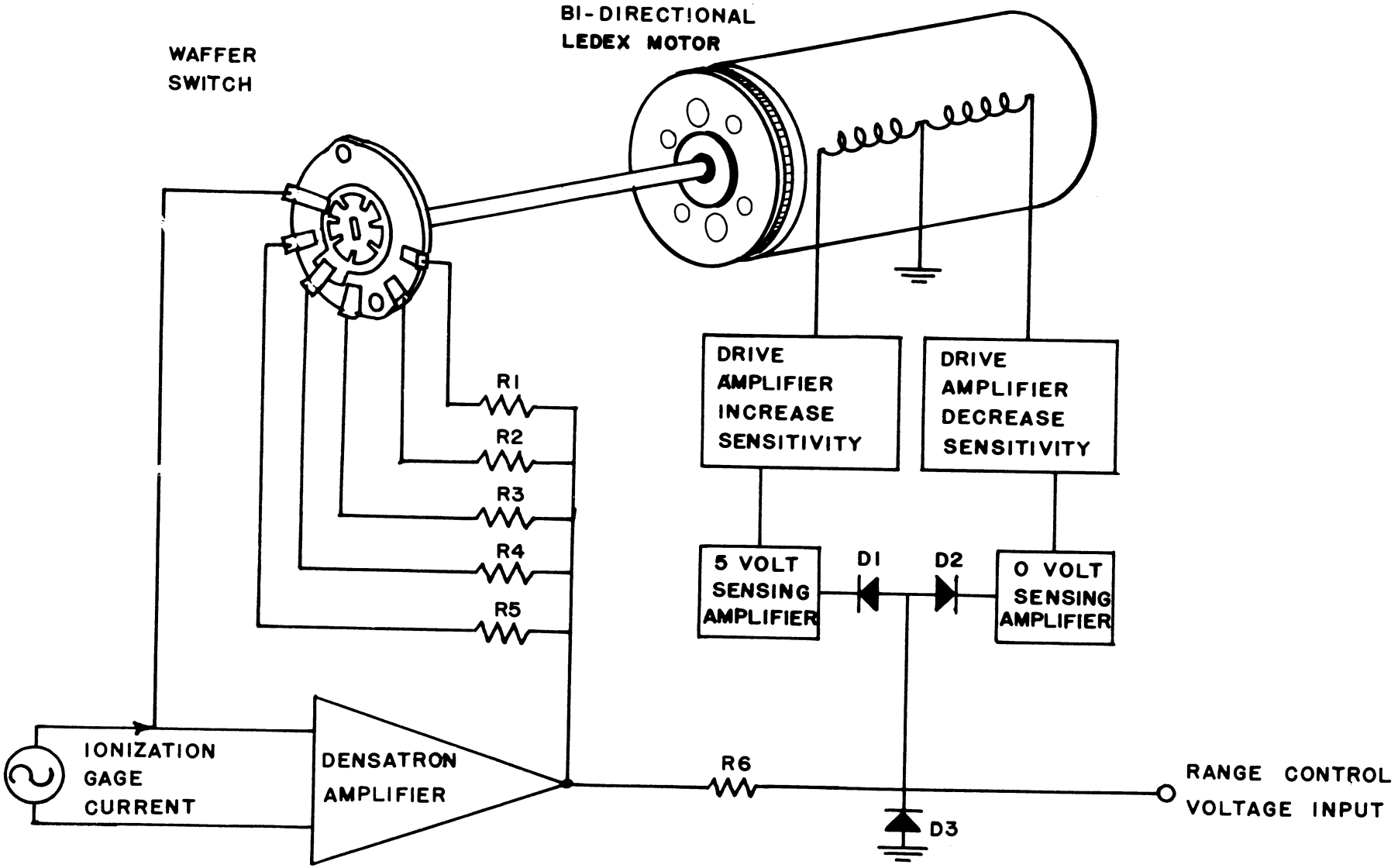

RANGE SELECTOR CIRCUIT
FUNCTIONAL DIAGRAM

Fig. 8

mentation needed to mold the payload into a completely independant measurement probe are located here. A block diagram of the system is shown in Fig. 9.

The payload operates from a nominal 28-v power source at approximately 400 ma load. All internal instrumentation is controlled by Ledex stepping switches through the pull away system, while the Densatron and other critical circuits are monitored in the same manner. A PAM/FM/FM telemeter system provides real time data transmission with 0.5 w RF power at 231.MHz. In-flight calibration is included for all except digitized subcarrier channels, and an electronics timer tests for Densatron amplifier drift after the data portion of the flight. The main data channel is also connected to the DOVAP telemeter input thus providing a back-up telemeter for the experiment.

Considerable effort was directed towards the mechanical as well as electrical development of this section in order to keep a close communication of basic objectives and design results. The circuits or components are mounted on a series of 5-3/8 in. diameter cylindrical shaped discs of variable thickness that are placed one on top the other forming a column similar to Fig. 10 and Fig. 11. The column is, in turn, fastened to the payload using four No. 10-32 threaded rods that pass through each deck and screw into a mounting platform. During final assembly, nuts are placed on the threaded rod and made to bear against the top deck causing the entire column to be held slightly in compression.

The resulting structure offers a high degree of protection from shock and vibration as well as providing accessibility to any part of the system. Each individual deck is pressure foamed with Ecco-foam* to further insure the protection of components. All of the decks are electrically joined to the system using Cannon D series connectors.

This modular design, so described, results in an extremely versatile payload that is easily tested and maintained. The electrical characteristics can be conveniently modified to satisfy varying demands of the system. For example, the data capacity of the telemeter system may be more than doubled without changing either the physical size or appearance of the section.

The individual decks found in the instrumentation section are described in more detail below, and the column deck arrangements are shown in Fig. 12.

2.31 Control Deck

Two Ledex programmers, mounted in the control deck Fig. 14, are remotely controlled through the umbilical pull-away system to energize internal instrumentation and select the proper functions to be monitored. The energizing

*Emerson and Cummings, Inc.

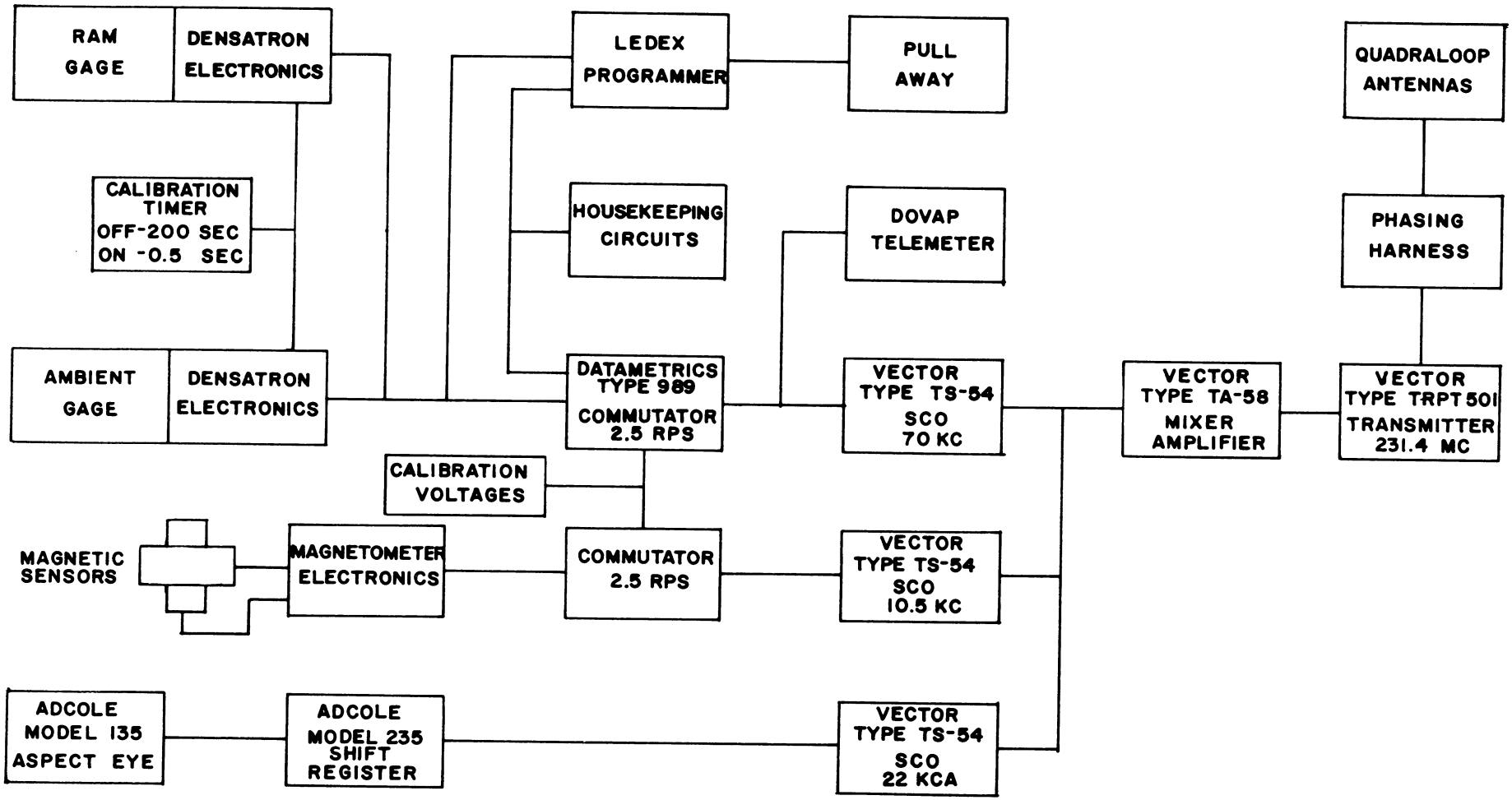

INSTRUMENTATION BLOCK DIAGRAM

Fig. 9

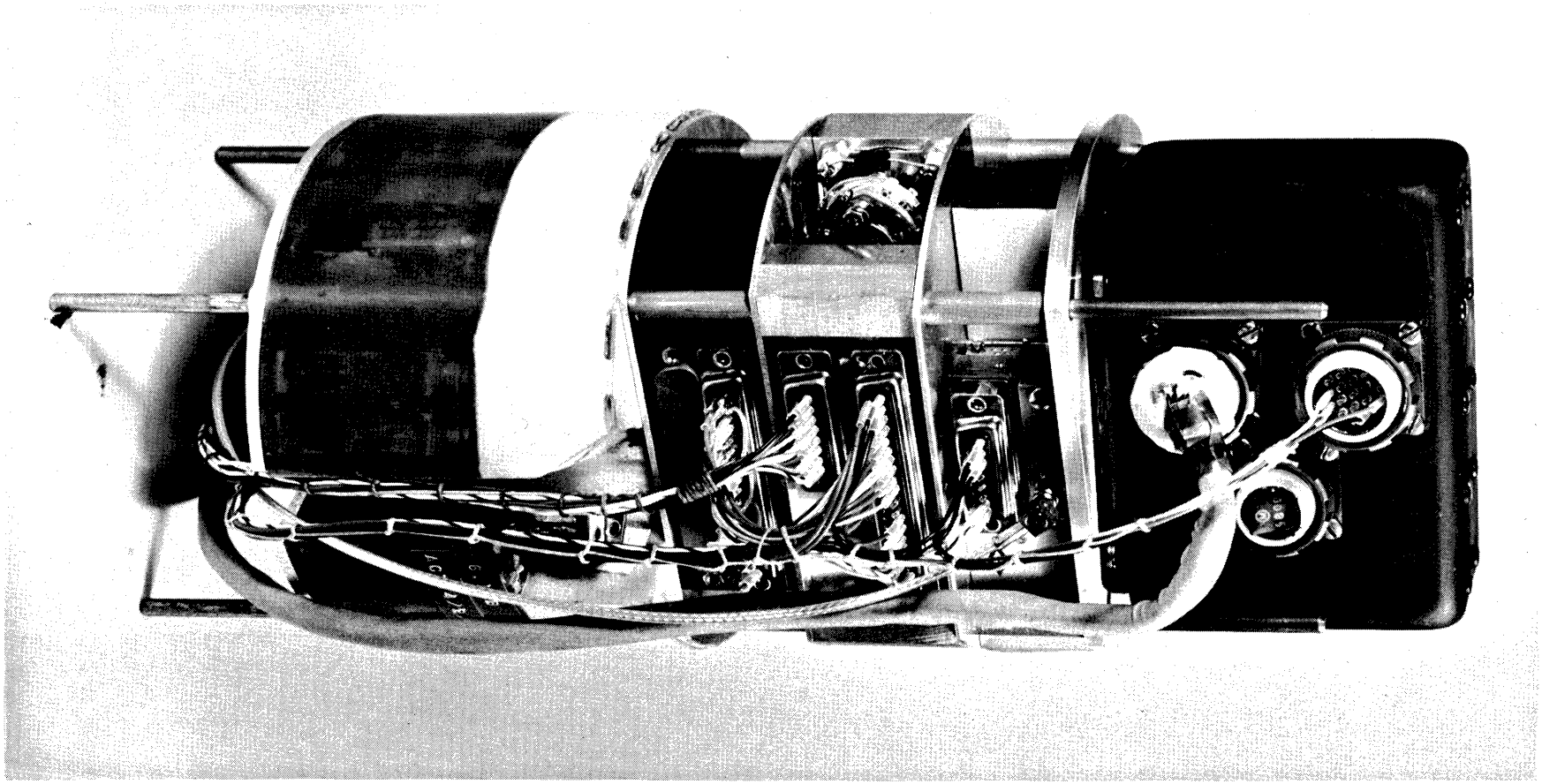

Fig. 10. Instrumentation with shift register—side view.

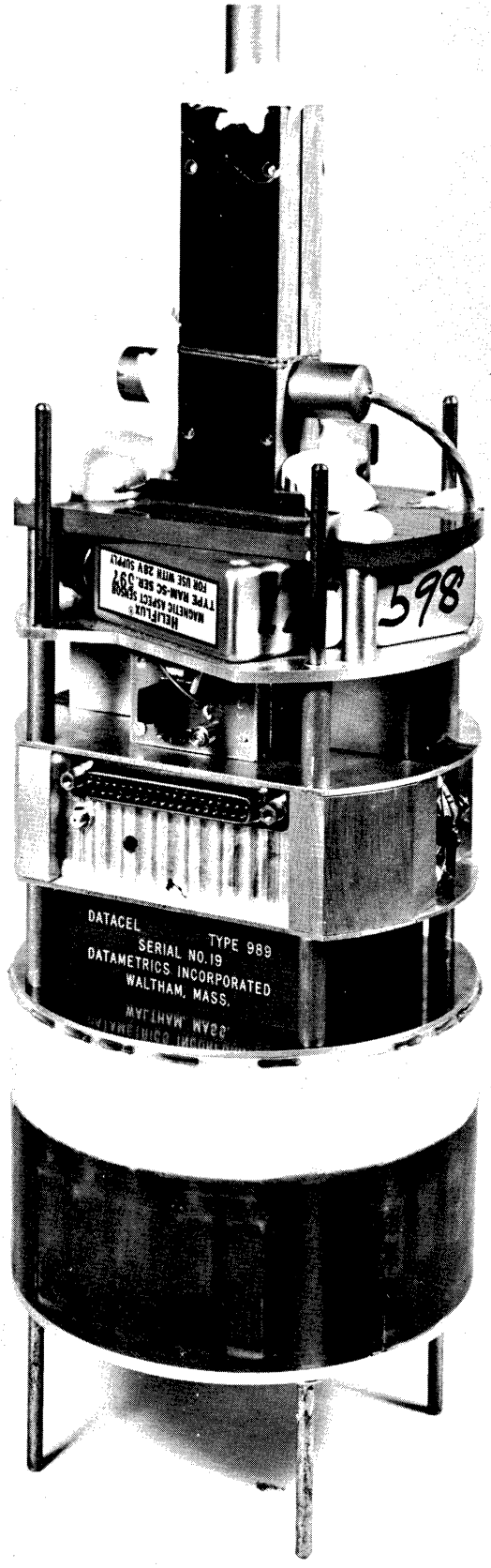

Fig. 11. Instrumentation with magnetometers—side view.

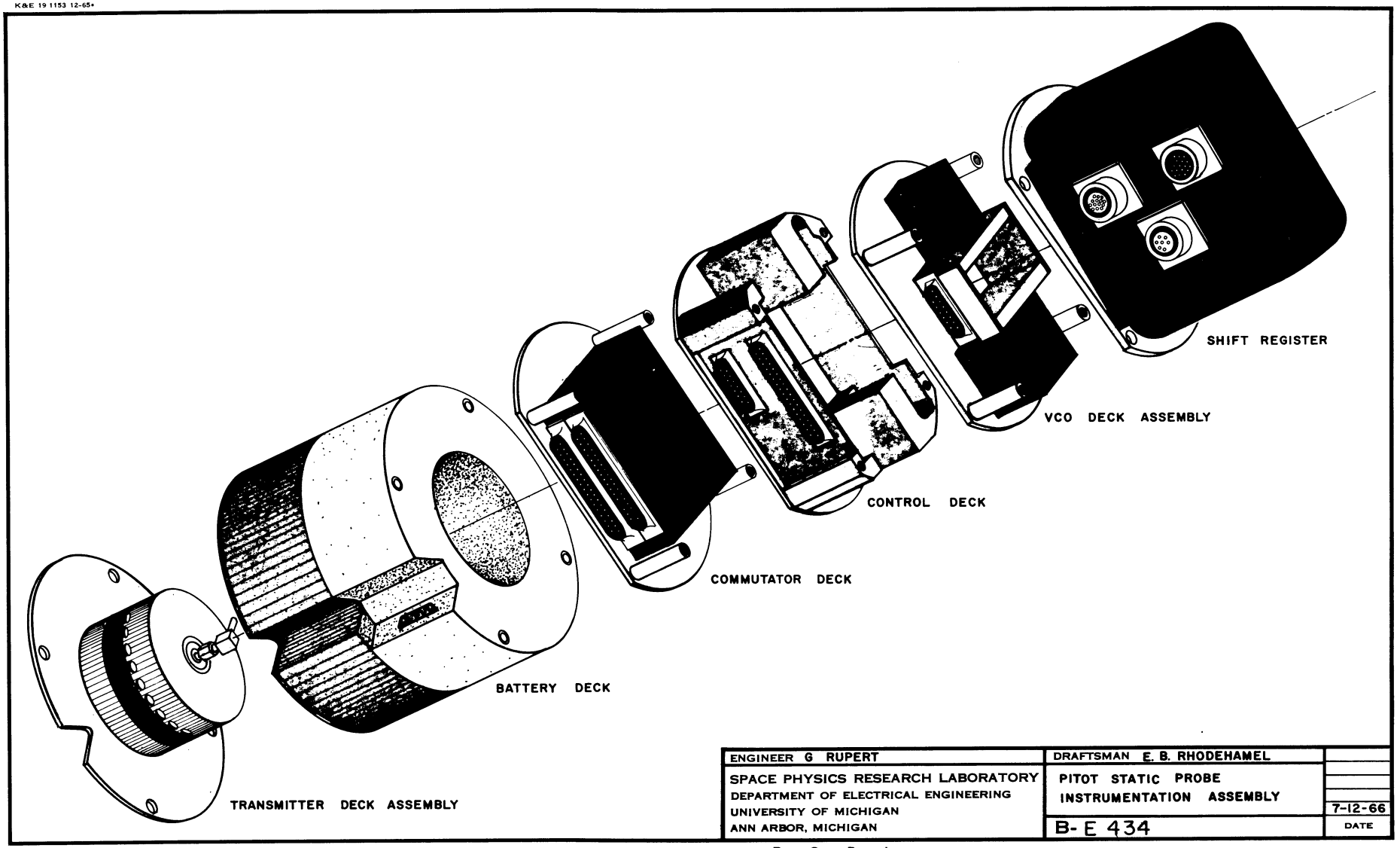
K&E 19 1153 12-65*
SHIFT REGISTER
VCO DECK ASSEMBLY
CONTROL DECK
COMMUTATOR DECK
BATTERY DECK
TRANSMITTER DECK ASSEMBLY
ENGINEER G RUPERT
DRAFTSMAN E. B. RHODEHAMEL
SPACE PHYSICS RESEARCH LABORATORY
DEPARTMENT OF ELECTRICAL ENGINEERING
UNIVERSITY OF MICHIGAN
ANN ARBOR, MICHIGAN
PITOT STATIC PROBE
INSTRUMENTATION ASSEMBLY
7-12-66
DATE
B-E 434
LAST USED R C D L

Fig. 12

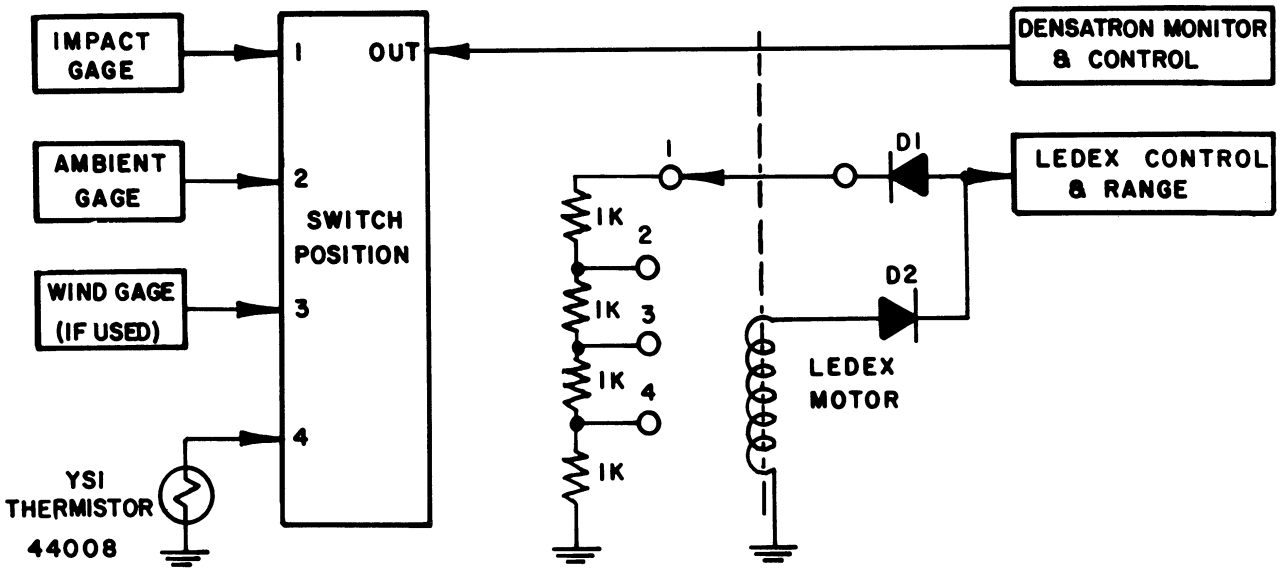

Fig. 13A

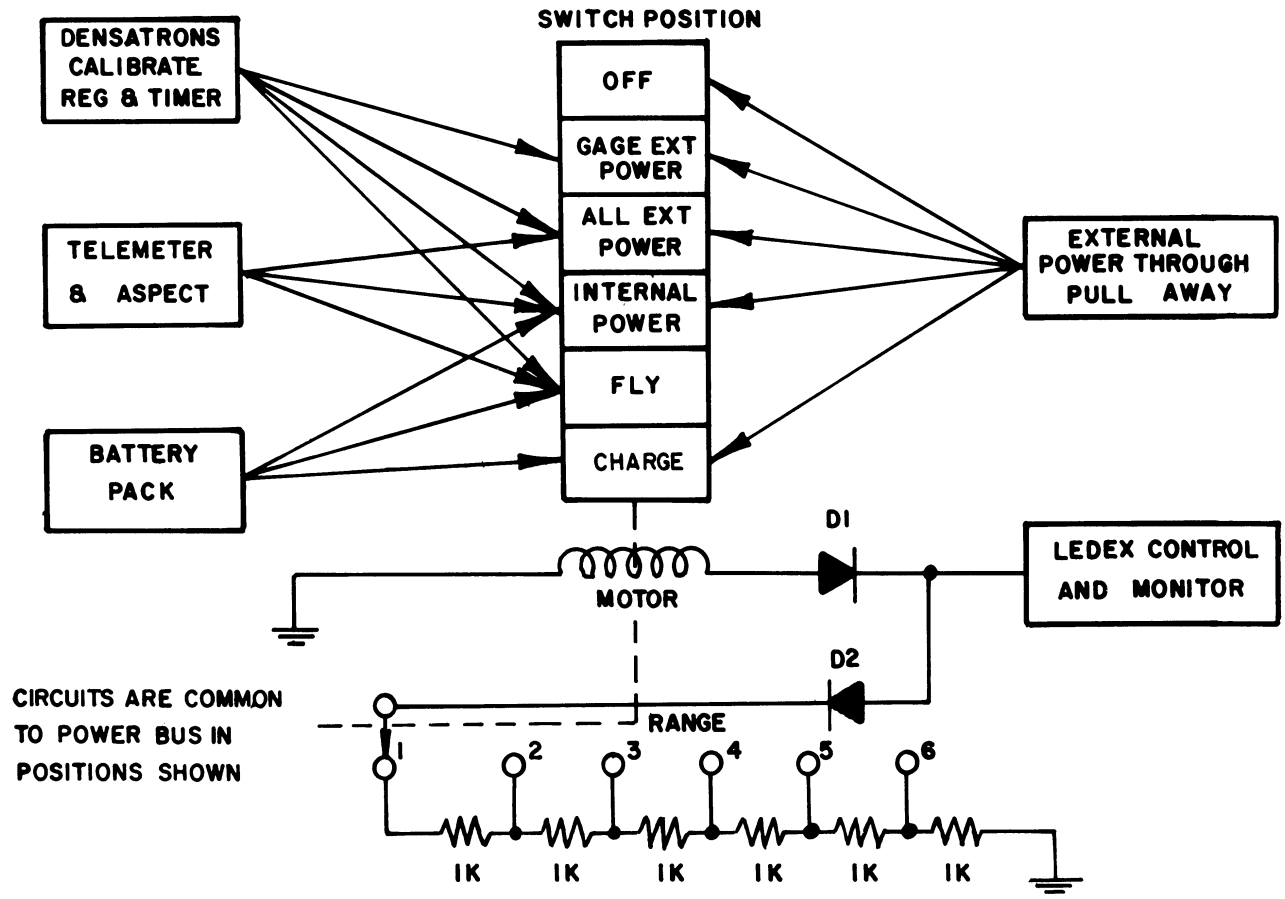

Fig. 13B

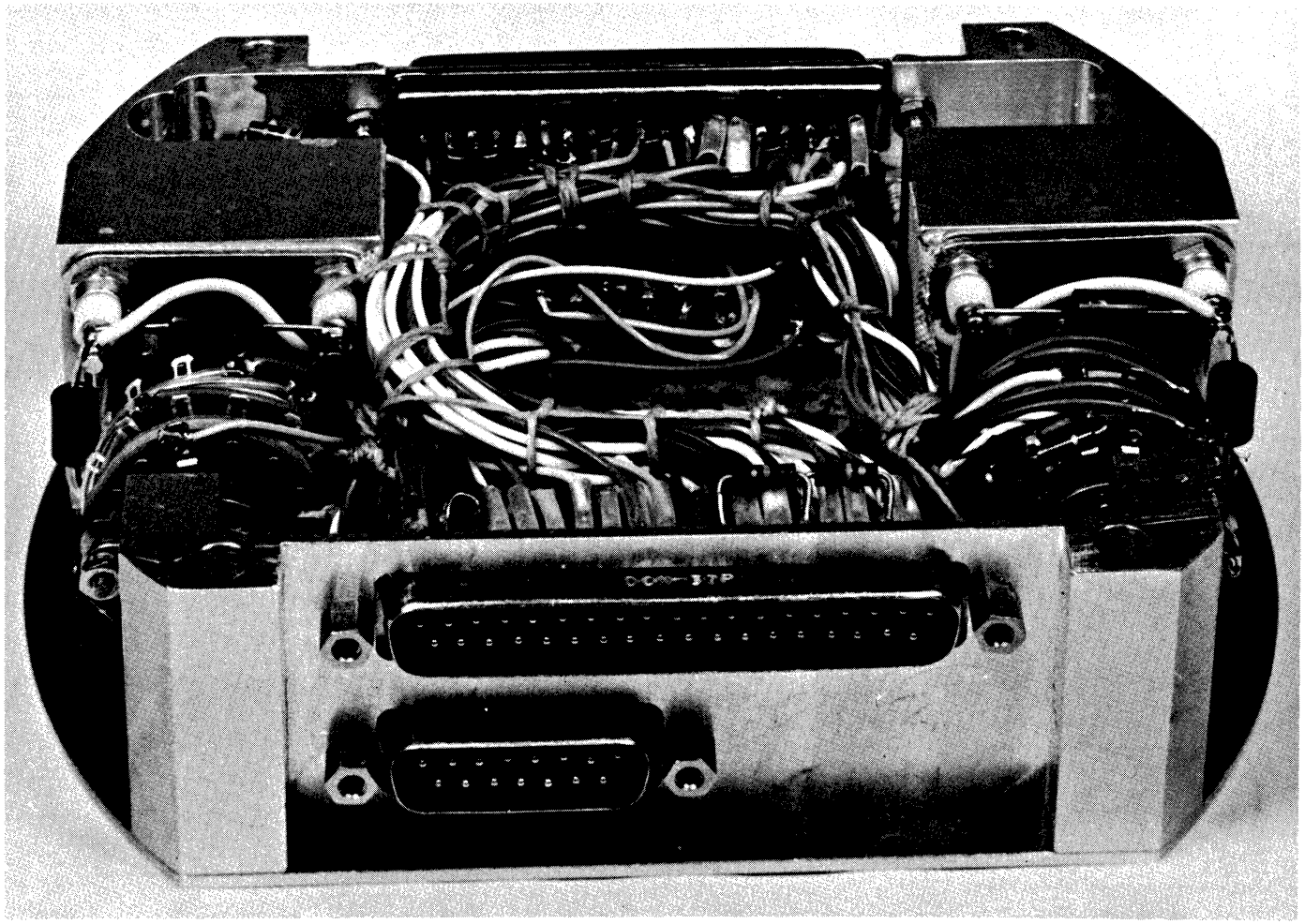

Fig. 14. Control deck—front view.

Ledex, commonly referred to as the telemeter Ledex, uses a specially designed six-position wafer switch to sequentially turn on the payload with provisions for external power operation and battery charging.

The remaining Ledex, referred to as the gage Ledex, uses two standard three-pole, four-position wafer switches to select leads from any one Densatron for ground monitoring through the pull away system. A separate position on each Ledex is used to disconnect all payload voltages from the umbilical during flight.

The functional aspects of the control circuitry is better understood from the block diagrams of Fig. 13A and Fig. 13B, also Tables I and II.

Each Ledex has a single control lead for switching the Ledex and also determining switch position. Blocking doides (D1 and D2 in Fig. 13A) are so arranged that a negative voltage pulse will actuate the Ledex motor, while a positive constant current source passing through a resistor network on a wafer switch, yields a voltage which then defines the switch position. For example, in position one of the gage Ledex, the 2 ma current source passes through four 1K resistors in series to ground, thus causing a voltage drop of 8 v. In position two, only three resistors are in series which then indicates 6 v.

TABLE I

GAGE LEDEX PROGRAM FORMAT

Switch Position	Designation	Function	Switch Position Monitor Voltage
1	Gage 1	Control and monitor ram gage	8
2	Gage 2	Control and monitor ambient gage	6
3	Gage 3	Control and monitor wind gage (if used)	4
4	Fly	Removes all internal voltages from pull away. Measures transmitter mounting plate temperature	2

TABLE II

TELEMETER LEDEX PROGRAM FORMAT

Switch Position	Designation	Function	Monitor	Position Monitor Voltage
1	Off	All circuits disconnected from pull away.		12
2	Gage external	Applies external power to all gages, calibration regular, and calibration timer.	External voltage at payload	10
3	All external	Applies external power to all remaining circuits.	External voltage at payload	8
4	All internal	All circuits switched to internal battery power.	Battery voltage	6
5	Fly	All voltages removed from pull away. All circuits energized from battery.		4
6	Charge	Connects battery to pull away for charging.	Battery voltage	2

Additional space in the control deck is used for the calibration timer and the calibrate voltage regulator. A test point jack for the 5-v calibration voltage and its adjustment pot is easily accessible at the so-called "rear" of the deck.

The control deck further serves as a center for all integration wiring. The Densatrons connect directly to the control deck via a 37-pin cannon connector at "rear" of the deck. The front side contains another 37-pin plug which connects to the main telemeter section wiring harness, and a 15-pin plug which goes directly to the umbilical plug.

The pull away system cable assignments are listed in Table III below.

TABLE III

PULL AWAY SYSTEM CABLE ASSIGNMENTS

Connector Pin Number	Function	Connector Pin Number	Function
1	Signal ground	7	Densatron range control
2	Power ground	8	Calibrate timer control
3	Telemeter Ledex control and range	9	External power input
4	Gage Ledex control and range	10	Power voltage monitor
5	Densatron output monitor	11	Amplifier temperature monitor
6	Densatron range monitor	12	Gage temperature monitor

2.32 Battery Supply Module

All of the instrumentation in the experiment is powered by a single battery pack specifically designed to fit in the base of the instrumentation section. The pack consists of 19 Yardney HR-1 Silvercels connected in series to yield a nominal supply voltage of 28.5 v. The module will supply a 1 amp load for greater than 1 hr and can be recharged at a 100-ma rate.

The cells are arranged on a 5-3/8 in. diameter deck, 3-3/8-in. high with a 2-5/8-in. diameter hole in the center. (The transmitter is fitted into the center hole during assembly.)

Construction of the pack is started by placing ventilation ports, made of heat shrinkable tubing over the vent caps in the cells. The cells are then arranged on an aluminum deck, placed in a mold, and scotchcast* in a tubular

*Minnesota Mining & Manufacturing Co.

shape to a height just above the cell terminals. A cannon plug bracket is then bonded to one of the forward deck supports. After wiring the battery leads to a cannon DEM-9S connector (Fig. 16) the whole assembly is returned to the mold where it is Ecco-foamed to its final configuration shown in Fig. 15.

2.33 Shift Register

The Adcole shift register "conditions," data received from the solar aspect eye. Information received in parallel form is "stored," and "read-out" in serial form by the shift register.

Whenever used (on all daylight firings) the shift register is located at the top end of the instrumentation column as shown in Fig. 10. The unit is first mounted on a 1/8-in. thick aluminum deck which then serves as the top plate of the column.

2.34 Magnetometer Deck

The magnetometer deck assembly, pictured in Fig. 17A, uses two Schoenstedt Engineering Model RAM-5C magnetometers. The sensors are mounted, one along the rocket axis, the other perpendicular to the first in a horizontal plane. The deck is constructed completely with the nonmagnetic material as are other surrounding structures to guard against field distortion and magnetic attenuation.

Electronically, the units operate from a nominal 28 v source at 11 ma current, are internally regulated, and provide an output linearly related to the magnitude of the magnetic input according to the following relation:

$$E = 2.40 + .004\ H \cos \Phi$$

where E is the output in volts, H is the magnetic field in millioersteds, and Φ is the angle between the magnetic field vector, and the sensor positive magnetic axis. The measurement range is ± 600 millioersteds resulting in a normal output swing from 0 to 4.8 v which is compatible with telemeter requirements. Typical calibration data for this magnetometer type are found in the Appendix. The deck wiring is shown in Fig. 18.

The deck is used for all nighttime launchings, and is physically located at the top of the instrumentation column in place of the shift register (Fig. 11).

For daytime launchings, a single axis magnetometer is mounted directly on the shift register as shown in Fig. 17B.

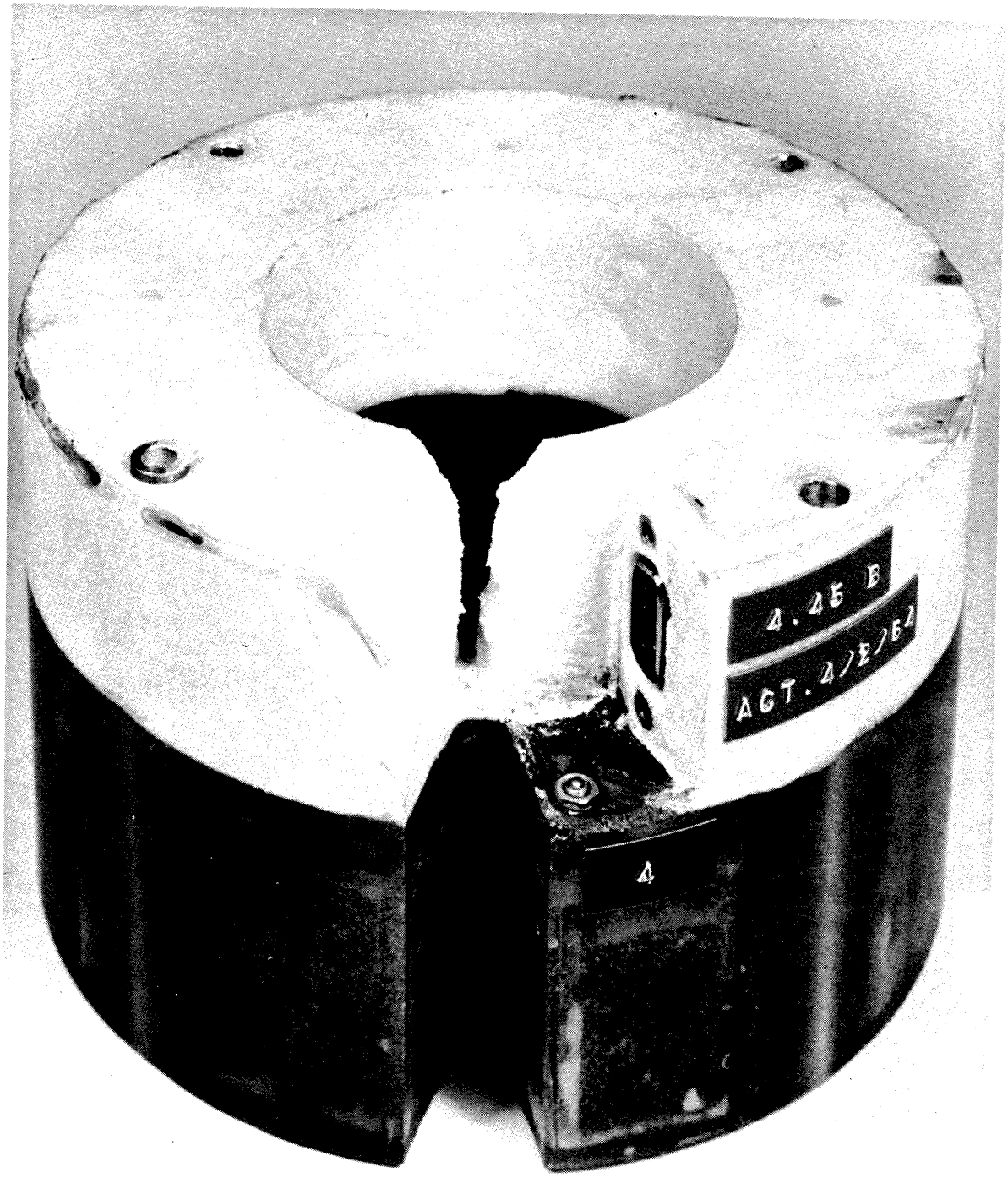

Fig. 15. Battery module—front view.

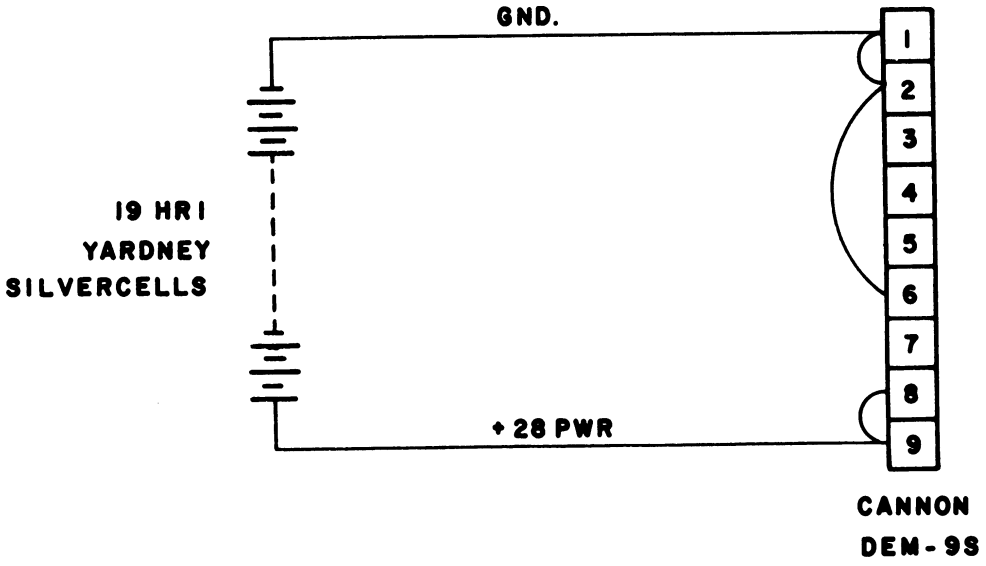

BATTERY SUPPLY MODULE WIRING

Fig. 16

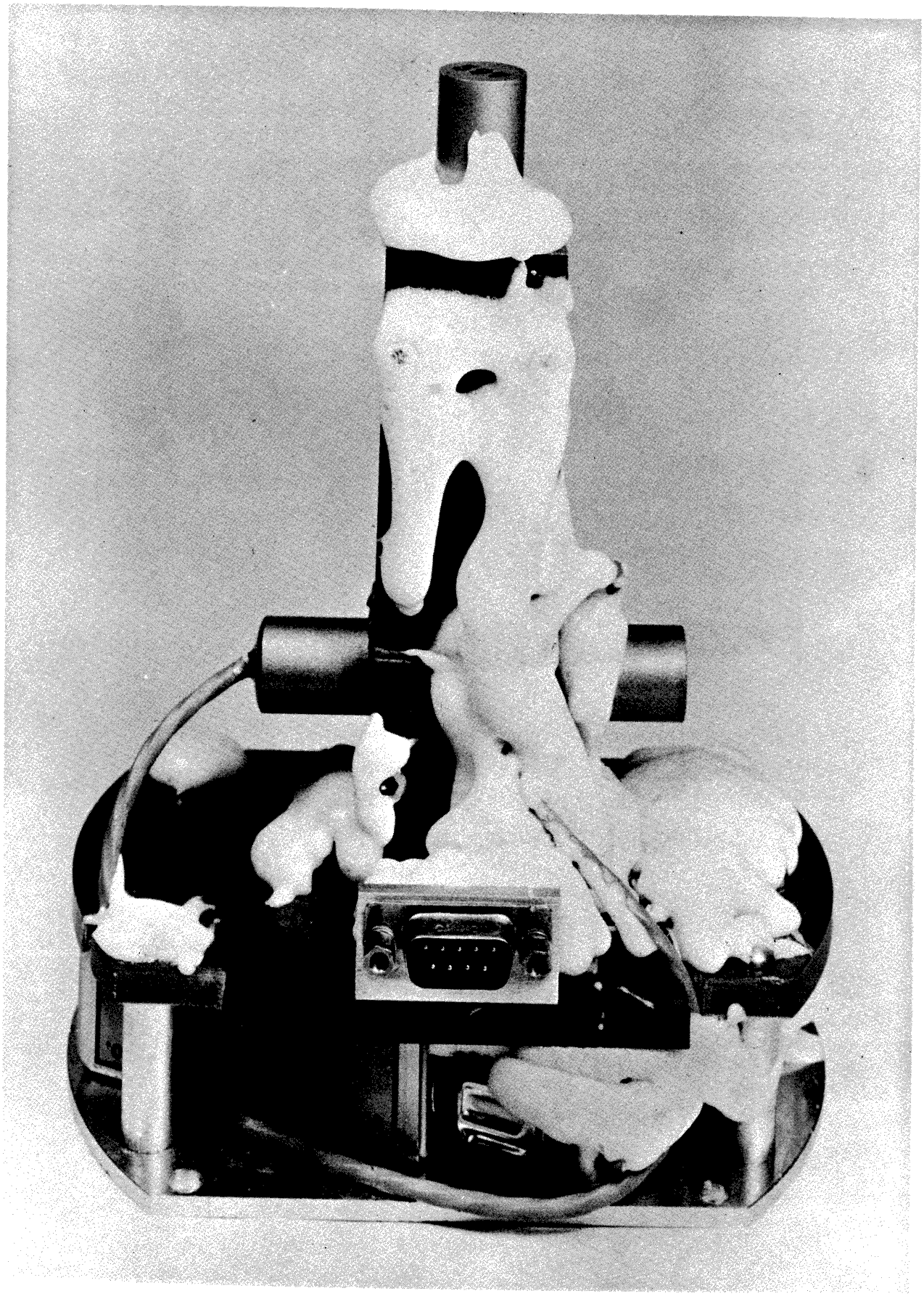

Fig. 17A. Magnetometer deck—front view.

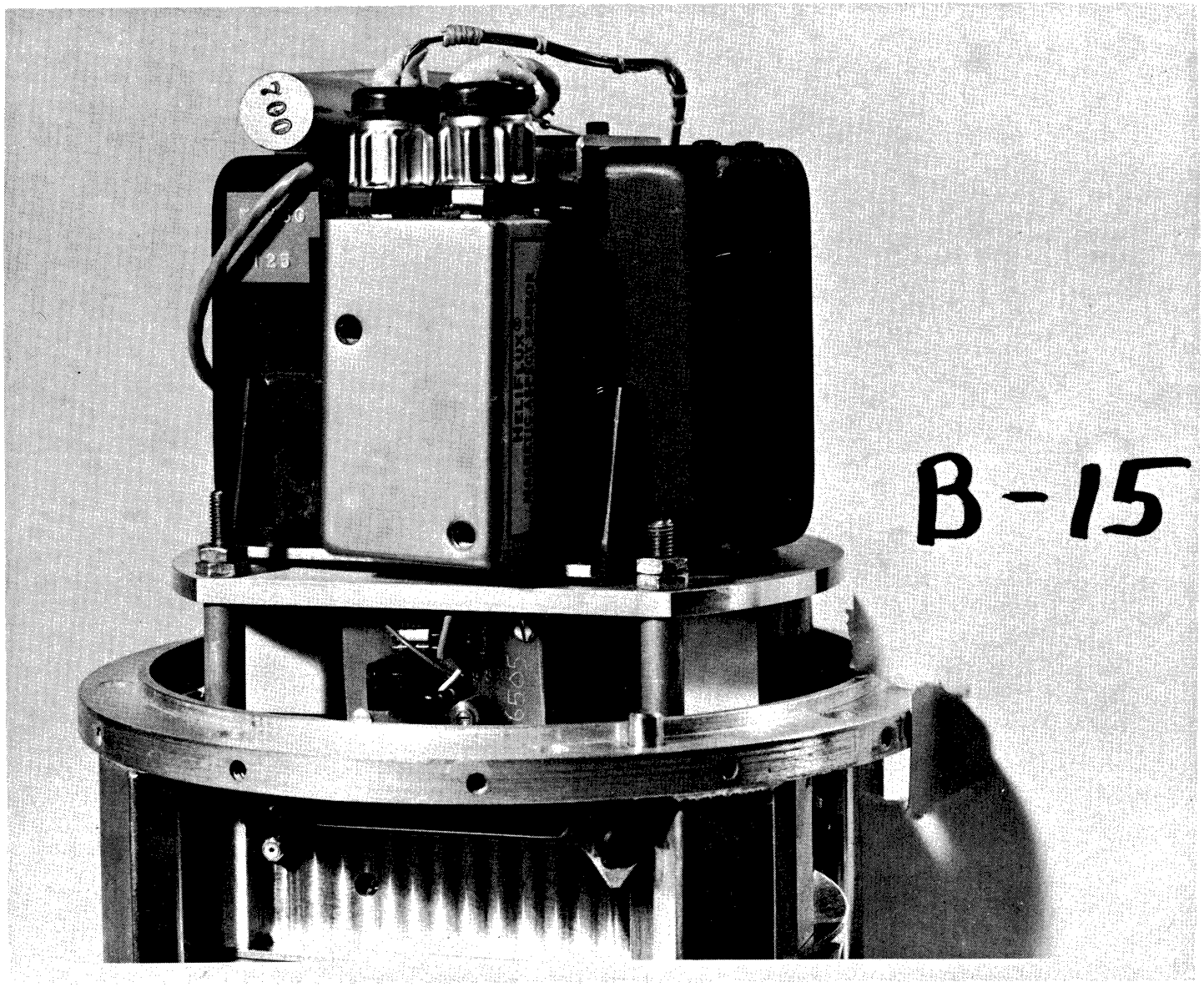

Fig. 17B. Magnetometer mounted on shift register.

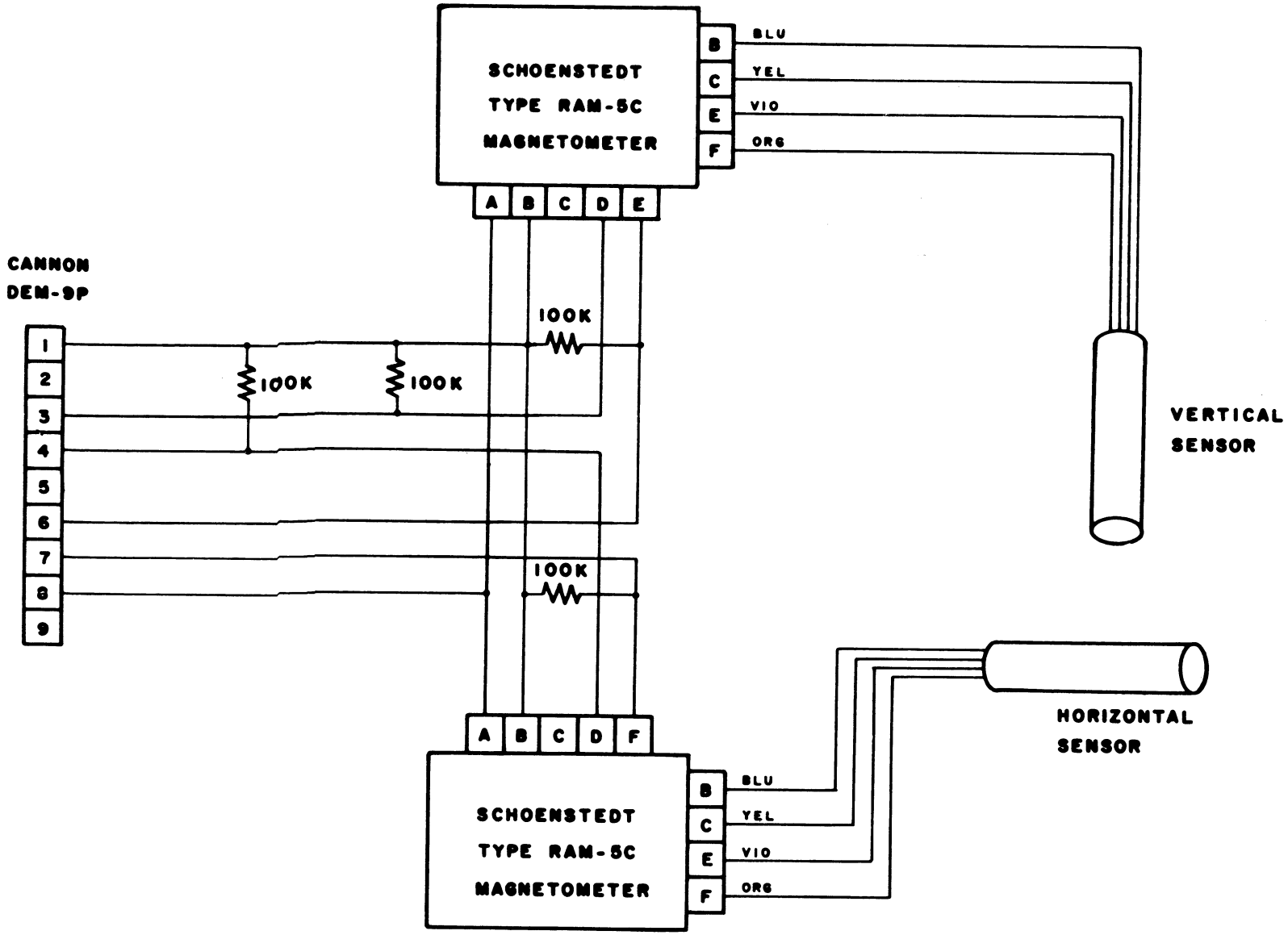

MAGNETOMETER DECK WIRING

Fig. 18

2.35 Special Circuits

Other circuitry, associated with the instrumentation section, were developed to satisfy specific requirements of the experiment. The operation of these circuits are discussed below.

2.351 Thermistor Supply

The temperature measurements needed in the experiment were greatly simplified by the availability of thermistors with 1% resistance/temperature characteristics. Thermistors have a large enough resistance change with temperature, that a voltage divider circuit with the thermistor in one leg, offers sufficient signal conditioning for telemeter.

The voltage/temperature curve of Fig. 19 results from the circuit of Fig. 20.

Most of the temperature measurements performed in the payload are for near ambient conditions, therefore a YSI-type 44008 thermistor is used most often which offers adequate resolution up to 60°C. Higher temperatures, up to 150°C, are measured using the same basic circuit and a thermistor probe selected to fit the desired temperature range. Most of the nose cone heating measurements graphed in the Appendix were performed in this manner. The appropriate thermistor probe required for certain temperature ranges are listed in the table below.

YSI* Part No.	R_o at 25°C	Nominal Temperature Range, °C	Minimum Sensitivity, mv/°C
44008	30K	10-60	50
44011	100K	45-90	42
44014	300K	60-120	35
44015	1 meg	85-150	30

*Yellow Springs Instrument.

The maximum temperature error expected due to the thermistor along is less than 0.5°C within the nominal temperature ranges specified. Telemeter may in the worst case add another 0.5°C error thus making a steady state RMS temperature error of about 0.7°C.

2.352 Calibration Regulator

Calibration voltages for telemeter are derived from the voltage regulator circuit of Fig. 21. This circuit is temperature compensated to within 0.05%

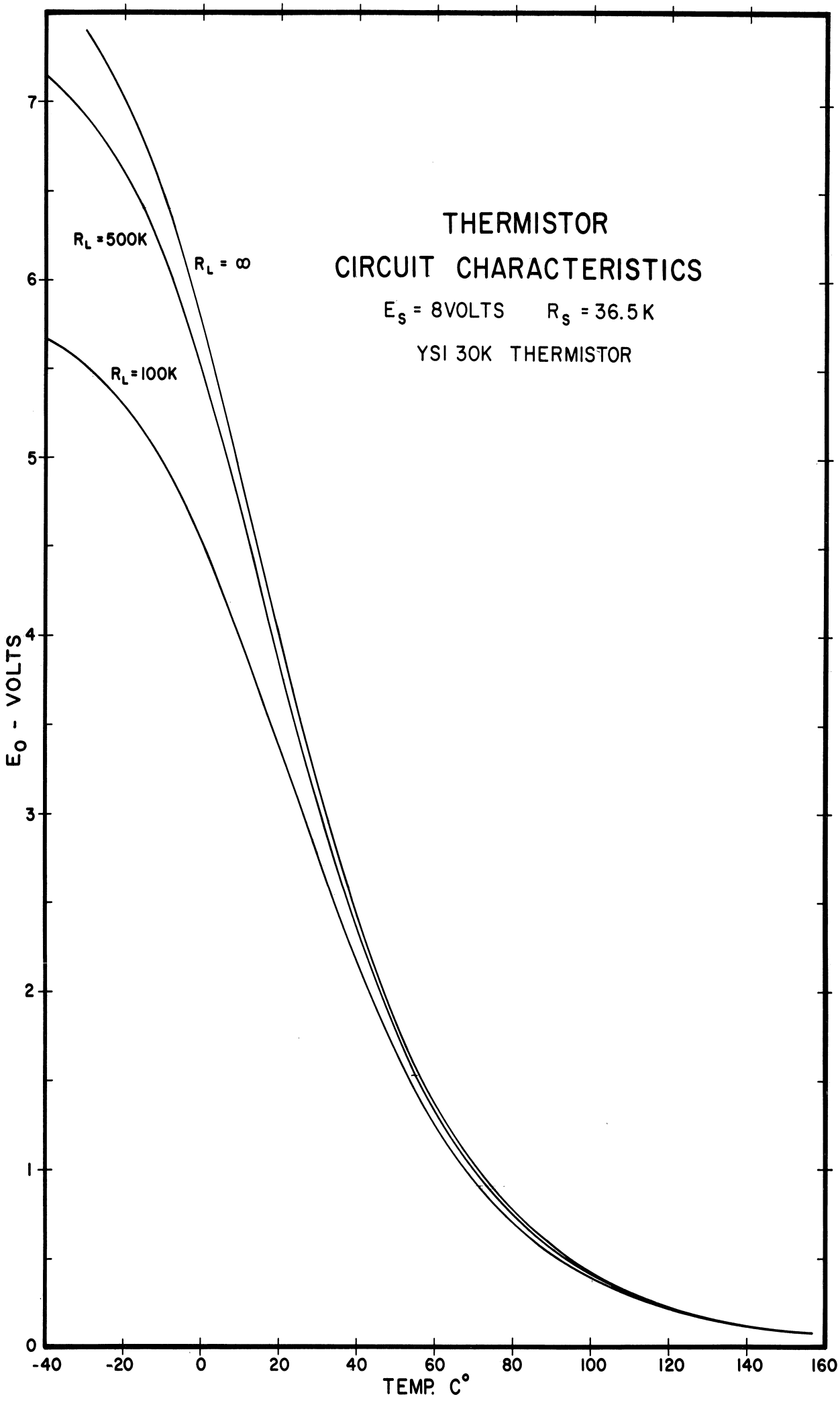
THERMISTOR
CIRCUIT CHARACTERISTICS
E_S = 8VOLTS R_S = 36.5K
YSI 30K THERMISTOR
R_L = 500K
R_L = ∞
R_L = 100K
E_O - VOLTS
TEMP. C°
0
1
2
3
4
5
6
7
-40
-20
0
20
40
60
80
100
120
140
160

Fig. 19

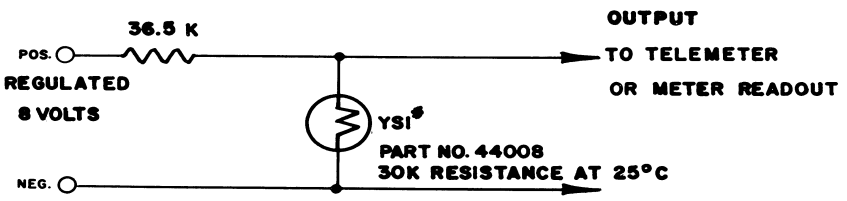

THERMISTOR SUPPLY

Fig. 20

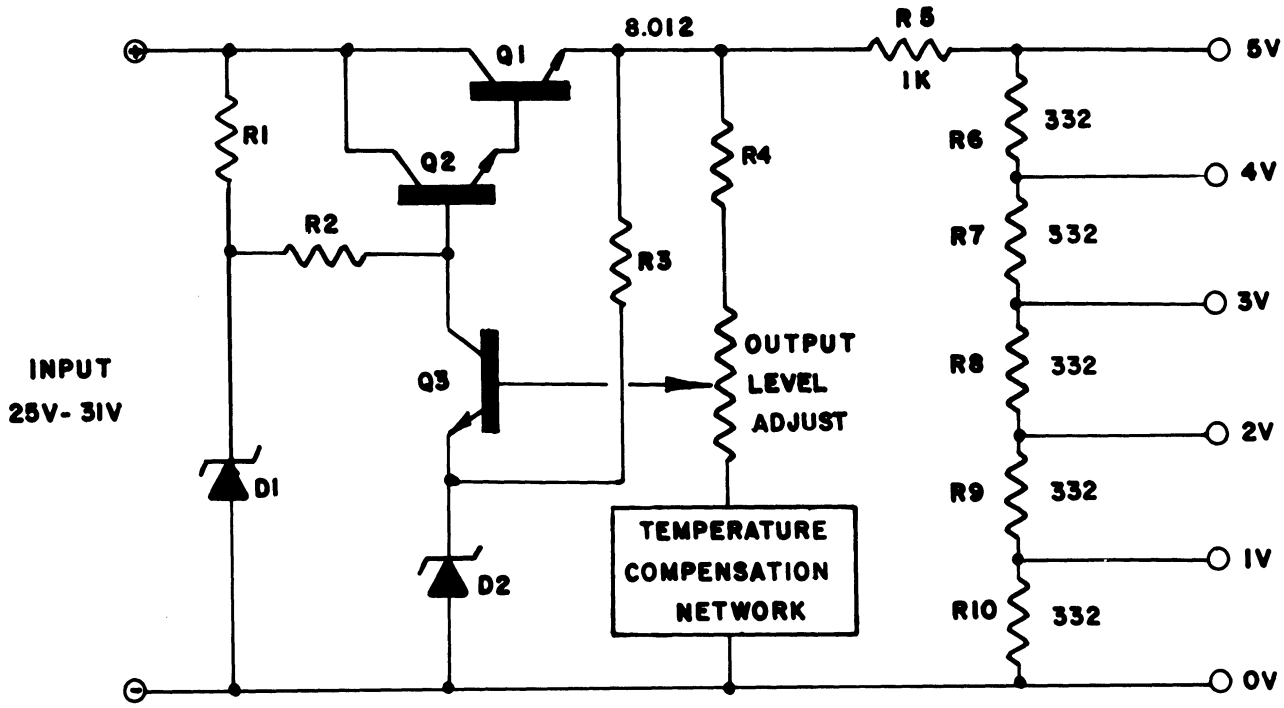

CALIBRATION REGULATOR

Fig. 21

from -20°C to +60°C. Supply voltage regulation is better than 0.01% and expected load changes effect the output less than 0.01%. Five calibration points are obtained with a voltage divider using 1-v steps. Overall accuracy of these voltages are within ±3 mv under all conditions of load, temperature, and input supply variations.

This circuit also provides an 8-v source for the thermistor circuits.

The design of the circuit follows standard patterns except for the temperature compensation method employed. The base of Q_3 is held at a voltage equal to the reference element D_2 plus the V_{BE} of Q_3. The voltage divider, consisting of R_4, the output level adjust and the temperature compensation network, then determines the output voltage. Q_1 is the control element, which drops the supply voltage to the required output while Q_2 is added to provide more loop gain to the amplifier, needed to obtain high stability. D_1 is a preregulator for the amplifier, which compensates for large input voltage swings.

While it is true that the circuit can be made temperature stable by biasing the reference amplifier (Q_3 and D_2) properly for zero drift, the characteristic may change considerably with circuit component changes because the point of zero drift is highly dependent upon maintaining precise bias conditions. For this reason, the reference amplifier is heavily biased so that changes in other components or conditions will not alter the bias conditions appreciably, which could lead to a change in the temperature characteristics.

The compensation network is easily determined by substituting a decade resistance box in place of compensation network and finding a curve of resistances versus temperature needed to keep the output constant. A curve obtained in this manner is shown in Fig. 22. The derivative of this curve taken at two or three points will yield a total resistance change or ΔR required for compensation. The compensation network can thus be selected by comparison of this data with the computed ΔR for various resistor-sensitor combinations. The chosen network can then be inserted into the circuit and the curve of temperature versus output obtained. The step may be repeated if better compensation is desired; however, other factors limit the degree of compensation possible with this method. The temperature response of a typical regulator is shown in Fig. 23. An important advantage to this method is that the shape of the curve remains essentailly the same over large periods of time.

2.353 Calibrate Timer

The Densatron amplifiers are calibrated periodically before and during flight primarily as a precaution against unforeseen or unnatural amplifier behavior. The amplifiers have very stable drift characteristics and normally require only a small correction factor for data reduction or none at all.

A free running unijunction transistor relaxation oscillator (Fig. 24) performs the basic timing function. The pulsed oscillator output triggers

VOLTAGE REFERENCE CIRCUIT
COMPENSATION NETWORK CURVE

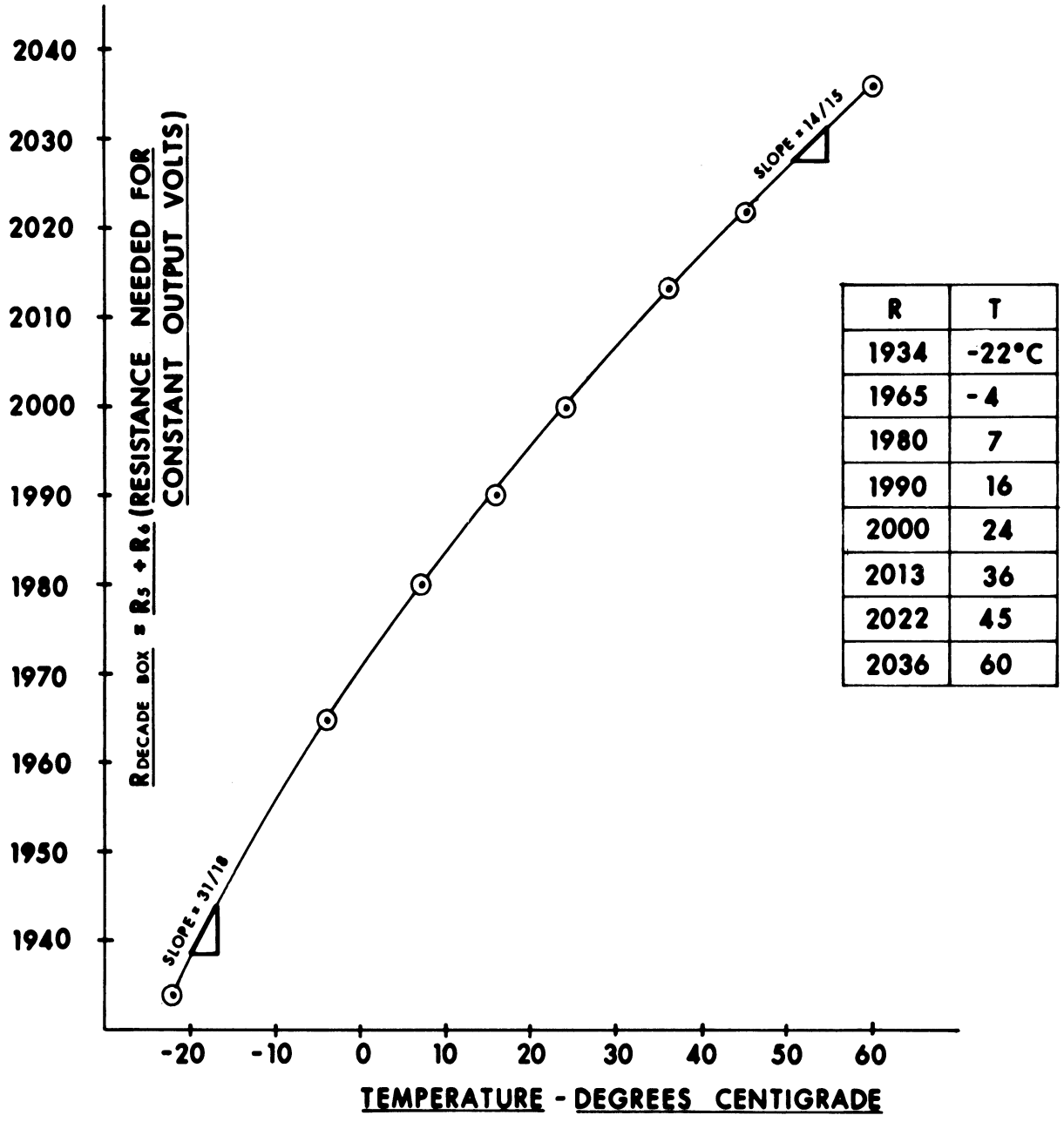

R	T
1934	-22°C
1965	- 4
1980	7
1990	16
2000	24
2013	36
2022	45
2036	60

Fig. 22

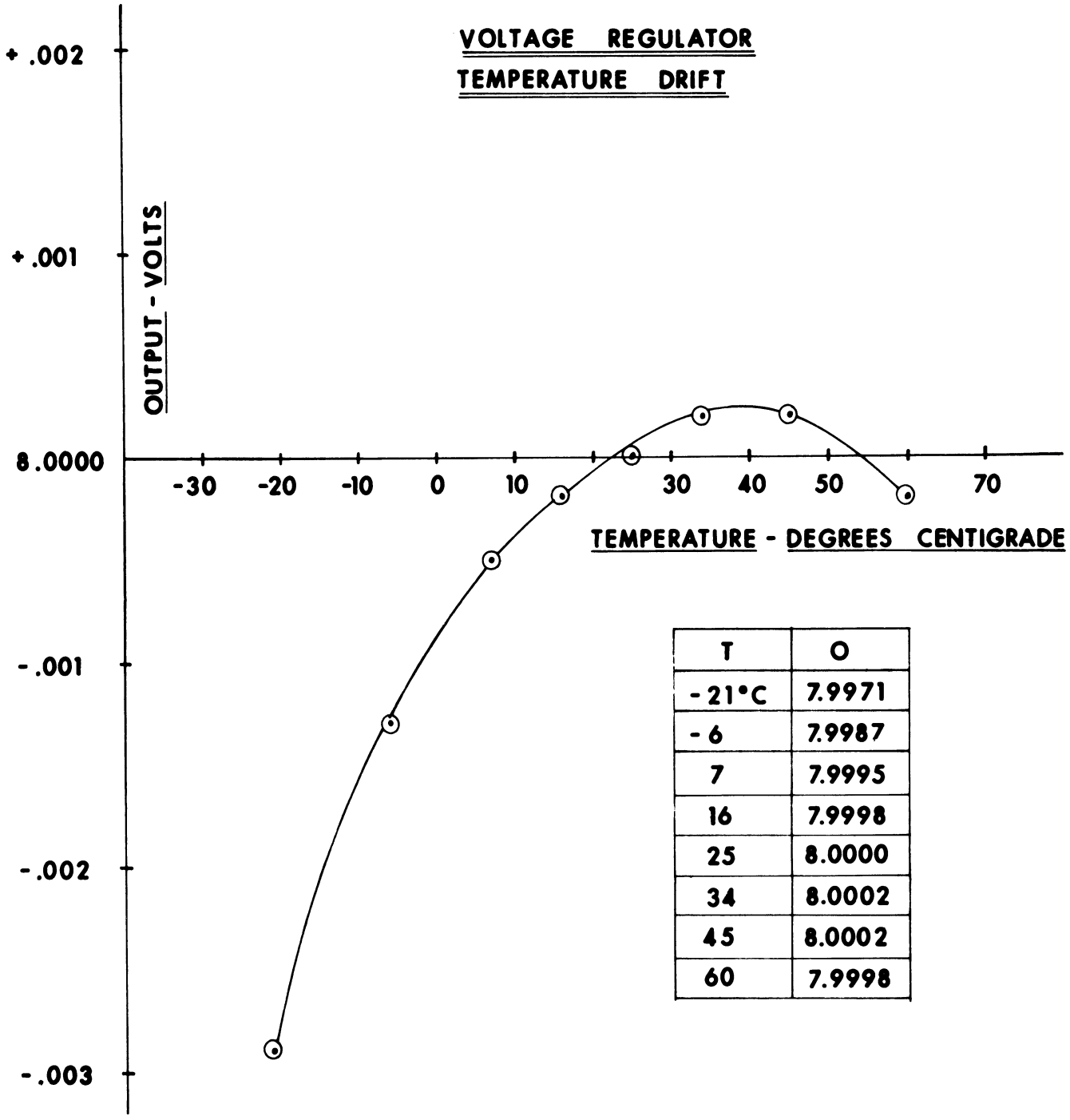

T	O
- 21°C	7.9971
- 6	7.9987
7	7.9995
16	7.9998
25	8.0000
34	8.0002
45	8.0002
60	7.9998

Fig. 23

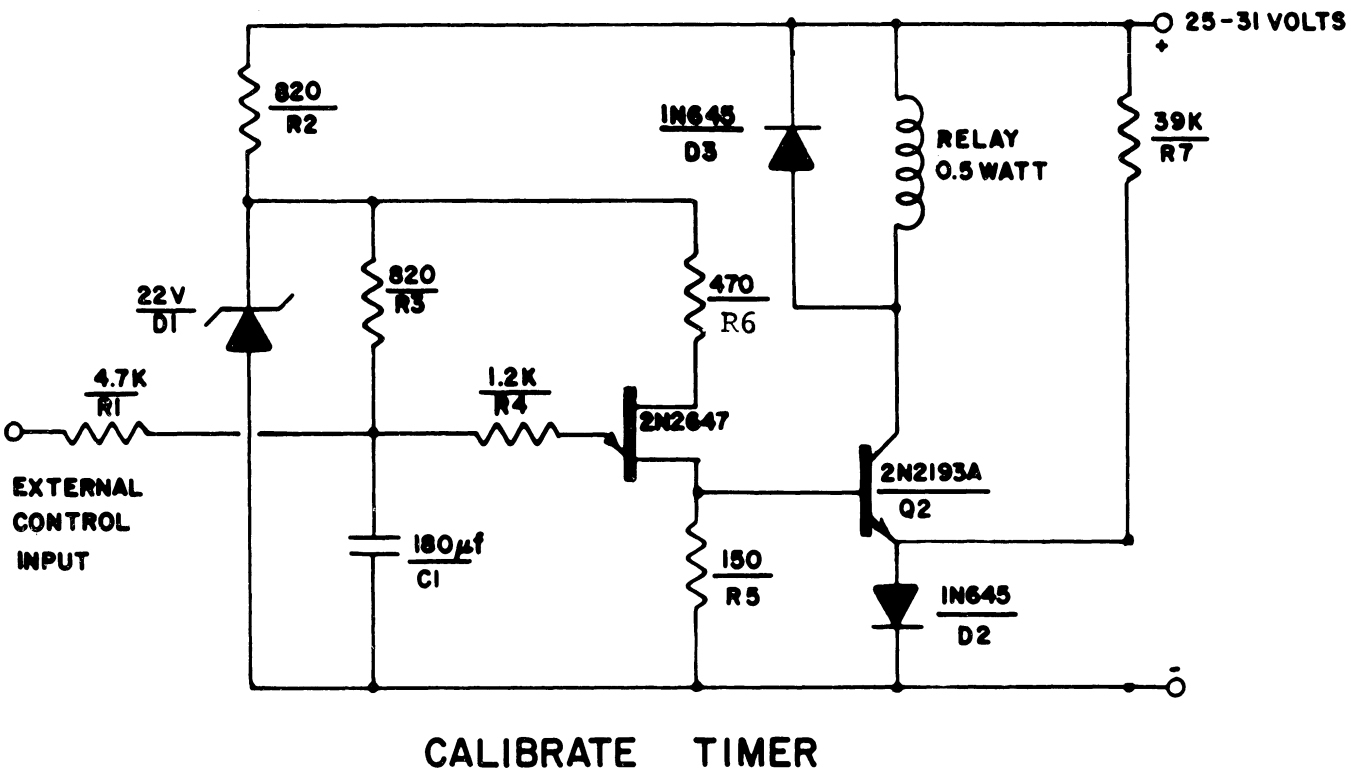

CALIBRATE TIMER

Fig. 24

a transistor switch (Q_2) that in turn drives a 1/2 w relay which then activates the calibration circuits in each Densatron.

Under normal operation, the off-time is adjusted for 200 sec. An external control lead can reset or start the timing function which in effect sets the first calibrate time after launch, thus insuring uninterrupted data recovery. The on-time is made as short as is necessary, usually about 0.5 sec.

The off-time is controlled primarily by the charging of C1 through R3 and by the intrinsic stand-off ratio (η) of the unijunction. The instantaneous voltage (V_c) on C1 is:

$$V_c = V_s \left(1-\varepsilon^{-\frac{1}{R_3C_1}t}\right) \tag{1}$$

when the effects of R4, R5, and R6 are ignored. The unijunction will fire at its peak point voltage (V_p) which is approximately

$$V_p = \eta V_s \tag{2}$$

where η is the intrinsic stand-off ratio and V_s is supply voltage across D1. The time required to achieve this level is found by substituting Eq. (1) into Eq. (2) which then yields:

$$\eta V_s = V_s \left(1-\varepsilon^{-\frac{1}{R_3C_1}t}\right) \tag{3}$$

which can also be written

$$(1-\eta) = \varepsilon^{-\frac{1}{R_3C_1}t} \tag{4}$$

then solving for t, the off-time:

$$t_{off} = R_3C_1 \ell n \left(\frac{1}{1-\eta}\right) \tag{5}$$

The value of $\ell n\ (1/1-\eta)$ will usually lie between 0.7 and 1.4 which means the time constant R_3C_1 must nearly equal the time required. The peak point current quite often limits the value of R3 to 1 meg or less so that capacitence required must be 200 μF or larger to obtain the desired off time.

It should be noted here that only high-quality, low-leakage capacitors can be used to obtain long off times.

The on-time is controlled by the discharge circuit of C1 which includes R4 and R5 and the unijunction characteristics. R4 may be used to adjust this time which, in practice, usually cannot be made longer than 0.7 sec due to other factors involved.

The transistor switch is held in cut-off, during the off-time with a diode, D_2, that keeps a slight reverse bias on the base of Q_2. The diode D_3 provides a current path for the relay current when the transistor is turned off thus avoiding high-voltage transients.

By proper selection of R5 and R6 the off-time can be made stable within $\pm 2\%$ over the temperature range of -20°C to +80°C. The on-time will vary considerably more by temperature changes than the off-time but is less critical in this application.

2.354 Pedestal Inverter Supply

Since there are no negative voltages available in the instrumentation section, the inverter circuit shown in Fig. 25 is used to provide the negative pedestal voltage needed in the IRIG commutator format. For simplicity, the circuit is represented in three parts: the first part is a Shockley diode relaxation oscillator composed of R1, D1, C1, and R2; the second part is a voltage doubler circuit with D2, D3, C2, and C3; while the third part is a voltage regulator composed of D4. Component selection is relatively uncritical except in the oscillator section where the circuit could "lock-up" due to the use of wrong combinations of components. It is best to use a high holding-current Shockley in this application so that the selection of other components are less critical.

The oscillator frequency lies between 300 and 400 cps. Typical circuit performance curves are presented in Fig. 26 and Fig. 27.

2.4 TELEMETER SYSTEM

Telemeter system design is the selection of many interrelated parameters in a manner devised solely to satisfy the demands or needs of a particular experiment or measurement. Each system is therefore unique in character and make-up.

Pitot-Static Probe telemetry are tailored to meet the experiment's requirements, within the scope of primary payload objectives, while at the same time maintaining compatibility with existing telemetry equipment.

For the most part, IRIG standards are used throughout the design except where modifications are more desirable and data quality are not effected. Flexibility is maintained wherever possible, so that each payload may be used to gather the most useful information—both engineering and scientific. System compon-

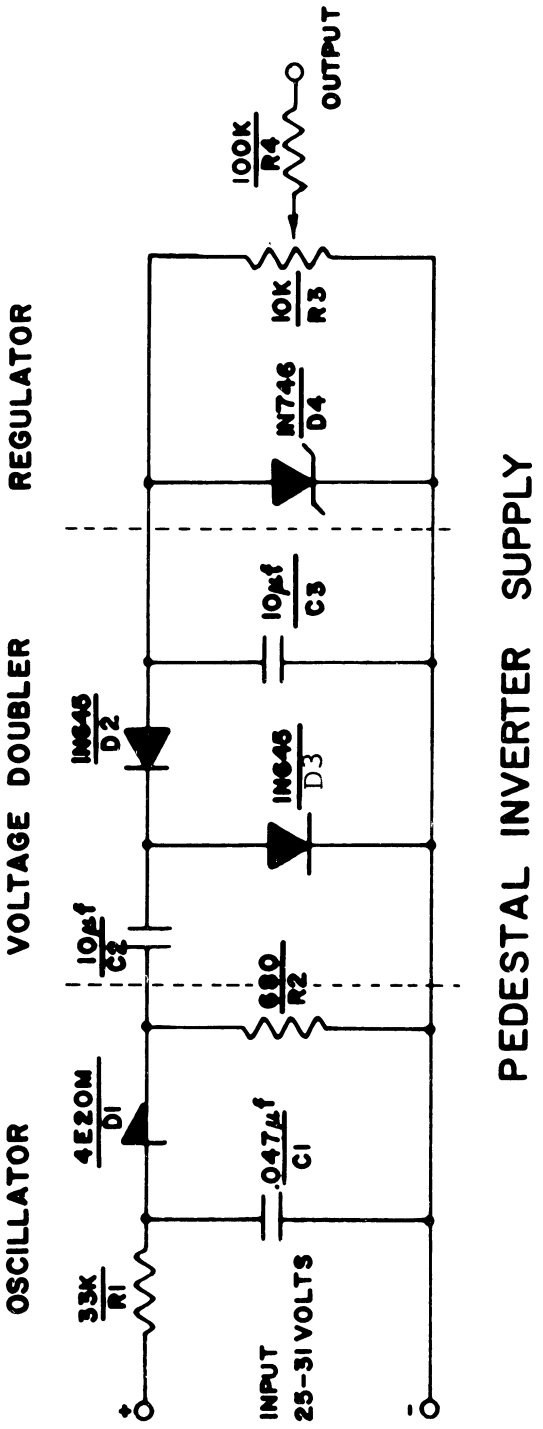
OSCILLATOR
VOLTAGE DOUBLER
REGULATOR
33K R1
4E20M D1
.047μf C1
10μf C2
IN645 D2
IN645 D3
680 R2
10μf C3
IN746 D4
10K R3
100K R4
OUTPUT
INPUT 25-31 VOLTS
+
-
PEDESTAL INVERTER SUPPLY

Fig. 25

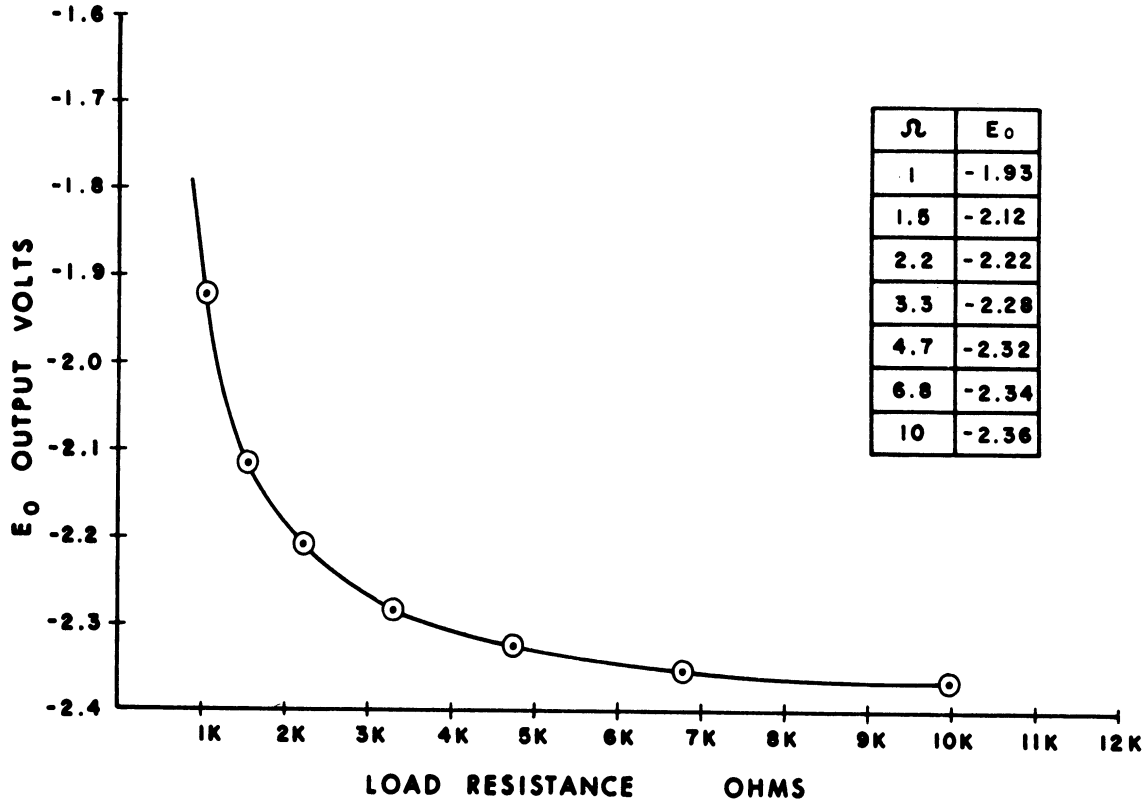

PEDESTAL SUPPLY CIRCUIT
LOAD CHARACTERISTICS

Fig. 26

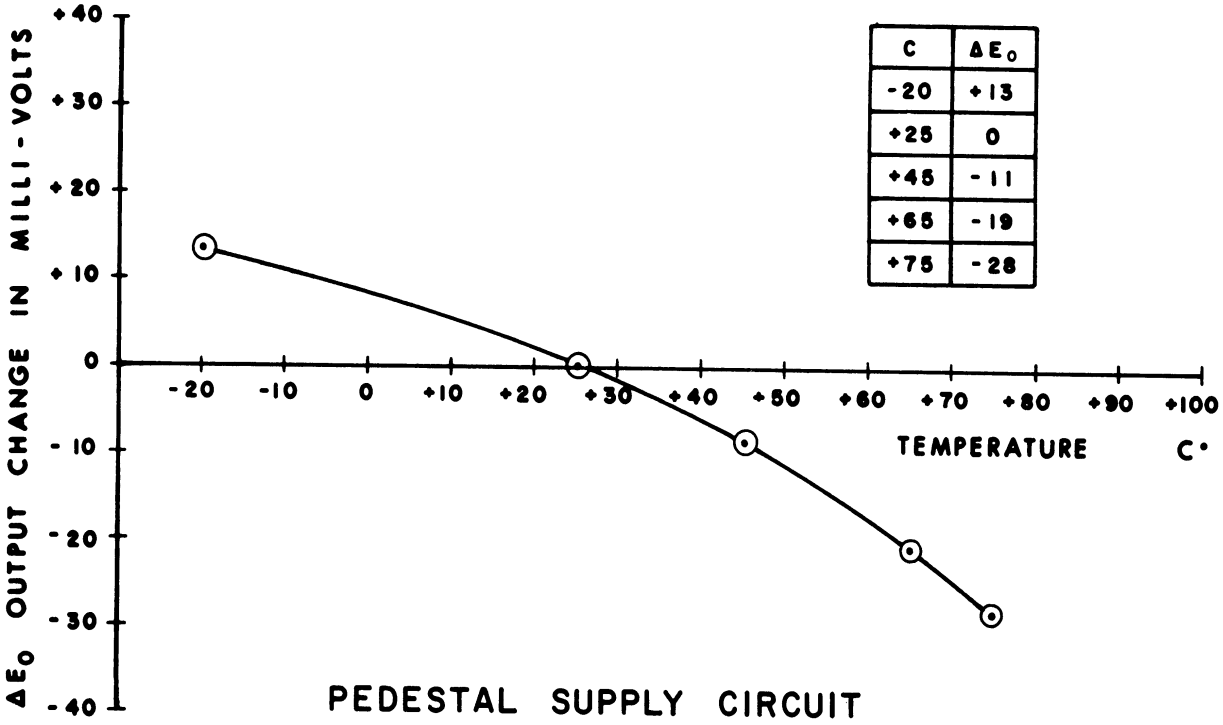

PEDESTAL SUPPLY CIRCUIT
TEMPERATURE CHARACTERISTICS

Fig. 27

ents are modularized in a manner similar to other instrumentation components to simplify payload check-out and testing.

Incoming data to the telemeter is nominally in the form of a variable dc voltage of 0 to +5 v magnitude. Slowly changing signals, such as engineering data, are multiplexed by a mechanically driven commutator resulting in a PAM pulse train that is, in turn, FM modulated in a SCO (Subcarrier Oscillator). The SCO outputs are paralleled forming a complex signal that is then passed through a mixer amplifier to the transmitter where frequency modulation is again performed. The expression PAM/FM/FM is thus defined by the data modulation conditioning processes prior to RF transmission.

A floating power ground system is used in union with a separate signal ground common to the chassis, thus reducing data degradation due to ground loops and cross-talk noise.

Other major considerations in the design, covered in more detail below, include: The RF link; data modulation processes and formats; and the system components used to accomplish the first two.

2.41 RF Link

The design of the transmitting system for the experiment is restricted to a large extent by the size of the vehicle and by the available power source. The weight of a transmitter including power source varies in direct proportion to the RF power output, which means a 3 db RF power increase will double the weight required.

Added weight to the payload will detract from the vehicle's altitude capability, which in the case of the Pitot-Static Probe configuration amounts to a loss of approximately 1 km/lb. The transmitter must be capable, however, of generating sufficient radio frequency power to allow reliable ground reception of the data. With these facts in mind, the minimum RF power requirements for the experiment are examined in detail below.

The design of the RF link for the experiment is dependent upon many nebulous factors, some uncontrollable, that add to the complexity of the problem. An example being that ground station parameters are not usually known since the experiment will be launched in a variety of locations using existing facilities.

A practical or beginning approach to the problem is to assume all "worst case" conditions that will take into account the unknowns and then include a reasonable margin of safety in the design.

The first step in the analysis is to establish a relation between the transmitted power and the signal power needed at the receiver. This can be done

somewhat intuitively by summing all of the factors that influence the signal. It is convenient to think of the radiation as occurring between isotropic antennas, and referencing all terms in decibels (db) in order to simplify calculations. The following relation is established by tracing the signal route from transmitter to receiver:

$$P_T + G_T + T_L + G_R = S/N_{db} + N_t \qquad (6)$$

where: P_T is transmitted power required;

G_T is the transmitting antenna gain over an isotropic reference;

T_L equals the free space transmission loss;

G_R refers to receiving antenna gain over an isotropic reference;

S/N_{db} is the signal to noise ratio desired at input to the receiver; and

N_t is the total noise power referred to receiver input.

The transmission loss is determined using the formula for free space transmission,[9,10] which is written:

$$P_r/P_t = A_r A_t/d^2\lambda^2 \qquad (7)$$

where P_r and P_t are, respectively, the received and transmitted powers; A_r and A_t are, respectively, the effective areas of the receiver and transmitter antennas, which for an isotropic antenna is $\lambda^2/4\pi$; d is the length of transmission and λ is the radio wave length.

The relation may be rewritten for isotropic antennas as:

$$P_r/P_t = (\frac{\lambda}{4\pi})^2/d^2 \qquad (8)$$

which after conversion to decibel form is written:

$$T_{loss} = 10 \log_{10} P_r/P_t = 20 \log_{10} \lambda - 20 \log_{10} 4\pi - 20 \log_{10} d \qquad (9)$$

Assuming a transmission distance of 150 miles (241 km) at a frequency of 231.4 mc (λ = 1.3 m,) the free space attenuation is approximately -130 db.

The noise power present at the input of a receiver is essentially Johnson noise and is found by the relation:

$$N = KTB \tag{10}$$

where N is the noise power in watts;

k is Boltzman's constant;

T is the noise temperature, °K; and

B is the receiver bandwidth, cps.

The total system noise must include the effect of noise generated in the receiver itself, the amount of which is a function of the receivers "noise figure."

The noise figure is defined as the S/N ratio at the input of the receiver, divided by the S/N ratio at the output and expressed in decibels. The total system noise referred to the input of the receiver is then:

$$N_t = 10 \log_{10} N + NF \tag{11}$$

which is approximately $N_t = 147$ dbw + NF at a temperature of 25°C using a receiver bandwidth of 500 kc.

Referring now to Eq. (6), and using the following assumptions:

Input power to receiver:	$S/N_{db} = 3$ db
Receiver noise figure:	NF = 10 db (5 db is reasonable)
Transmitter Antenna Gain:	$G_T = 0$ db (isotropic)
Receiver Antenna Gain:	$G_R = 8$ db (using six turn helicals).

The required transmitter power is calculated as $P_t = -12$ dbw or 60 mw.

This figure then represents the minimum RF power required for reliable data reception under the conditions stated. The conclusion of the design then rests with the selection of a reasonable safety factor. Again, many parameters become involved that are not and probably cannot be determined. Additional noise may enter the picture, antenna response fluctuations may occur due to the spinning vehicle, the system may experience some deterioration due to battery-voltage decline or other unknown factors. Earlier Pitot-Static flights used a nominal 2-w transmitter which certainly proved more than adequate. Subsequent flights have used a 500 mw transmitter which has proven to be a near optimum choice. Decreasing the size further will not effect the payload size or weight nor will it decrease the cost noticeably.

It should be noted here also that higher transmitter powers than are actually needed during flight are beneficial during ground check-out of the payload where "line of sight" transmission between the rocket and ground station may not exist--a condition certainly expected at some remote launching sites.

An examination of past Pitot-Static flights indicates that RF signal reception is good except during the latter phase of the flights where drop outs do occur, usually due to tumbling.

2.42 Data Formats

Data inputs to telemeter are either multiplexed (time shared) or sent directly to subcarrier oscillators. From the standpoint of maximum information content in minimum bandwidth, PAM is considered the best modulation method to use.[10] Multiplexing is possible, and therefore desirable whenever interruption of the data does not destroy its content. Direct channels are used for continuous or analog data inputs, which for the most part include fast changing or unpredictable data.

A block diagram of the Pitot-Static Probe data distribution through telemeter are shown in Fig. 28 and described below. PAM data formats are found in Table IV and V. Normal system requirements are for two or three SCO's to be used with a single two-channel commutator.

The IRIG section of the commutator (J2) supplies twenty-eight data channels of which five are used for calibration voltages. The frame sync pulse carries the 5-v calibration. Seven channels are assigned to each Densatron output and the remaining nine channels carry engineering data.

The PAM commutator output is sent to the DOVAP telemeter, in addition to modulating a SCO in the regular telemeter system; thus providing two separate RF links for a major share of the experiment's data.

The remaining commutator section (J1) has 30 data channels. Two are used for 0- and 5-v calibration voltages; the rest are divided between two magnetometers. The output usually modulates a channel 10 (10.5 kc) SCO.

The remaining SCO channel is used to transmit solar aspect information. The shift register output is a digital representation of the solar aspect data that also includes earth cell information. A command eye, associated with the optics, "tells" the shift register to "store" the instant it "sees" the sun, and to "read-out" a short time later. The earth cell output shifts the dc level of the pulsed sun information during the time the earth telescope views the earth. The resultant aspect data, being unpredictable in time, requires exclusive use of a SCO--usually an IRIG channel A (22 kc).

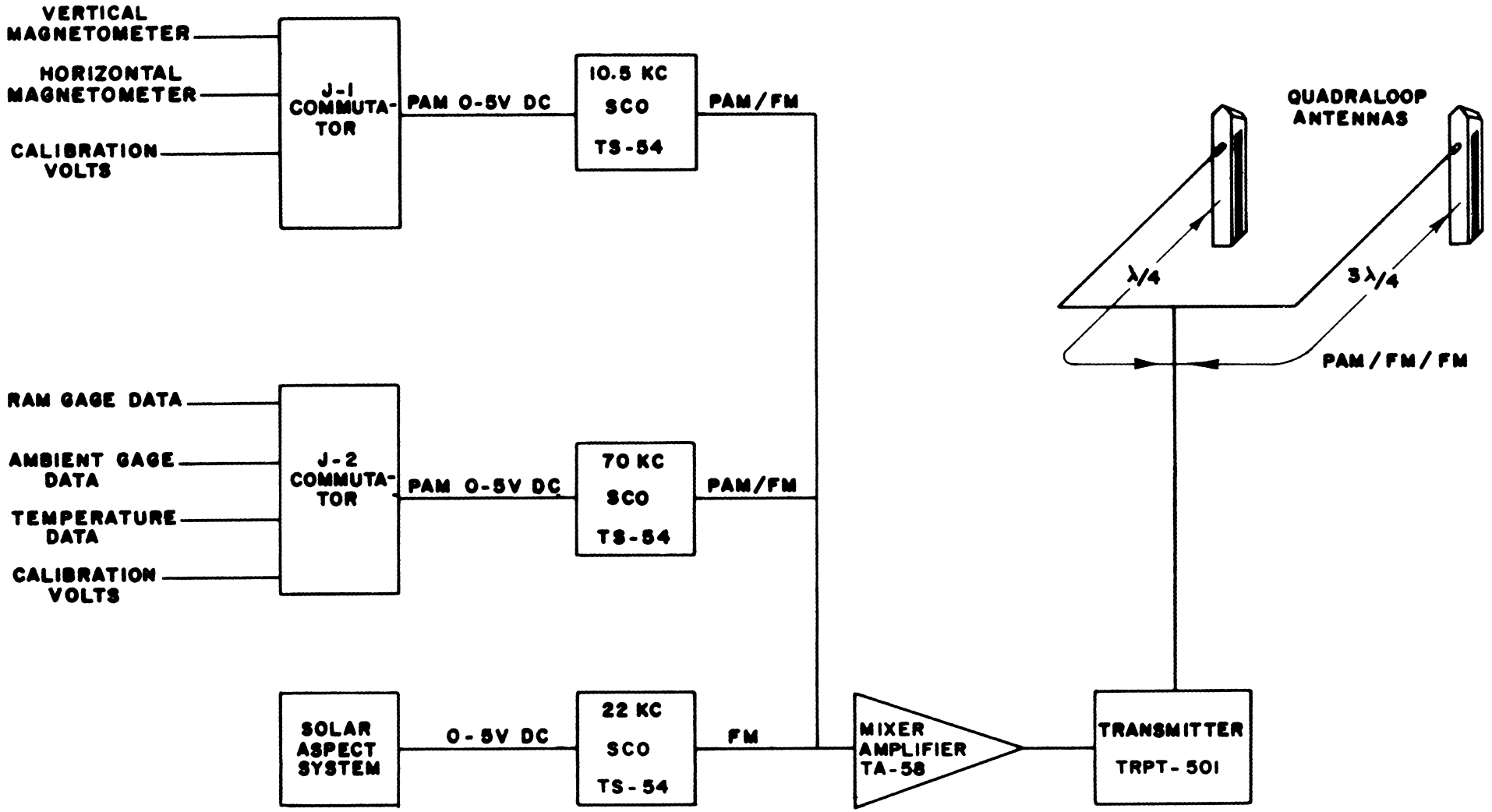

TELEMETRY SYSTEM DATA FLOW DIAGRAM

Fig. 28

TABLE IV

PAM CHANNEL ASSIGNMENT

Channel Number	
1	Ram gage output
2	Ambient gage output
3	Ram gage amplifier range monitor
4	Ambient gage amplifier range monitor
5	Nose cone temperature
6	Ram gage out
7	Ambient gage out
8	Ram gage electronics temperature
9	Ambient gage electronics temperature
10	Ram gage output
11	Ambient gage output
12	Ram gage temperature
13	Ambient gage temperature
14	Ram gage output
15	Ambient gage output
16	Nose cone temperature
17	Battery voltage monitor
18	Ram gage output
19	0-v calibration
20	Ambient gage output
21	1-v calibration
22	Ram gage output
23	2-v calibration
24	Ambient gage output
25	3-v calibration
26	Ram gage output
27	4-v calibration
28	Ambient gage output
29	5-v calibration
30	5-v calibration

TABLE V

MAGNETOMETER CHANNEL ASSIGNMENTS

Channel Number	Function
1	0-v calibration
2	5-v calibration
3 - 16	Vertical sensor magnetometer
17 - 30	Horizontal sensor magnetometer

A representation of the data is displayed in Fig. 29, which is a photographed portion of a real time paper recording for NASA 14.251. Time codes and the ground receiver AGC characteristic curve showing variations in received signal strength are included with subcarrier discriminator output data.

Basically, the data formats are as shown in the figure; however, modifications are periodically implemented to optimize the data recovery scheme consistant with updating the instrument.

2.43 System Component Description

2.431 Transmitter Deck

A Vector Manufacturing Model TRPT-501 transmitter, shown fastened to its mounting plate in Fig. 30, was chosen for telemeter because of its small size, stability, rugged construction, and reliability. It may be operated from an unregulated power source and is relatively uneffected by environmental changes. The transmitter will drive a 50-ohm antenna with a nominal 0.5 w of RF power at 10% efficiency. Complete specifications are listed in the Appendix.

The transmitter deck is assembled in the system at the base of the instrumentation column (Fig. 12) where the transmitter actually protrudes up into the center of the battery pack (Fig. 31). Except for the RF output cable, which passes through the foamed section of the battery pack, the lead connections are made at the bottom of deck through a nine-pin series DEM cannon connector (Fig. 32). Additionally, signal and power ground systems are tied to each other, and to the transmitter chassis through the connector, thus establishing the instrumentation's true ground point.

2.432 Commutator Deck

A two-section Datametrics Commutator, Model 989 (Fig. 33 and Fig. 34), performs the telemeter multiplexing. One section, designated J1, has 30 MMB (make before break) contracts while the other section (J2) uses a standard IRIG format with 28-data channels of 60% duty cycle. A pedestal voltage (negative 0.7 v) inserted between each data channel provides channel syncronization for automatic decommutation. The frame rate is 2.5 rps, and the unit requires 1 w at 28 v to operate.

2.433 SCO Deck

The combination of a Vector Model TA-58 mixer amplifier with Vector Model TS-54 SCO's complete the telemeter system. The units are mounted on a deck as shown in Fig. 36. The experiment normally used three SCO's; however, the deck can accommodate up to five SCO's in the event future data requirements

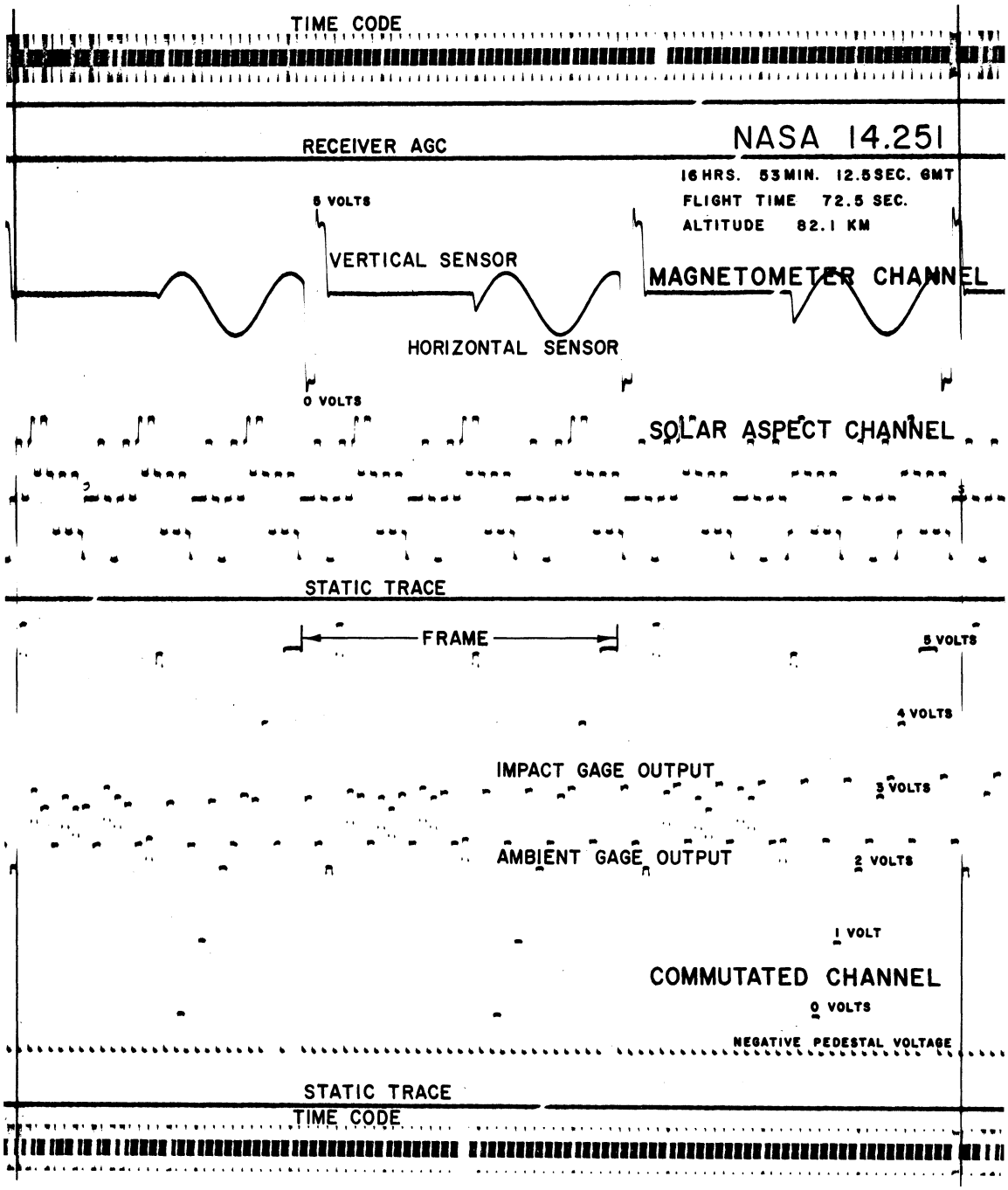
TIME CODE
RECEIVER AGC
NASA 14.251
16 HRS. 53 MIN. 12.5 SEC. GMT
FLIGHT TIME 72.5 SEC.
ALTITUDE 82.1 KM
5 VOLTS
VERTICAL SENSOR
MAGNETOMETER CHANNEL
HORIZONTAL SENSOR
0 VOLTS
SOLAR ASPECT CHANNEL
STATIC TRACE
FRAME
5 VOLTS
4 VOLTS
IMPACT GAGE OUTPUT
3 VOLTS
AMBIENT GAGE OUTPUT
2 VOLTS
1 VOLT
COMMUTATED CHANNEL
0 VOLTS
NEGATIVE PEDESTAL VOLTAGE
STATIC TRACE
TIME CODE

Fig. 29

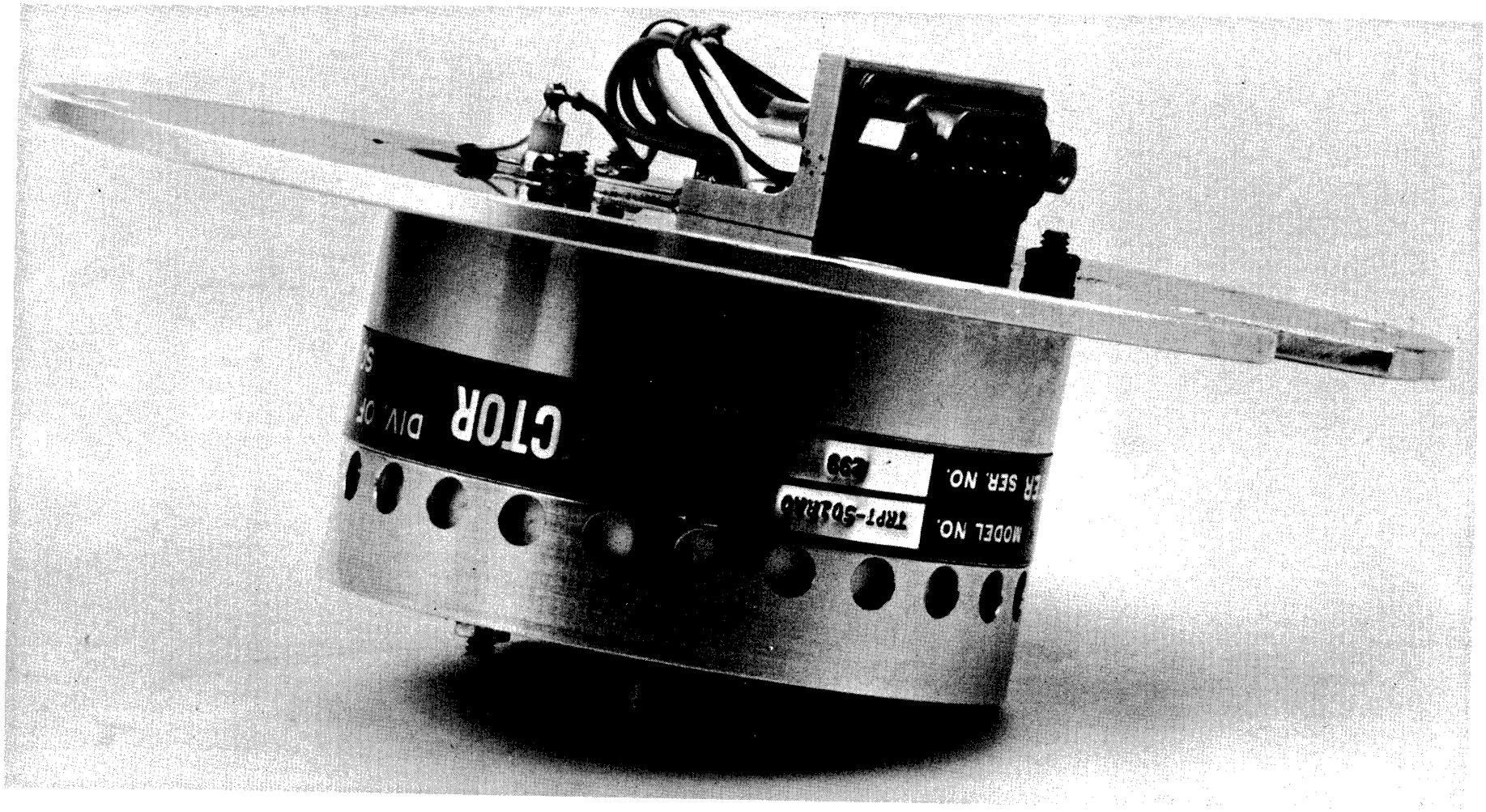

Fig. 30. Transmitter deck—side view.

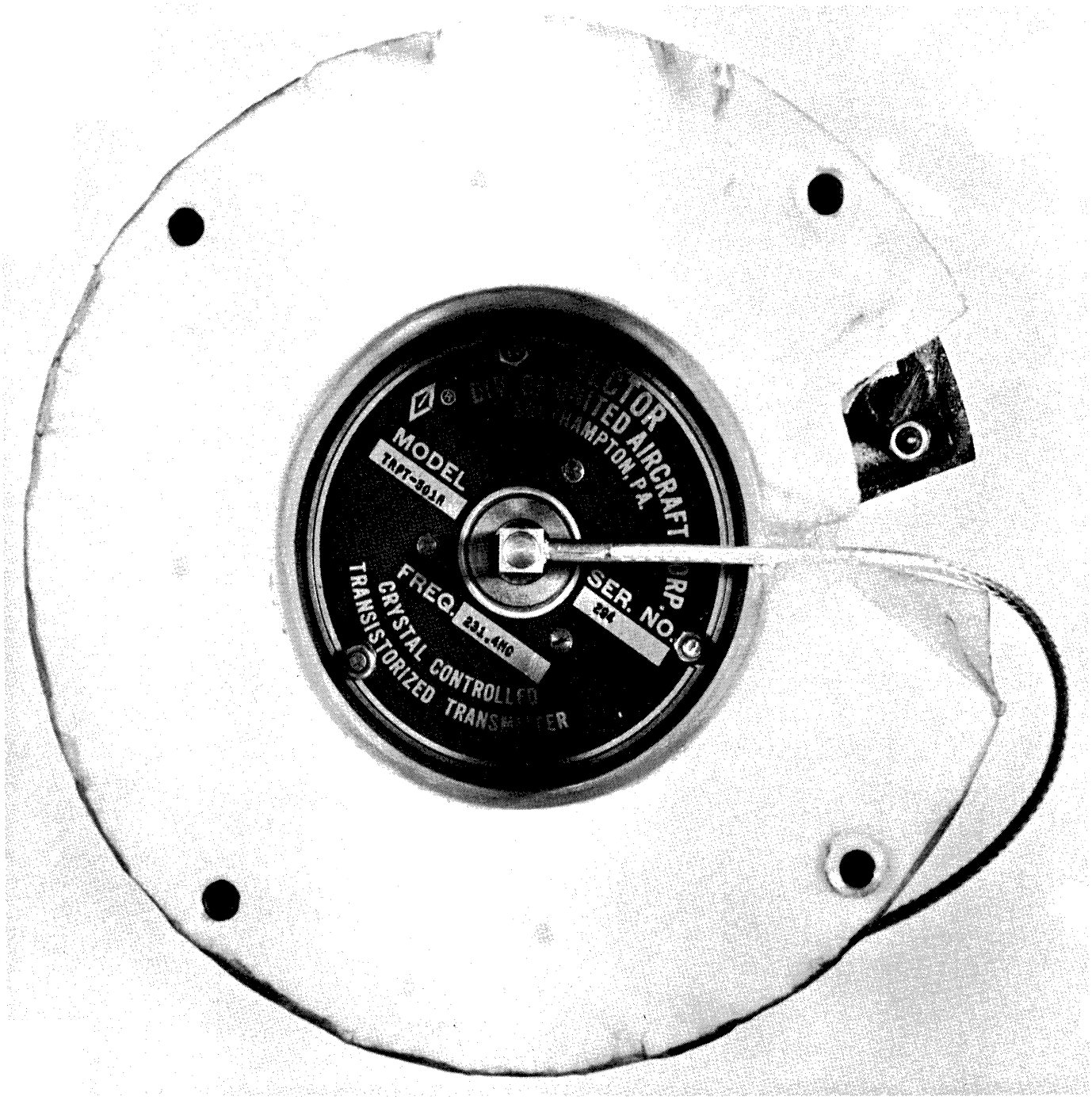

Fig. 31. Transmitter deck and battery module—top view.

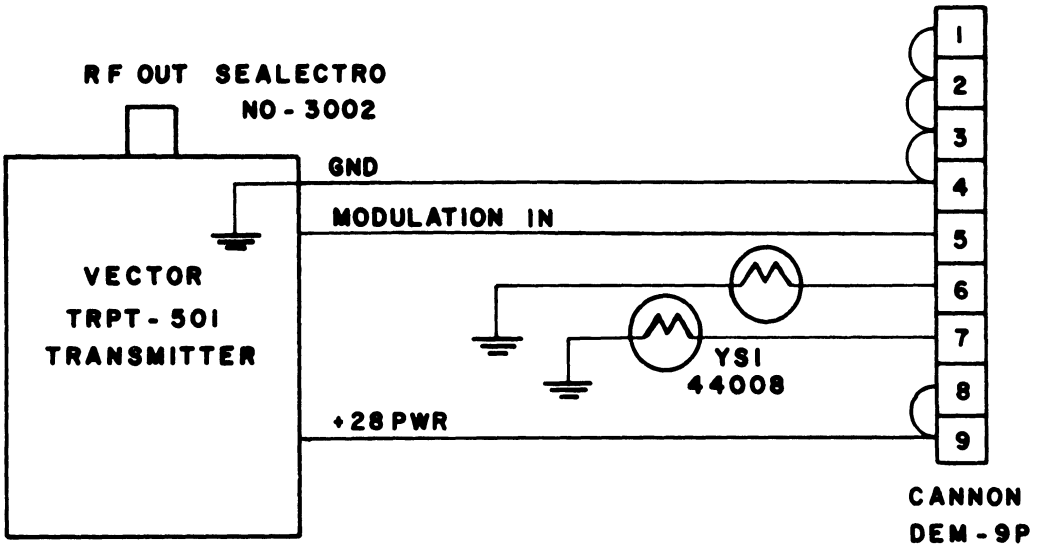

TRANSMITTER DECK WIRING

Fig. 32

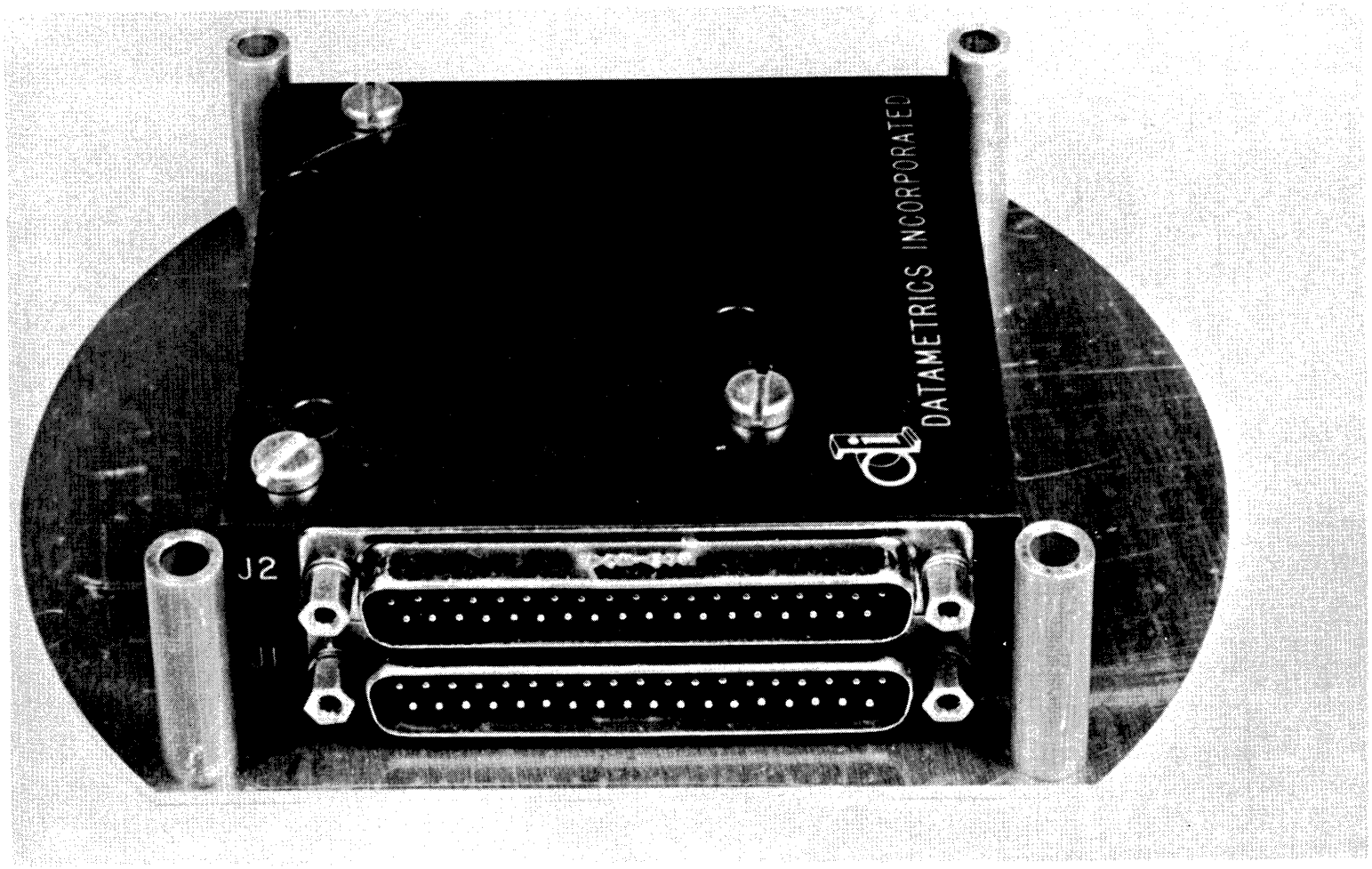

Fig. 33. Commutator deck—front view.

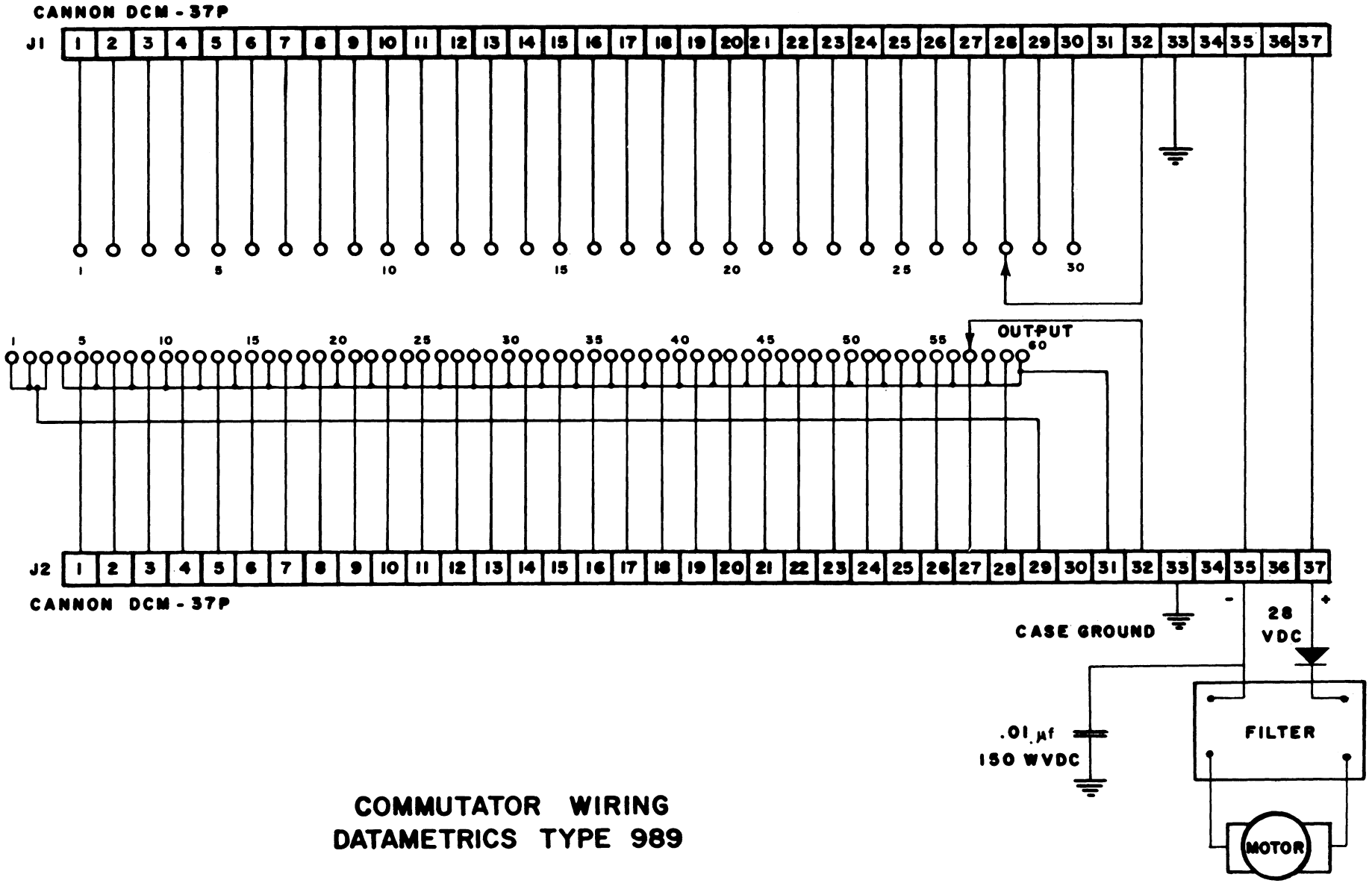

COMMUTATOR WIRING
DATAMETRICS TYPE 989

Fig. 34

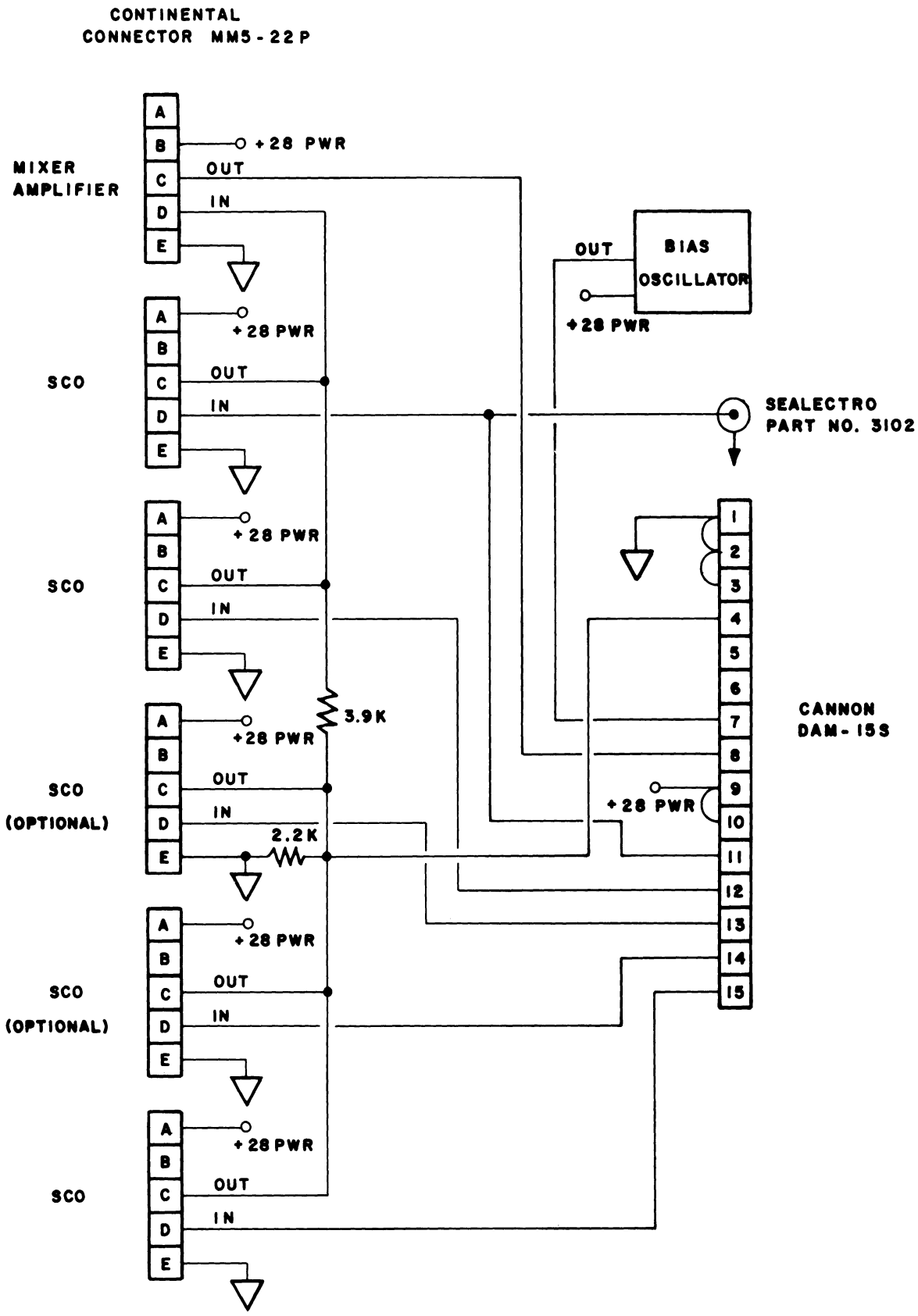

SCO DECK WIRING

Fig. 35

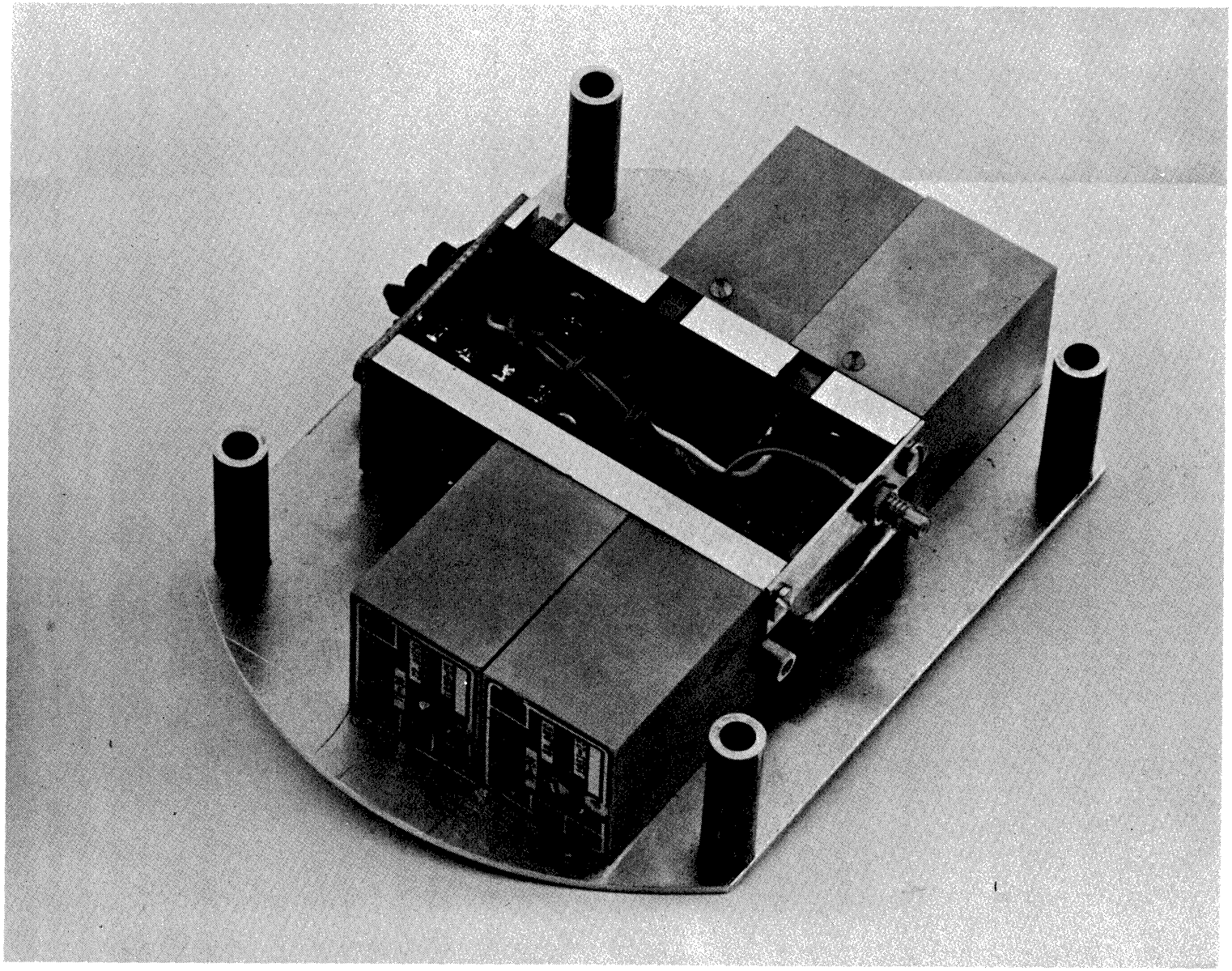

Fig. 36. SCO deck.

increase. The deck wiring is shown in Fig. 35.

The TS-54 SCO has an input impedance greater than 500 k, a linearity better than 0.1%, and an open circuit output of 2 v RMS.

The mixer amplifier is used for mixing or "summing" the SCO outputs into a single complex signal in addition to increasing the output levels sufficiently for proper transmitter modulation. The TA-58 has an adjustable voltage gain from 0 to 20 and a frequency response within 0.5 db from 20 cps to 100 kc. The gain is adjusted at the lowest required level to minimize distortion.

Also located on the SCO deck is the commutator pedestal bias oscillator explained in an earlier section (see Section 2.354).

2.434 Telemetry Antenna

The antenna system uses a pair of model 2.003 quadraloop antennas,[11] mounted on the skins covering the instrumentation section (Fig. 37A). These antennas are designed specifically for high spin rate vehicles, and with a low profile to keep aerodynamic drag forces low.

A phasing harness (Fig. 28) is used to feed the antennas in parallel, 180° out of phase, which gives good fore and aft coverage. The antenna driving point impedance is selected near 100 ohms; and by using a one-half wavelength feed line in parallel with a one wave length feed line made of 50-ohm transmission cable, the combination will match a 50-ohm transmitter. As might be expected, the impedance is critical with frequency (a typical curve is shown in Fig. 37B) so that transmitters and antennas must be compatible.

The radiation pattern, using the right circular component, is that of a toroid whose axis is normal to the vehicle axis. The VSWR is generally 1.5:1 or less in the range of interest.

2.5 GROUND CONTROL SYSTEM

Payload development was paralleled by the design of a ground control system that is needed to provide remote payload control and monitor functions. Divided into three sections, the entire system includes the control deck mounted in the instrumentation section and explained in an earlier section; the umbilical system: and a specially designed ground control console. For the most part, design objectives are similar to those of flight instrumentation with reliability and portability being major considerations. The main function of the system is, of course, to activate the payload; however, additional features include provisions for external power operation and battery charging. The finished design utilizes a step-by-step turn on procedure that, in effect, automatically checks system operation without relying on operator decisions and without jeopardizing payload circuits. Other considerations in the design

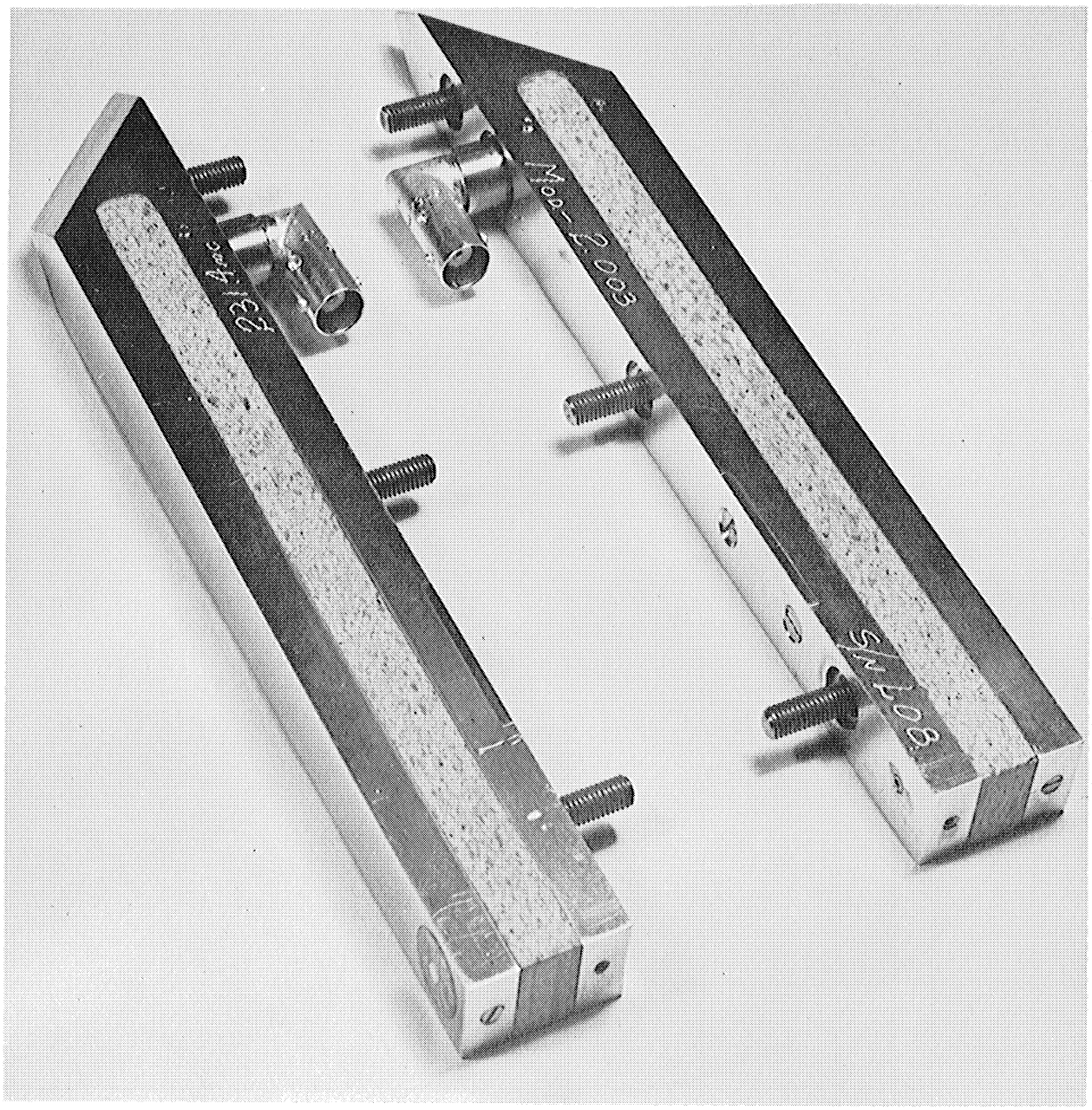

Fig. 37A. Model 2.003 telemetry antennas.

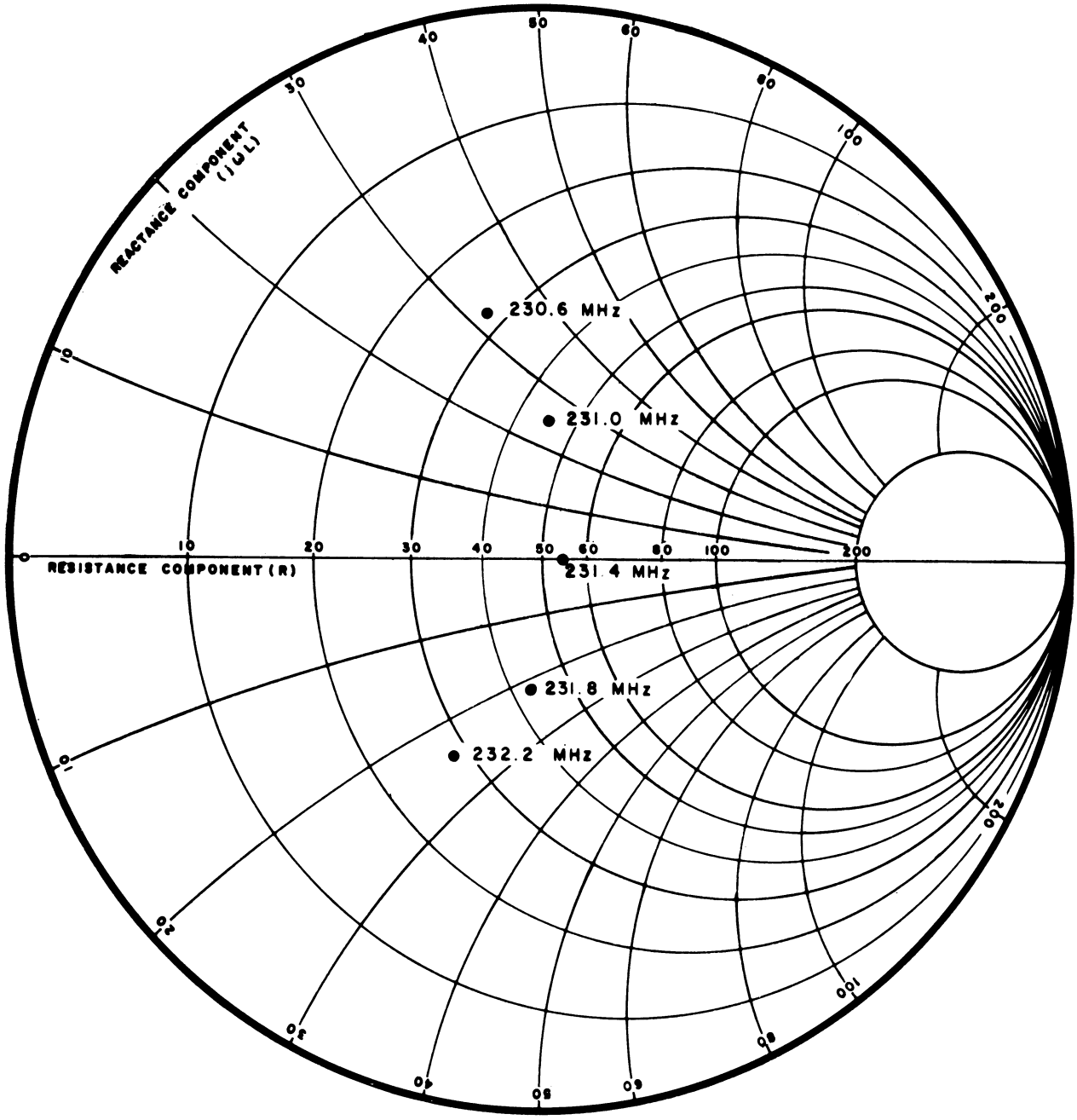

IMPEDANCE / FREQUENCY
FOR MODEL 2.003
QUADRALOOP TELEMETRY ANTENNAS

Fig. 37B

are covered below.

2.51 Umbilical System

A 12-conductor pull-away system was somewhat arbitrarily selected as a compromise between using a large plug and cable capable of accommodating all of the required control functions or using a smaller cable and plug that are less bulky and suited more for pull-away operations.

By using Ledex programmers, the lead availability is in effect multiplied, which allows use of the latter system.

Because it is desirable to keep the operation of the main payload and DOVAP instrumentation isolated and independent of one another, a separate 8-conductor ground control cable is used for DOVAP.

Each ground control cable to the vehicle is wired to a Jones plug that mates to a female Jones plug mounted in the instrumentation section. The Jones plugs are particularly useful for this application because they have low contact resistance and they can be easily pulled apart without jamming.

Control of payload functions and DOVAP instrumentation is possible through the pull-away cables until actual launch time when motion of the vehicle initiates a so called "fly away" umbilical release. The system is simple to use and requires no special equipment other than a few weights to anchor the cable to the ground behind the launcher. The principal of operation is explained as follows using Fig. 38 reference.

Consider first, that the system is in a static condition just prior to release. At this time, the cable is tied securely to the ground at point A and is fixed at point B. The impending movement of the vehicle imparts a force F1, at point B which acts in the direction of motion. This force may be resolved into two components, F2 acting along the cable axis, and F3 which is directed up and away from the vehicle. Since the cable cannot support bending, the force F3 must be located at point B.

Due to the cables restriction, a force F4 exists which is opposite to F2, whereby the effects of each force are cancelled leaving only the resultant force F3. Upon release, point B on the cable is accelerated in the direction of F3 along an arc described by the line BC which is the desired result.

In actual practice, the cable is taped at various intervals along the length of the Apache motor housing thereby creating a point "B" at each tape point, resulting in a whipping action that carries the plug and cable up and away from the rocket and exhaust gasses.

All indications from past flights are that the system has worked very

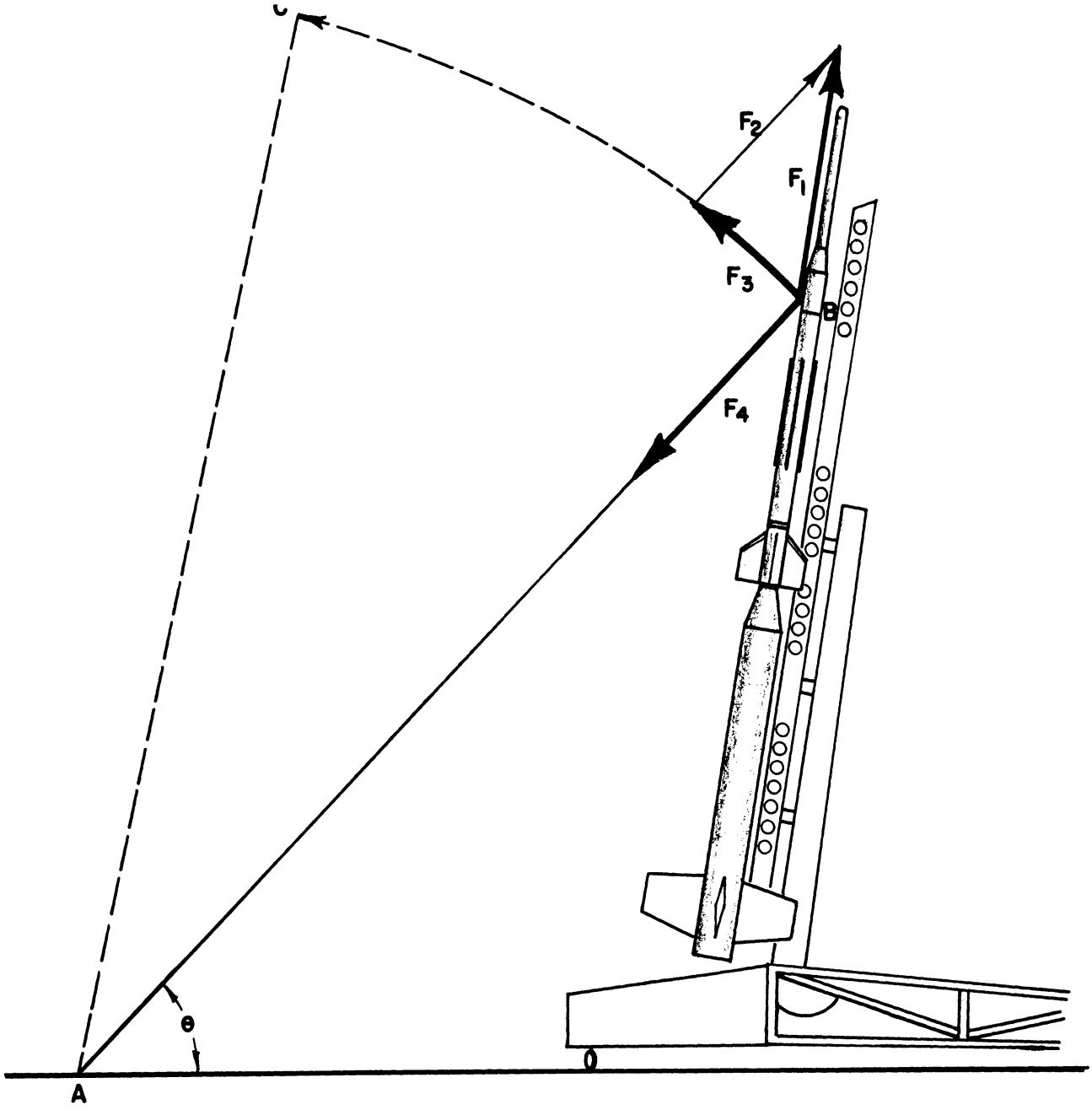

UMBILICAL FLY AWAY RELEASE SYSTEM

Fig. 38

well. Cables and plugs are generally left undamaged to the point of being reusable.

2.52 Control Console

A functional block diagram of the control console is shown in Fig. 39. Two programming Ledexes, similiar to those located on the control deck described in an earlier section, are used to select the proper control or monitor circuits inside the console and direct them through the pull-away cable to the payload. Each control console Ledex is synchronized to a "companion Ledex" mounted on the payload control deck which, as explained earlier, then directs the pull-away leads to proper circuits to be controlled or monitored. For example, when the instrumentation Ledex is synchronized to the payload telemeter Ledex in the OFF position, there are no circuits connected to the pull-away leads either at the payload or at the control console. In the next position, GAGE EXT, the power supply output from the control console is connected to the appropriate pull-away leads. Then, on the payload side of the pull-away cable, the telemeter Ledex directs the power supply leads to the gage circuits. Each succeeding Ledex position correspondingly selects the proper circuits or meters as requested by the payload telemeter Ledex.

A single push button switch simultaneously switches both the control console Ledex and its companion Ledex in the payload. To reduce the possibility of a Ledex not switching, each Ledex is driven from a separate 500 MFD capacitive power source.

Control console Ledex positions are displayed by indicator lamps driven from switch wafers D1 and D5. Payload Ledex positions are determined using the range resistors mounted on wafers D4 and D6. Voltages derived by constant 2 ma current sources flowing through these resistors and similiar circuits on the payload Ledex switch wafers, are compared in error amplifiers. A different voltage greater then 1 v (indicating the Ledexes are out of step) will activate a relay (SW-6 or SW-8) which in turn causes the push button switch (either PB1 or PB2, whichever the case may be) to glow red by turning on L2 or L4. Normally, when the Ledexes are in step, the push buttons glow green by the lamps L1 and L3.

Should the case arise where the Ledexes are out of step, the payload Ledexes can be disconnected by SW-5 (or SW-7) from the stepper switch PB 1 (or PB 2) thereby allowing the control console Ledex to "catch-up" to the payload Ledex.

The payload operational turn-on sequence begins with the telemeter Ledex in the "OFF" position while the gage Ledex is usually left in the "FLY" position. When the telemeter Ledex is switched to "GAGE EXT" position, the Densatrons, the calibration timer, and the calibration regulator circuits can be operated on external power. A manually operated switch (SW-1) connects the

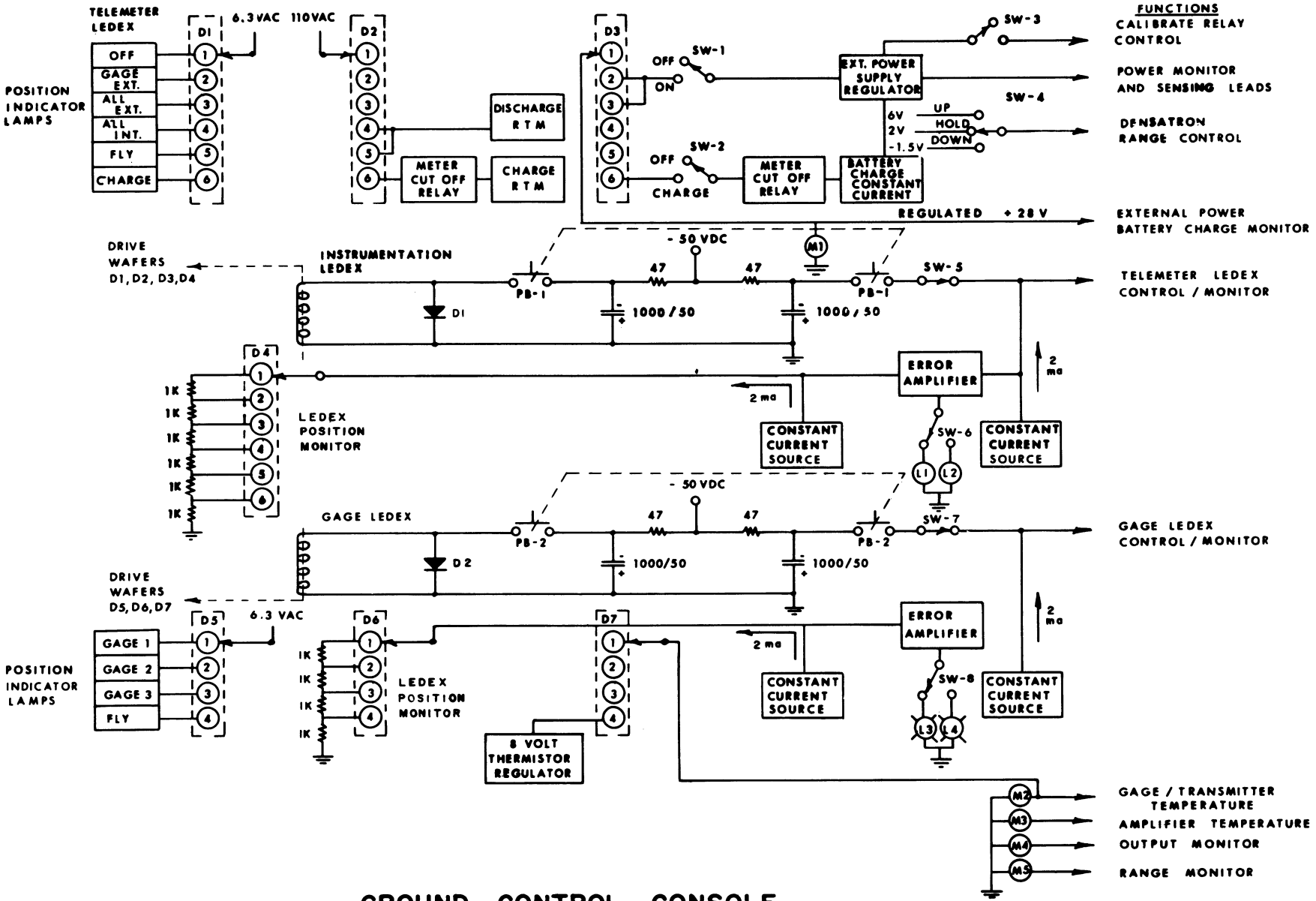

GROUND CONTROL CONSOLE

Fig. 39

"external power supply regulator" output to the pull away. Additional power leads, separate from the current carrying leads, are used for "sensing" the voltage at the payload thereby reducing the effect of line voltage drop on the voltage appearing at the payload. Diodes between the sense leads and the output leads at the control console, clamp the maximum available output voltage at a safe level in the event the sensing leads are disconnected.

The gage Ledex, operating independently from the telemeter Ledex, can be used to select any one of three Densatrons for monitor or control purposes irrespective of the telemeter Ledex position. The Densatron output, amplifier range, amplifier temperature, and gage temperature are monitored using meters M2 through M5, while a three-position switch, SW-4, is used to select one of three required range control voltages.

The calibrate relay control switch (SW-3) is tied in parallel to each Densatron and may be activated in any position including the "FLY" position.

When the telemeter Ledex is switched to "ALL EXTERNAL," the complete payload is operating on external power. The next position is used to switch from external power to internal power--again, all circuits are operating. At this time the internal battery voltage is monitored at the control console, and a RTM (running time meter) is turned on to record the battery discharge time. The next step in the turn-on procedure, puts all circuits in a flight condition and removes all internal payload voltages from the umbilical plug. The "discharge RTM" is still activated. The following position, turns off all of the instrumentation, and puts the payload internal batteries in a position for charging. The output of a 100 ma constant current source can be manually connected to the batteries by the switch SW-2. When a predetermined voltage level (usually 38 v) is measured by the meter M1, the meter cut off relay automatically disconnects the charge circuit from the batteries. A separate "charge RTM" records the battery charge time.

The control console, pictured in Fig. 40, is mechanically built to withstand the rough handling environment often time encountered during shipping and operating the equipment at remote launching sites. The unit is built in two sections which are rack-mounted with shock mounts in the shipping container. By removing the front and back panels of the shipping container, the console is ready for operation by merely plugging in the appropriate cables.

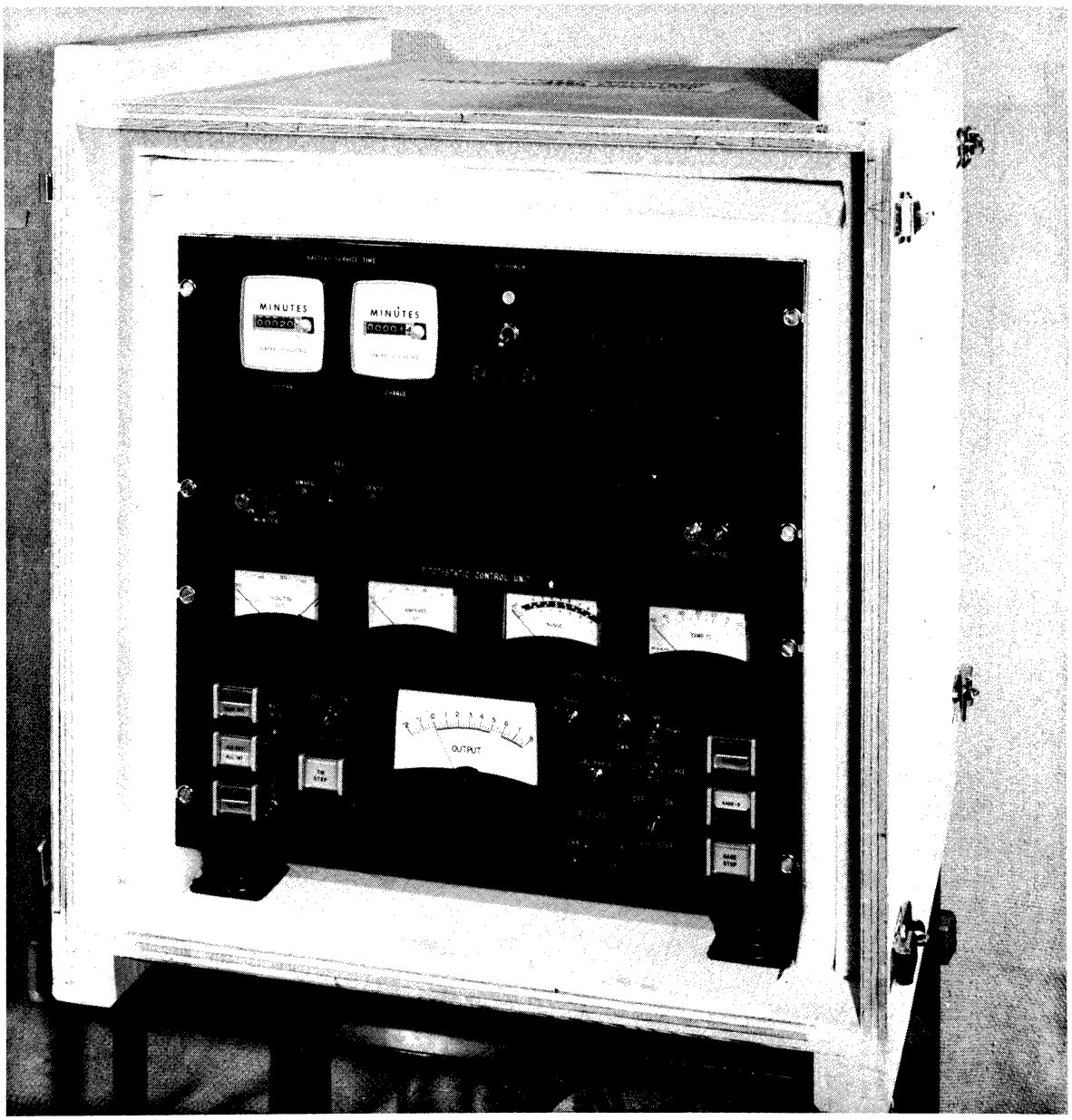

Fig. 40. Ground control console—front view.

3. MECHANICAL DESIGN

The complete nose cone is fabricated in three sections for housing the Densatrons, telemeter instrumentation, and the DOVAP transponder respectively; and hereafter described as the probe section, the instrumentation section, and the DOVAP section. Each section is independently assembled, both electrically and mechanically, before mating to remaining payload sections (see Figs. 41A, 41B, and 41C).

The basic structure is described starting at the top or forward end of nose cone, then proceeding along its length until reaching the Apache second stage.

The ram pressure orifice and gage chamber are contained in a 3.5-in. diameter hemispherical nose tip (Fig. 42A) that fastens directly to a 30-in. long stainless steel tube (Fig. 42B), which then connects to a stainless steel center section (Fig. 43) that contains the ambient pressure chamber on the forward side, and either a wind gage chamber, or else no chamber at all on the aft side. (A few later model nose cones were modified to include an additional ambient chamber on the aft side.) Proceeding further, the center section then mates to a magnesium casting (Fig. 44), that serves as a transition section between the probe section and the larger diameter of the instrumentation section. Four Unistrut* columns welded to steel rings (Fig. 45) at each end form the instrumentation structure with a mounting platform included between the columns for the instrumentation decks. A second Unistrut section provides space for the DOVAP transponder and connects to the Apache motor coupling adapter. In the final configuration, a pair of rolled aluminum skins enclose each Unistrut section.

The multiple sections of the payload are kept in alignment using dowels and other means explained in detail later, and tight tolerances are maintained between sections to increase strength and rigidity of the structure.

The overall length of the payload is 74.2 in. with a nominal weight of 62 lb including DOVAP and all internal instrumentation. The center of gravity is located 37 in. behind the nose tip. A semi-assembled view of the nose cone including a despin module, but without DOVAP, is shown in Fig. 41B.

3.1 PROBE SECTION ASSEMBLY

Figure 47 shows the probe section assembly as well as individual gage as-

*Unistrut Corporation, Wayne, Michigan.

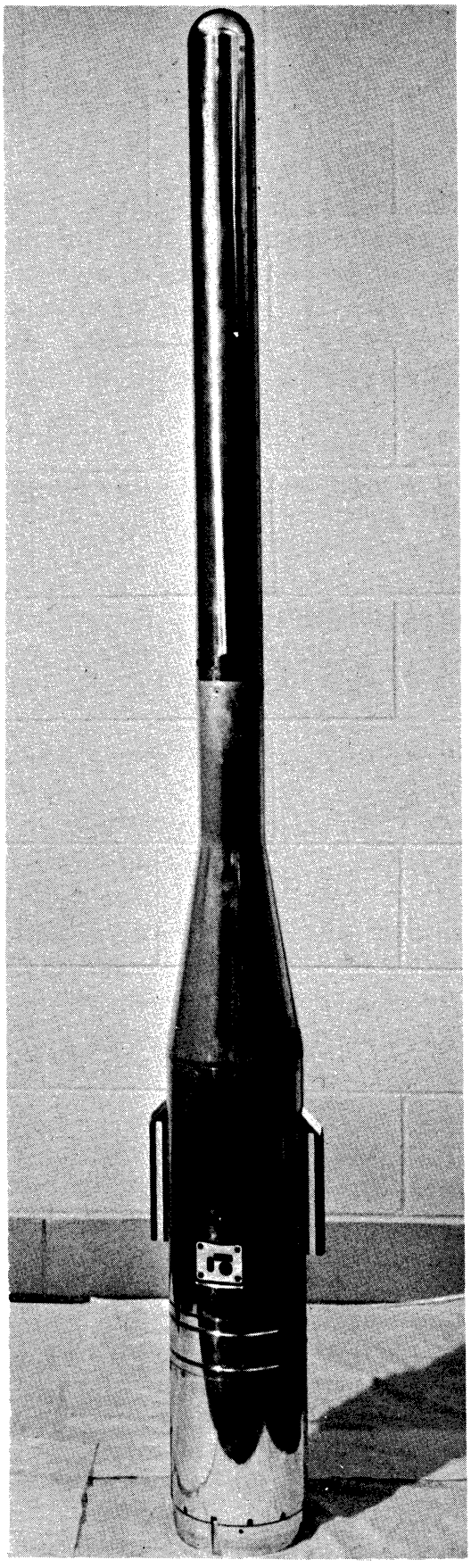

Fig. 41A. Nose cone—rear view.

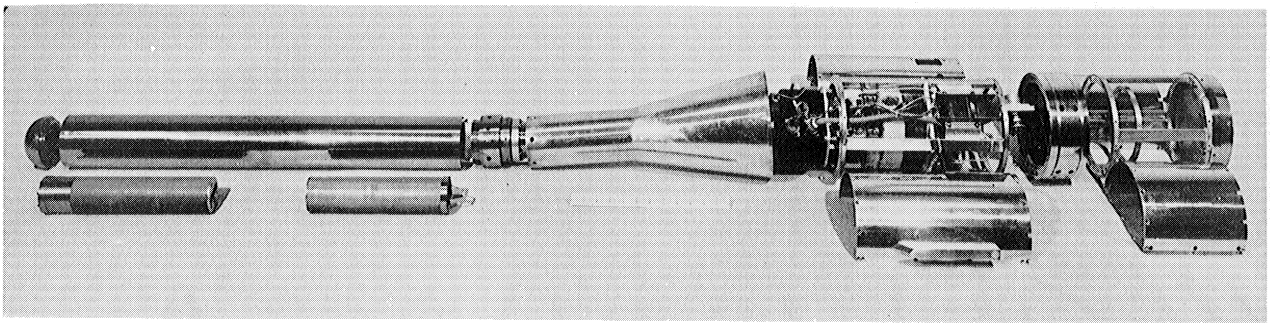

Fig. 41B. Disassembled nose cone.

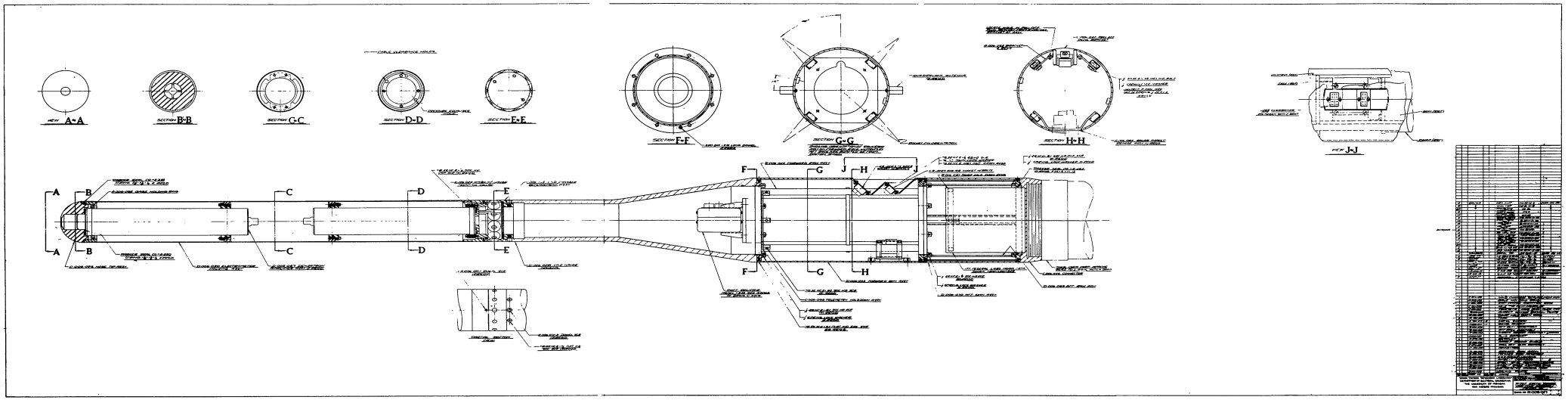
VIEW A-A
SECTION B-B
SECTION C-C
SECTION D-D
SECTION E-E
SECTION F-F
SECTION G-G
SECTION H-H
VIEW J-J
A
B
C
D
E
F
G
H
J

Fig. 41C

Fig. 42A. Nose tip—front view.

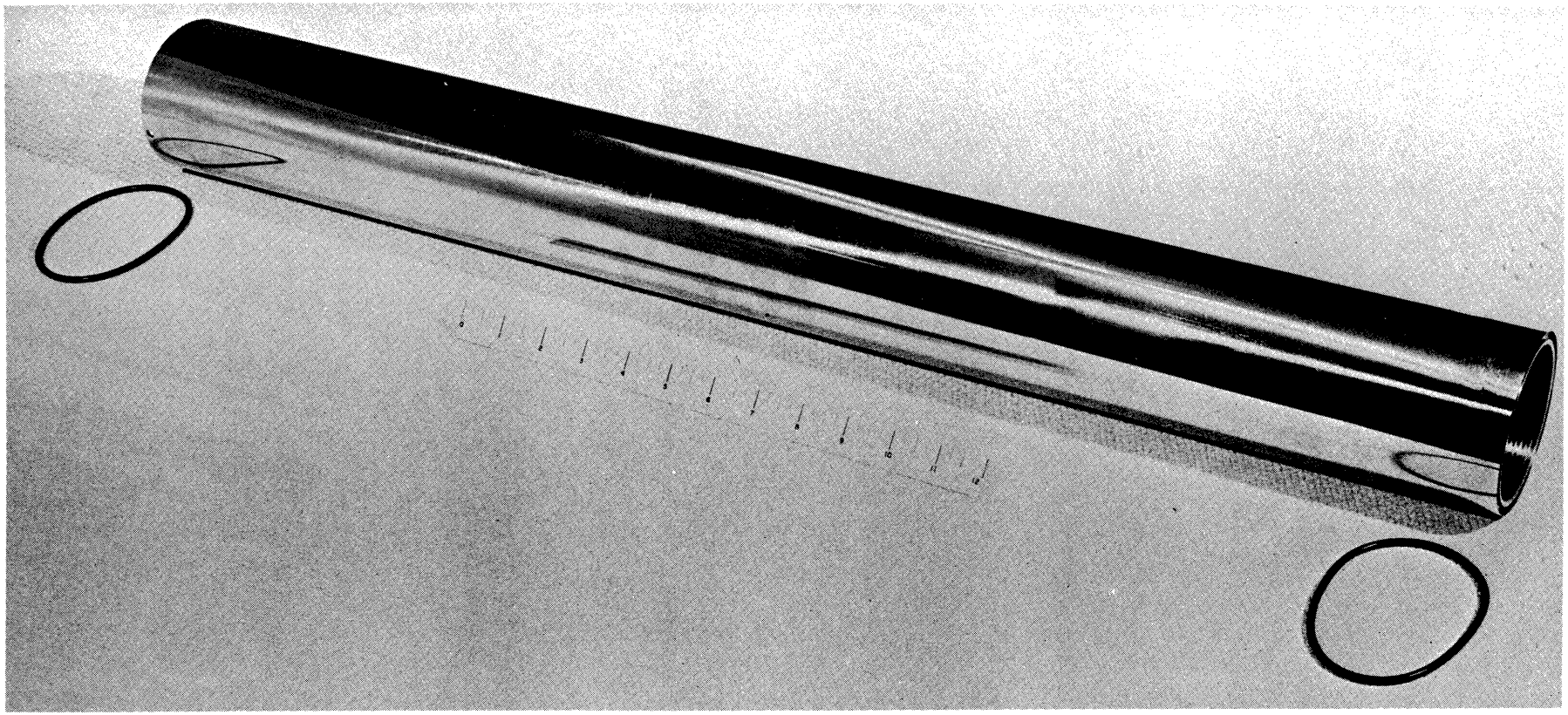

Fig. 42B. Nose tube—side view.

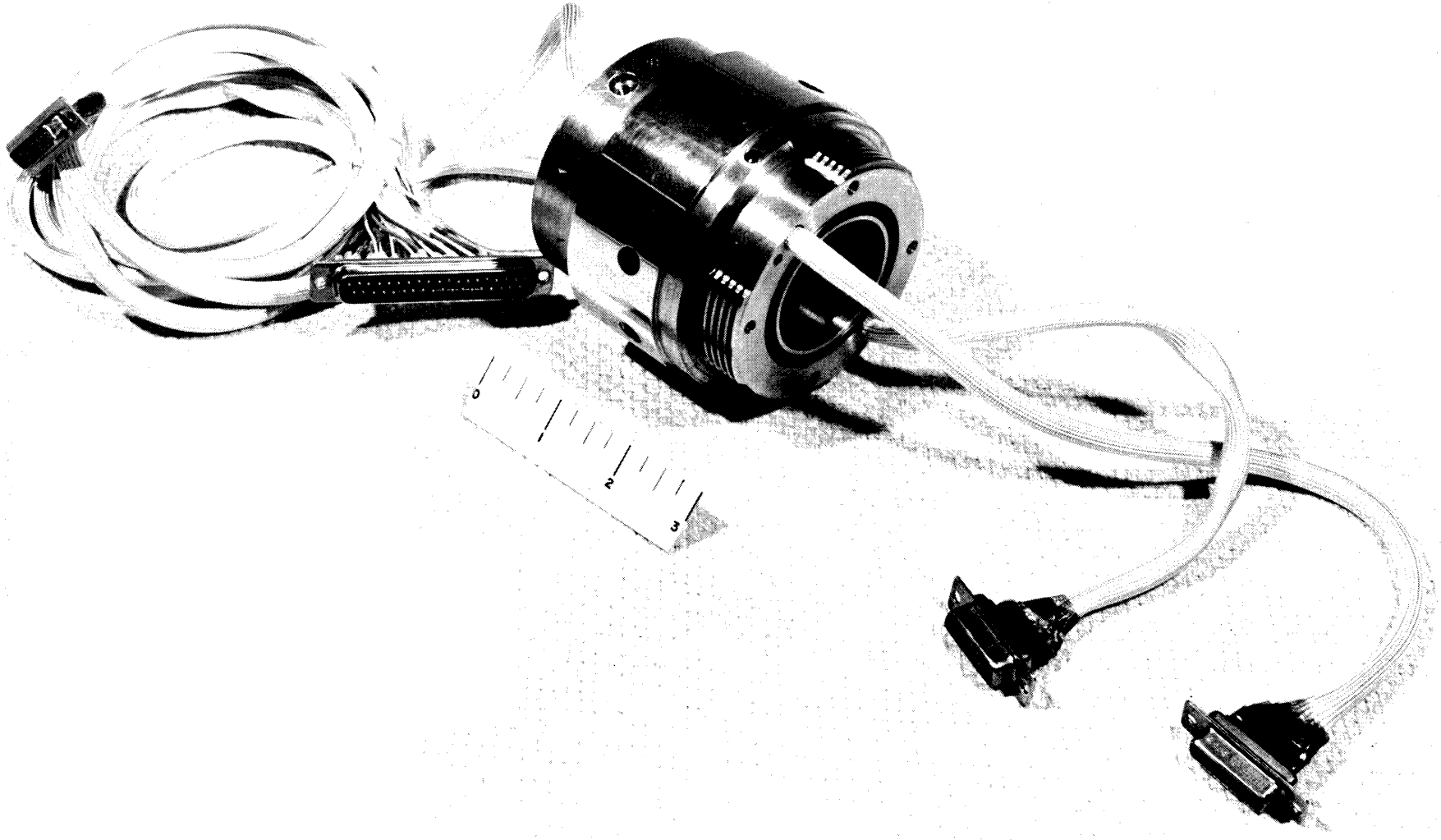

Fig. 43. Nose cone center section.

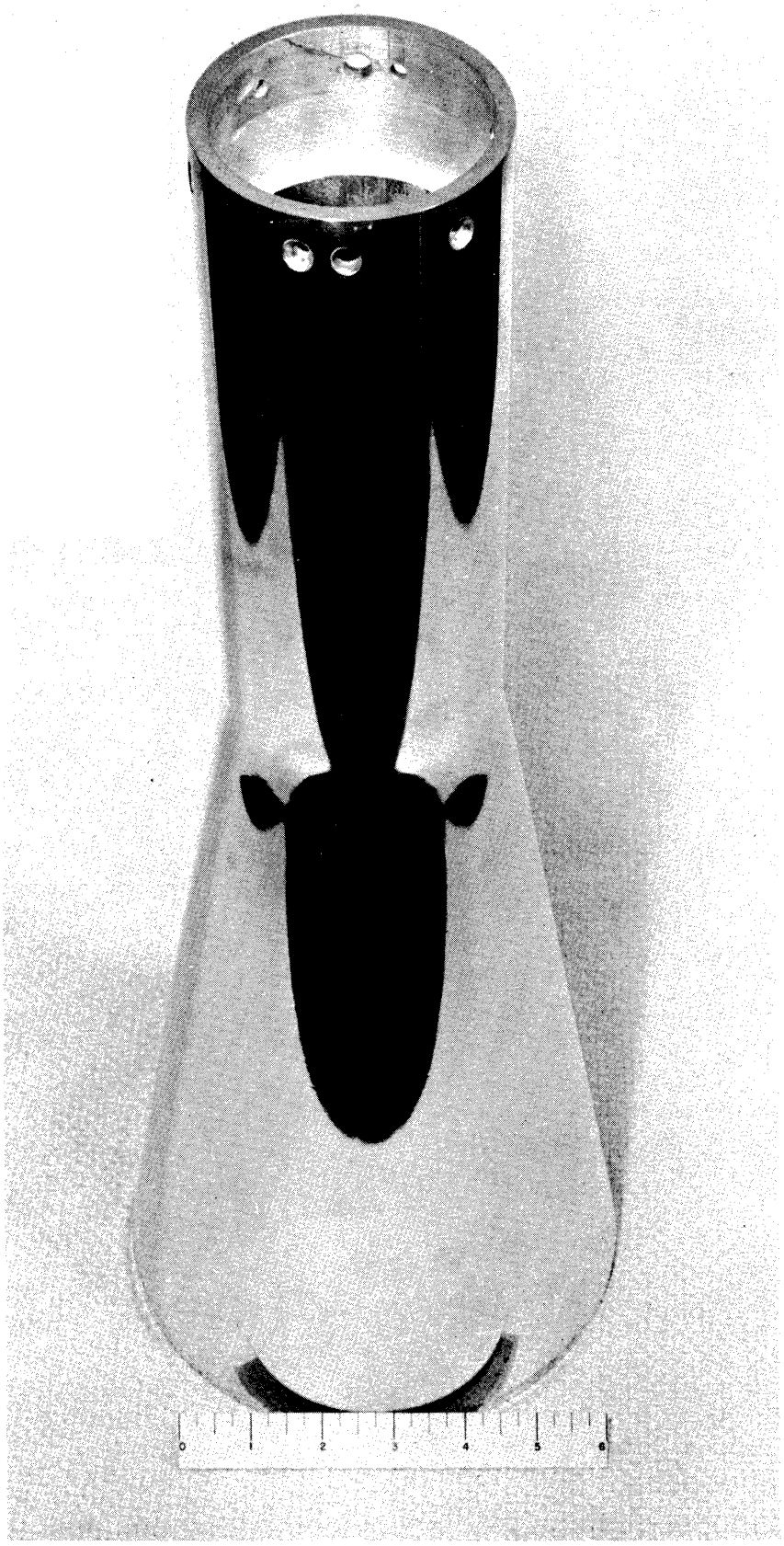

Fig. 44. Nose cone transition section.

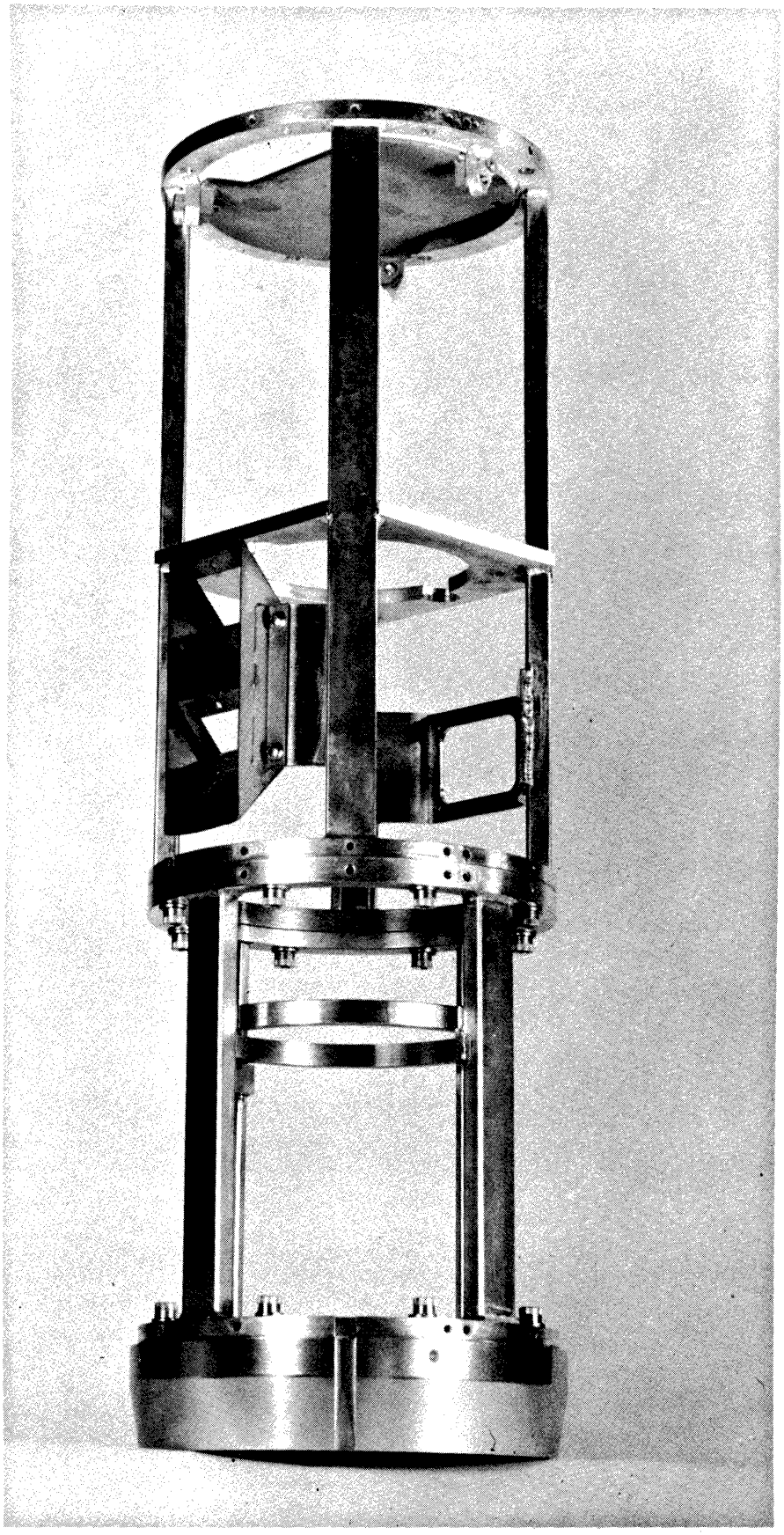

Fig. 45. Unistrut assembly for instrumentation and DOVAP.

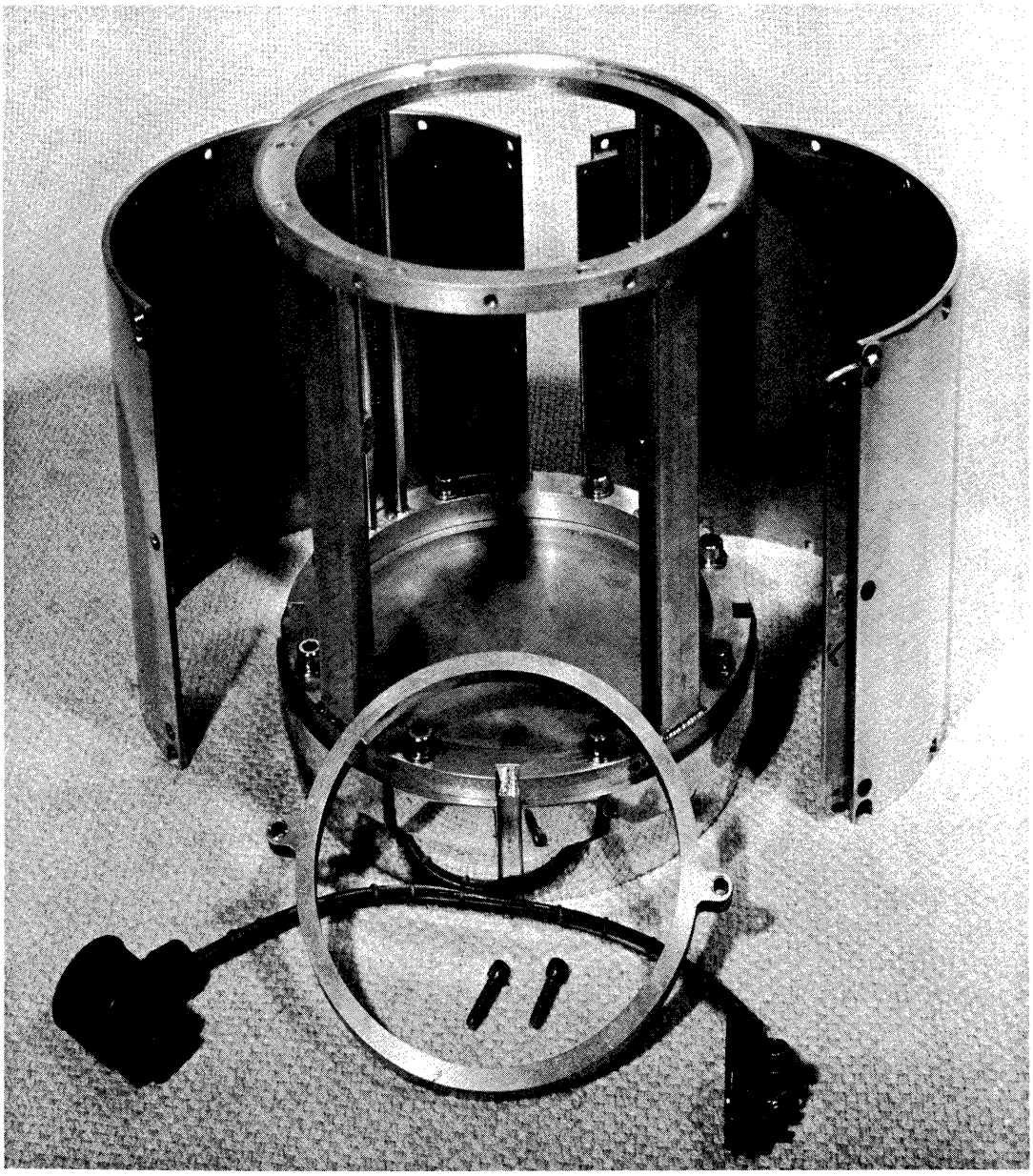

Fig. 46. DOVAP section with hardware.

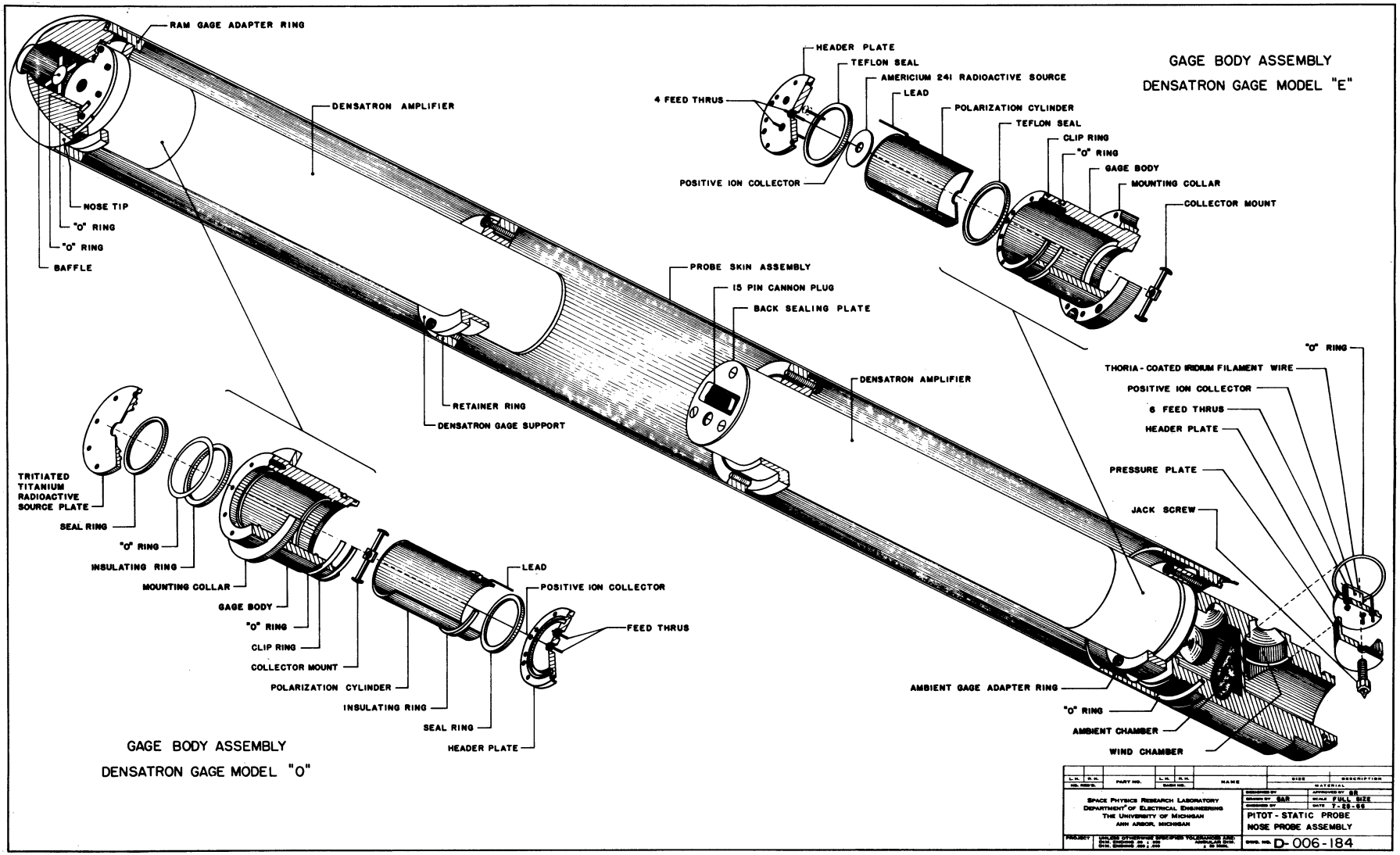
RAM GAGE ADAPTER RING
DENSATRON AMPLIFIER
NOSE TIP
"O" RING
"O" RING
BAFFLE
HEADER PLATE
TEFLON SEAL
AMERICIUM 241 RADIOACTIVE SOURCE
LEAD
4 FEED THRUS
POLARIZATION CYLINDER
TEFLON SEAL
CLIP RING
"O" RING
GAGE BODY
MOUNTING COLLAR
POSITIVE ION COLLECTOR
COLLECTOR MOUNT
GAGE BODY ASSEMBLY
DENSATRON GAGE MODEL "E"
PROBE SKIN ASSEMBLY
15 PIN CANNON PLUG
BACK SEALING PLATE
DENSATRON AMPLIFIER
RETAINER RING
DENSATRON GAGE SUPPORT
"O" RING
THORIA-COATED IRIDIUM FILAMENT WIRE
POSITIVE ION COLLECTOR
6 FEED THRUS
HEADER PLATE
PRESSURE PLATE
JACK SCREW
TRITIATED TITANIUM RADIOACTIVE SOURCE PLATE
SEAL RING
"O" RING
INSULATING RING
MOUNTING COLLAR
GAGE BODY
"O" RING
CLIP RING
COLLECTOR MOUNT
POLARIZATION CYLINDER
INSULATING RING
SEAL RING
HEADER PLATE
LEAD
POSITIVE ION COLLECTOR
FEED THRUS
AMBIENT GAGE ADAPTER RING
"O" RING
AMBIENT CHAMBER
WIND CHAMBER
GAGE BODY ASSEMBLY
DENSATRON GAGE MODEL "O"
SPACE PHYSICS RESEARCH LABORATORY
DEPARTMENT OF ELECTRICAL ENGINEERING
THE UNIVERSITY OF MICHIGAN
ANN ARBOR, MICHIGAN
PITOT-STATIC PROBE
NOSE PROBE ASSEMBLY
DWG. NO. D-006-184

Fig. 47

semblies. Each radioactive ionization gage is an integral part of the Densatron amplifier system, and the two are mounted in the nose cone as a single unit.

The probe assembly begins by mounting the appropriate Densatron(s) to the center section (Fig. 43). The chamber shown has been modified to include two ambient measurements. A further modification is to be made to include a wind chamber (see Section 7.1). Each gage is vacuum sealed from the amplifier section by "O" rings and in turn each chamber gage assembly is vacuum sealed from the remainder of the payload.

The Densatron mated-center-section is next connected to the magnesium structure with the lower Densatron protruding down into the transition section. The two parts are secured using screws located externally along the periphery of the magnesium section. A close tolerance is needed at this point to insure a rigid junction. A screw type coupling is not used here because Densatron electrical cables would be twisted during assembly.

Next, the steel tube is fitted down over the upper Densatron and connects to the center section via a quarter-turn acme threaded coupling. Finally, the ram gage Densatron is dropped into the steel tubing and rests against a lip provided. With an "O" ring attached, the hemispherical nose tip then screws into the tubing, thus completing the probe assembly.

Inside the steel tubing the Densatrons are held in place by nylon supports, which in turn are supported by steel retainer rings welded to the inside diameter of the steel tubing. Densatron cables pass through the nylon supports and feed directly through the center section to the rear of the magnesium section where they connect to the telemeter section via a 37-pin cannon connector.

Before assembly to the payload, each Densatron is wrapped in alternate layers, usually three each, of armalon and aluminum foil which effectively forms a radiation heat shield against the high skin temperatures caused by aerodynamic heating (see Appendix).

3.2 TELEMETER SECTION ASSEMBLY

With the exception of the aspect eye and pull-away plugs, all of the telemeter instrumentation are located on standard cylindrical shaped decks. The decks are assembled into a column such as Fig. 48, and fastened to a steel mounting platform by four 10-32 threaded rods that pass through each deck. Additional support for the structure is gained using a bracketed plate (Fig. 49) that attaches to the top steel ring of the Unistrut section.

Two pull-away plugs, one for DOVAP, the other for the main payload, are mounted to a bracket (Fig. 45) which in turn screws to brackets attached to two of the Unistrut columns. Located opposite to the pull-away is a mounting plate for the aspect eye which is welded to the remaining two Unistrut columns (Fig. 45).

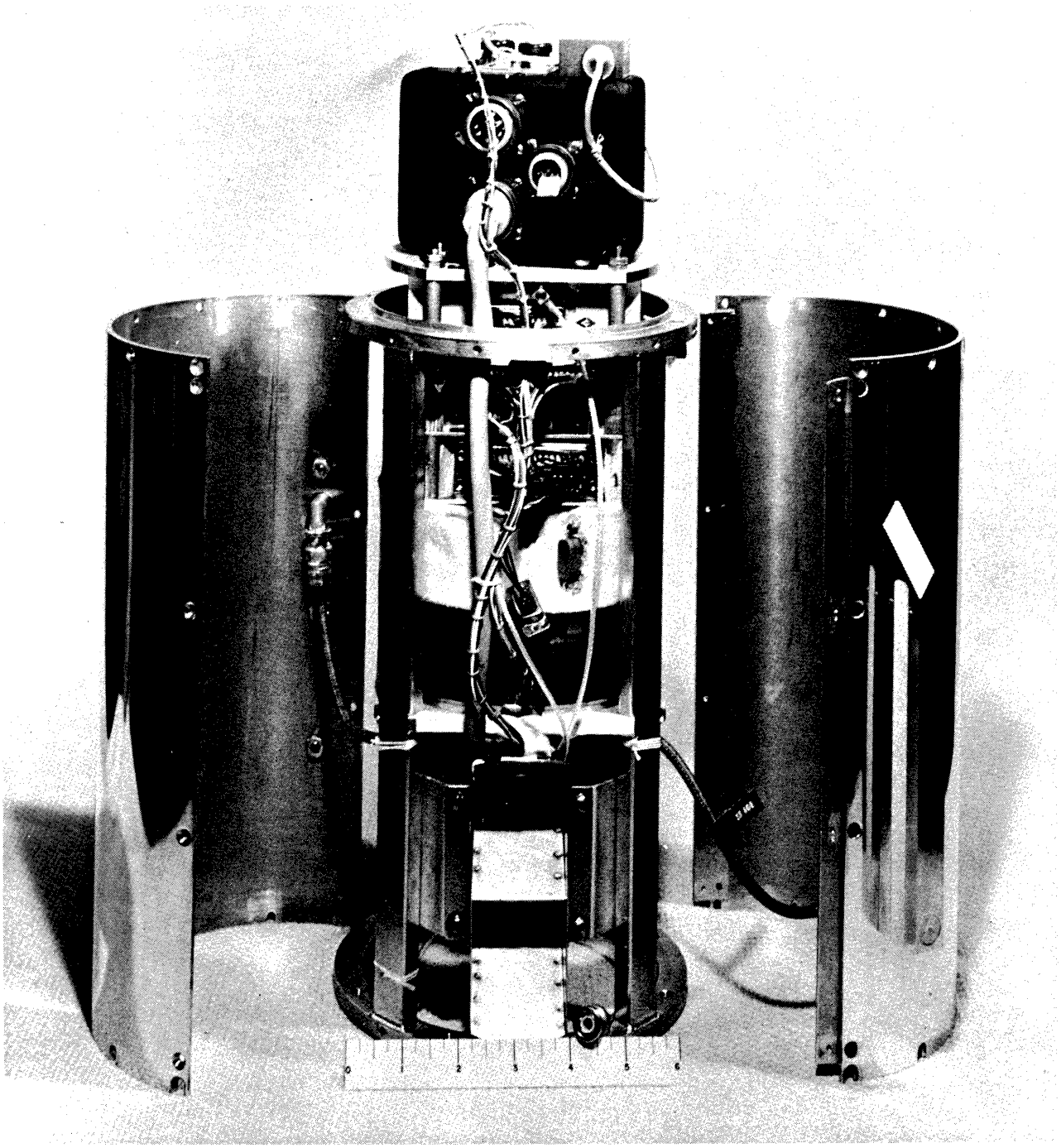

Fig. 48. Instrumentation section with electronics—front view.

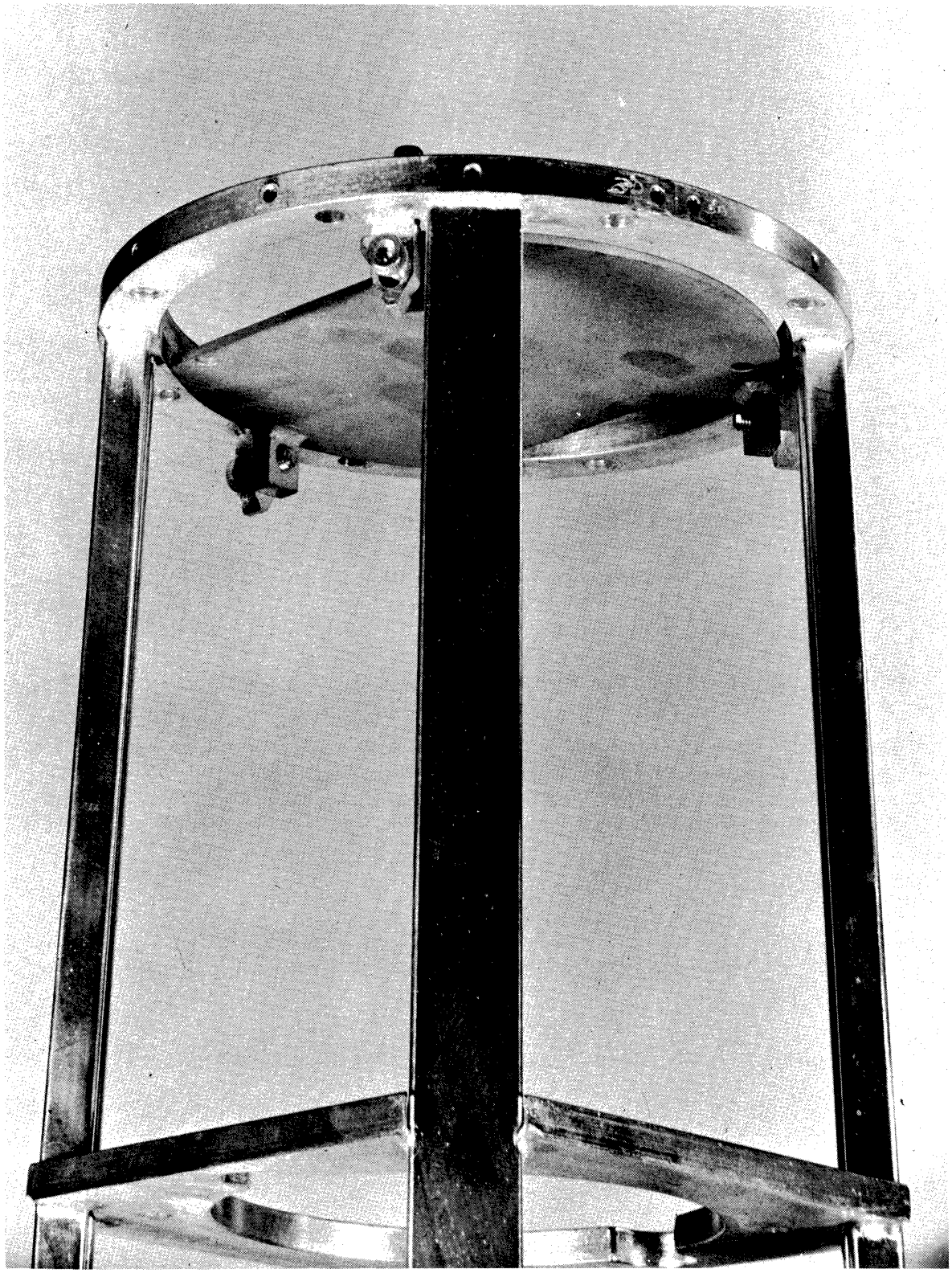

Fig. 49. Top of instrumentation structure showing column support bracket.

The quadraloop telemetry antennas (Fig. 48) are fastened by screws to the aluminum skins surrounding the telemeter section.

The completed telemetry section connects directly to the magnesium casting using eight 1/4-in. stainless steel bolts. The upper steel ring of the Unistrut section is snug-fit piloted to the magnesium section, and a keyway is used to maintain alignment and rigidity.

3.3 DOVAP ASSEMBLY

DOVAP instrumentation fits into another Unistrut section, Fig. 46, located to the rear of the payload. The Apache motor coupling adapter is used also for the mounting base for the DOVAP "can." A hold-down ring (shown in Fig. 46) that fastens to welded brackets in two of the Unistrut columns is all that is needed to hold the can in place as shown in Fig. 52.

In the past, the DOVAP antenna coupling networks were fastened to the "can" as shown in Fig. 50 and 51. Brackets for the networks are now provided which are screwed to the Unistrut columns as shown in Fig. 53.

Piloting and keying arrangements similar to those employed in the telemeter section are used on both ends of the DOVAP section to help maintain strength and rigidity of the structure.

Since DOVAP antennas are mounted directly on the second-stage Apache, it is desirable to split the payload at this point and consider DOVAP to be a part of the rocket. Therefore, final assembly of the payload to the rocket involves installing the DOVAP can, joining the two Unistrut sections with eight 1/4-in. bolts, and putting skins around the DOVAP can to finish the operation. The entire sequence is usually accomplished in less than 30 min.

3.4 DESPIN MODULE

A yo-yo despin module,[18] which will be used in the future payloads for wind measurements (see Section 7.1 and Figs. 54, and 55), is designed to fit between the telemeter section and the DOVAP section using the same mounting holes, keys, etc., that are used to mate the two sections. Electrical wiring is independent of the remaining payload, therefore no modification or integration other than mounting are necessary when a despin module is used.

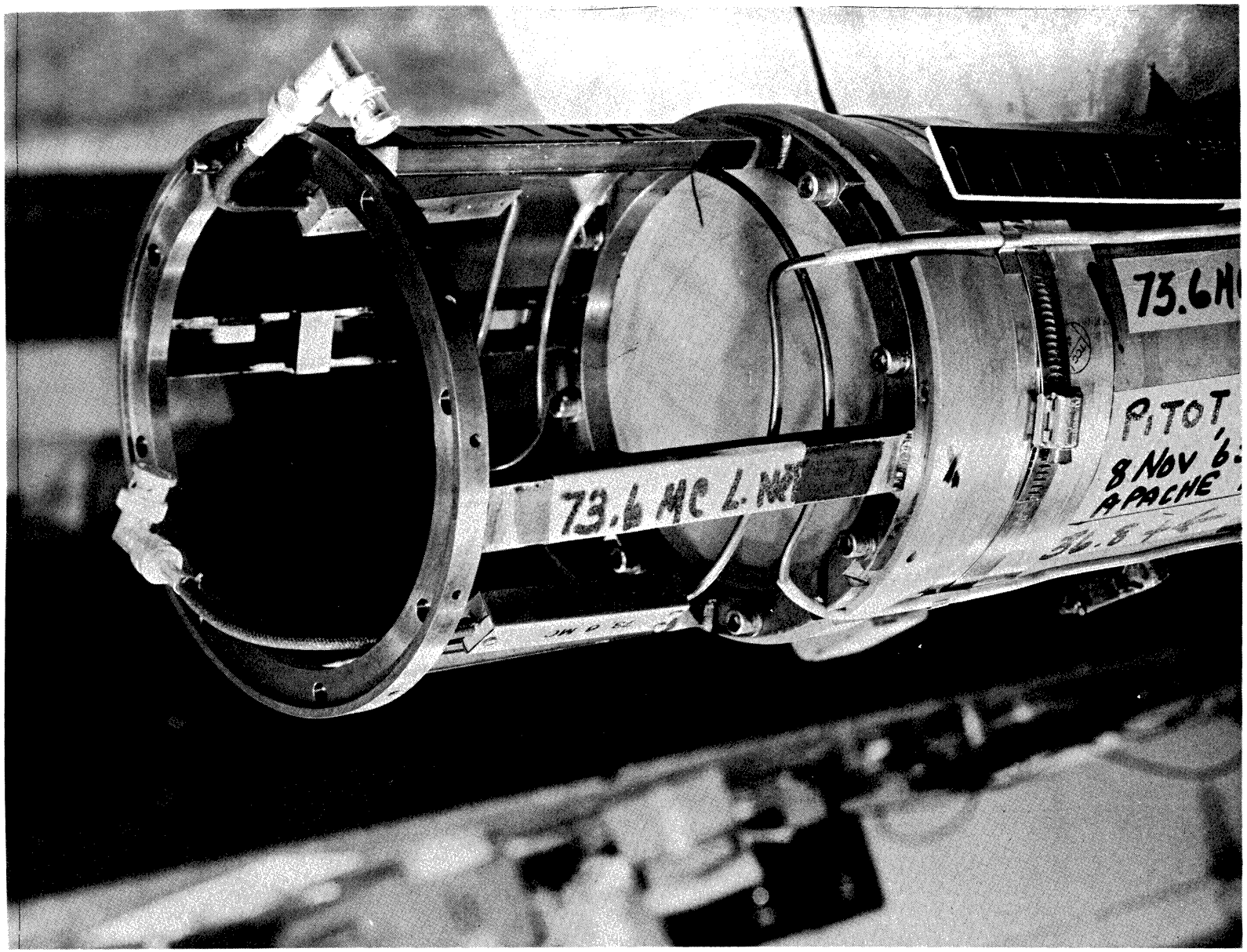

NASA W-63-336

Fig. 50. DOVAP section mounted on Apache.

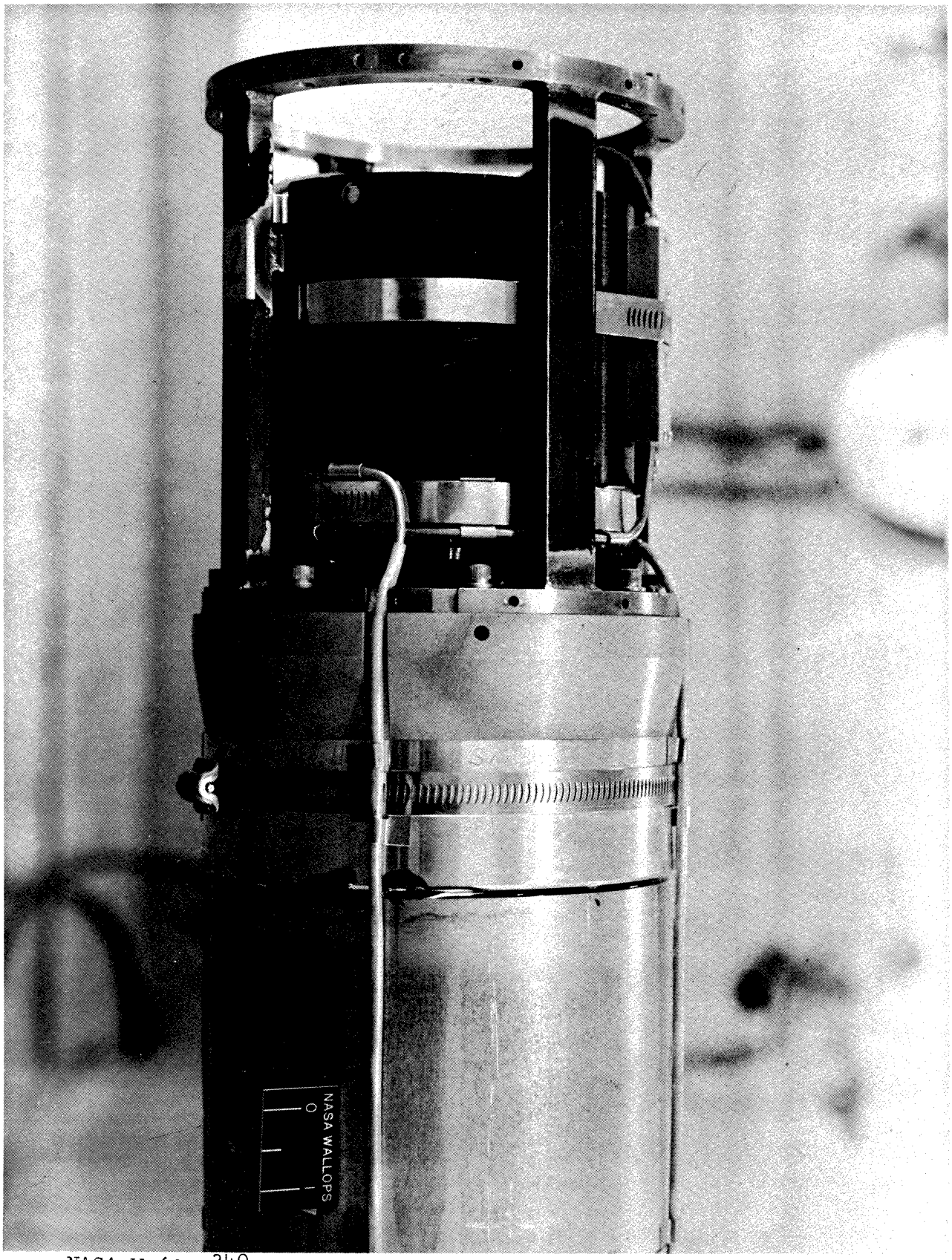

NASA W-63- 340

Fig. 51. DOVAP transponder installed--side view.

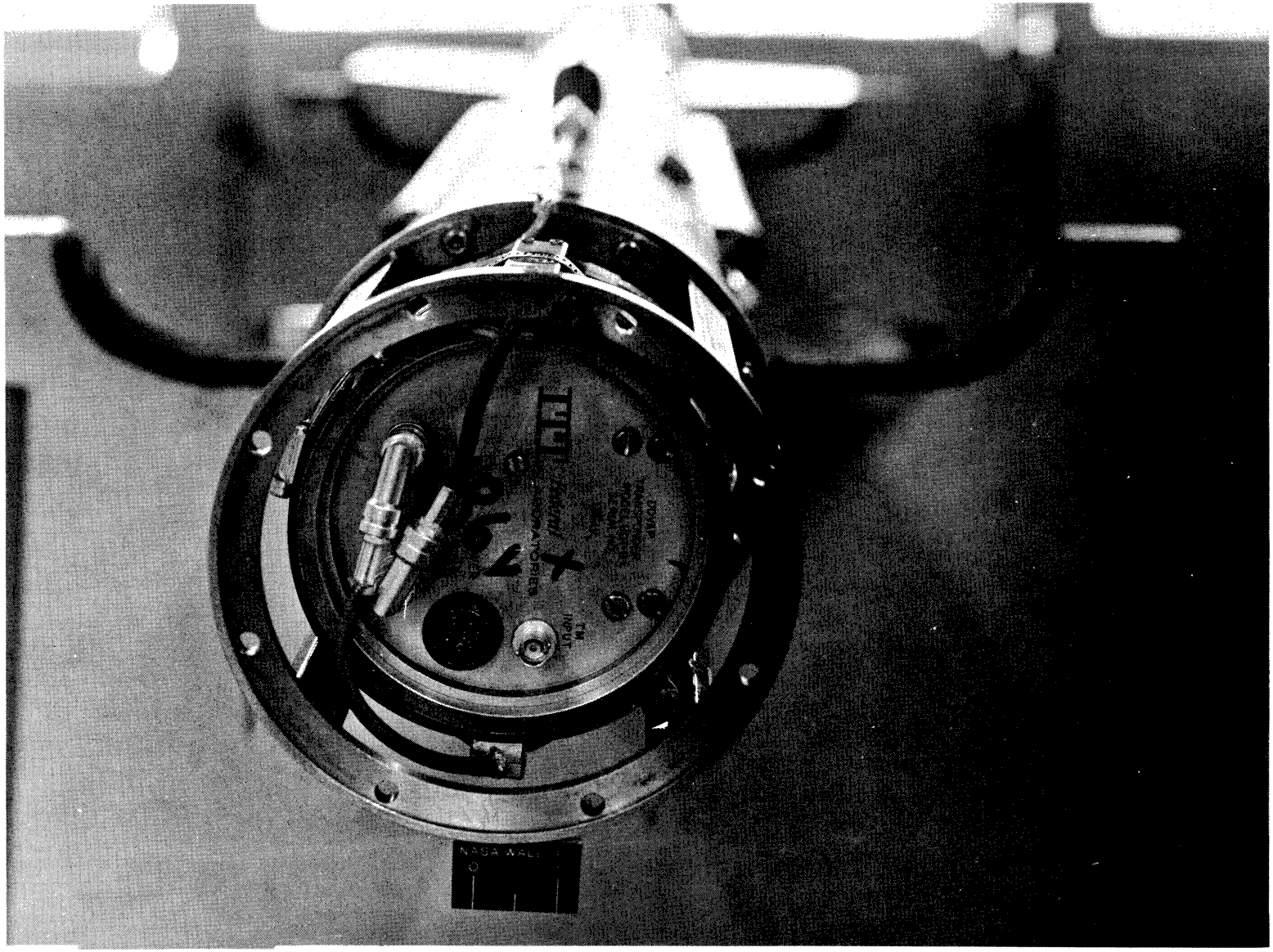

NASA W-63- 338

Fig. 52. DOVAP transponder installed—top view.

Fig. 53. DOVAP section showing brackets for antenna coupling networks.

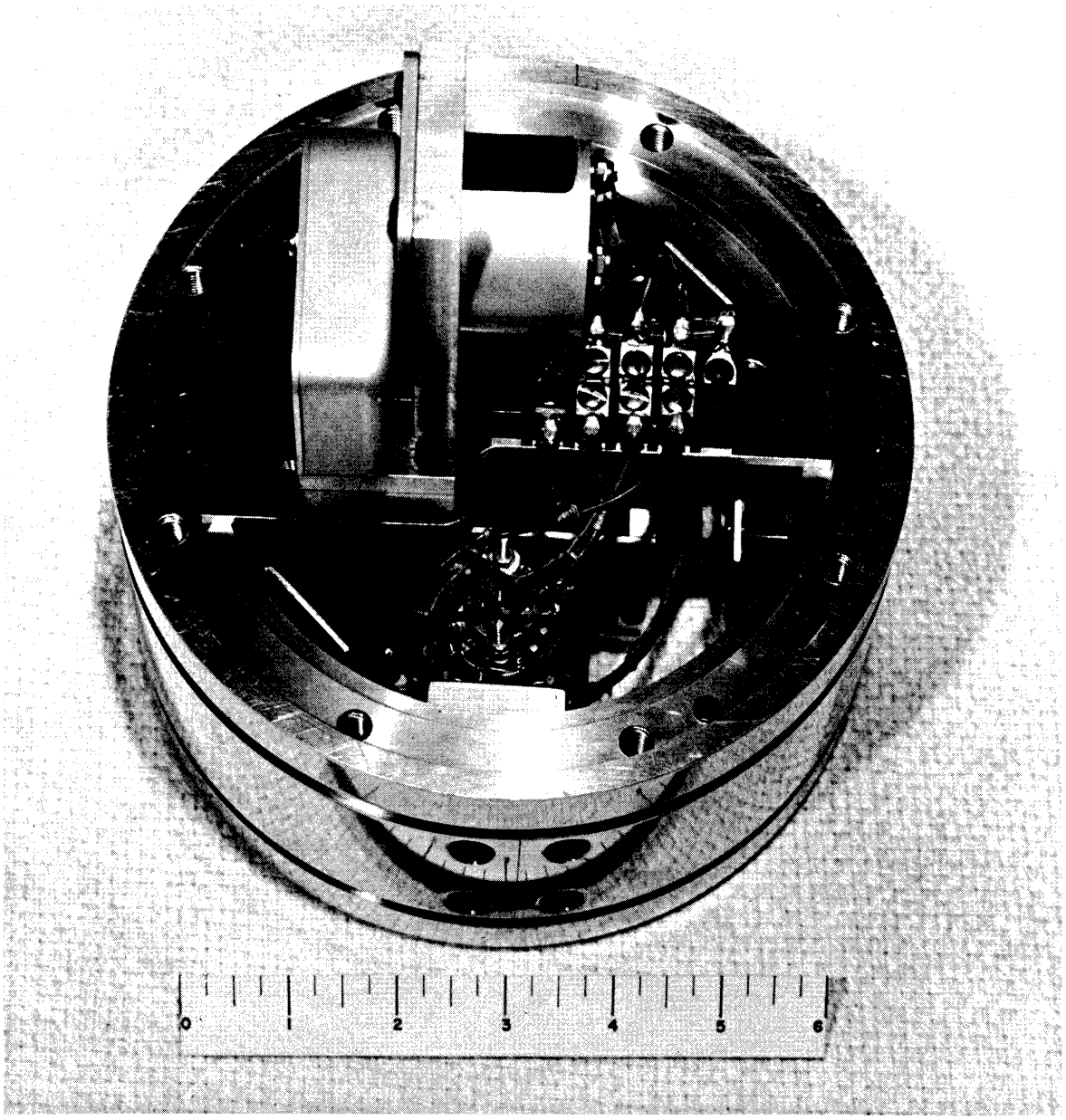

Fig. 54. Despin module assembled.

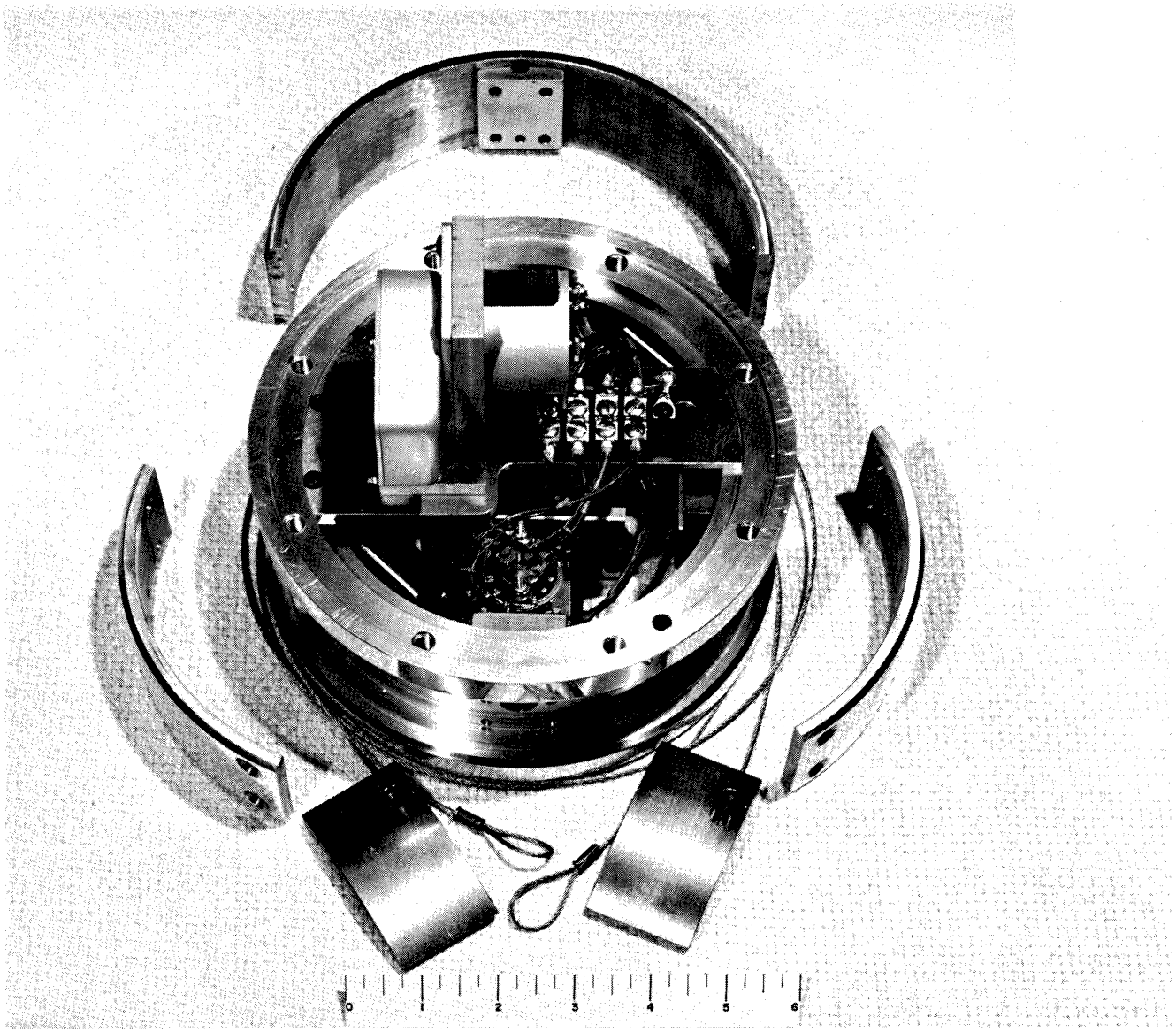

Fig. 55. Despin module—showing weights, steel wire, and skins.

4. TESTING

4.1 SYSTEM TESTS

The objectives of payload testing are (1) to prove design adequacy, and (2) to define operational characteristics and improve the reliability of each payload. The first part is accomplished through simulated methods testing and test launchings. In the case of the Pitot-Static Probe experiment, the basic design was proven by the prototype nose cone launching AA6.340 and since verified by a number of successful launches that followed. The environmental tests, explained in more detail below, performed on NASA 14.19 at Goddard Space Flight Center give further support to the design. In addition, a theoretical study for aeroelastic flight loading of the nose cone was made by Thiokol Chemical Corporation,[12] which concluded only moderate loading was to be expected during flight. Nevertheless, static load tests using parameters dictated by the study were conducted on NASA 14.285 at Goddard Space Flight Center to determine whether or not structural deficiencies exist. Almost negligible payload distortion was observed during the test.

The second objective of determining operational characteristics and reliability, is basically directed towards individual payload testing with emphasis on fabrication and assembly techniques rather than design aspects.

For the most part, testing is done at three levels of payload development. First, each circuit is individually performance tested with respect to temperature changes, voltage changes, etc. Then every solder connection is visually inspected before a circuit or connector is considered usable. Next each subassembly, such as the Densatron, or the telemeter system, is throughly checked out before being installed in the nose cone. Before any commercially purchased equipment is used, the units are tested against manufacturer's specifications. The nose cone is periodically inspected during fabrication, and the gage assemblies are vacuum tested for leaks. The battery pack is carefully monitored during all charge and discharge operations.

The last tests are concerned with the system as a whole and include a vibration test using test levels applicable to the Apache payload (see Section 4.21). Instrumentation tests associated with rocket check out concludes individual payload testing.

By the time a particular nose cone is ready to launch, considerable data is available on the performance and history of the components as well as the complete assembly, and a reasonable confidence in its capability to perform the measurement exists.

4.2 ENVIRONMENTAL TESTS

Formal testing of Pitot-Static Probe payloads originated with NASA 14.19 at Goddard Space Flight Center in the spring of 1962, where vibration and thermo-vacuum tests were performed and the payload was dynamically balanced.

4.21 Vibration

The vibration test consisted of shaking the payload along three mutually perpendicular axes in accordance with specified levels for the Nike-Apache vehicle, which are;

Thrust Axis - 1 g (gravitational constant) sinusoidal survey sweep from 10 cps to 2000 cps followed by a constant maximum velocity of 3 in./sec. from 10 cps to 145 cps and 7 g from 145 cps to 2000 cps.

Lateral X axis - same as thrust

Lateral Y axis - same as thrust, except no 1 g survey.

Anticipated high loading areas of the nose cone, such as the nose tip and the rear of the ambient Densatron gage housing, were instrumented with accelerometers for evaluation purposes.

Results of the tests indicated no structural weakness in the design, and there were no failures of internal instrumentation. Data from the test showed a strong resonance with a Q (amplification factor) of approximately 6 in the range between 350 cps and 400 cps along the thrust axis. In the lateral axes, the major structural resonance occurred at approximately 14 cps with a Q of 9. Other minor resonances ($Q \leq 4$) appeared in the 150 cps to 200 cps range.

The same vibration test parameters are used on every Pitot-Static Probe payload as part of a standard check out procedure. Visual and operational examinations after the shake test together with observations during the test determine the payload's launch status.

4.22 Thermal Vacuum Test

This test examined the Pitot-Static Probe's capability to function in a space environment. The nose cone was placed in a Tenny Thermal Vacuum Chamber where the temperature was stabilized at -15°C. The chamber was then evacuated to a pressure of 10^{-5} mm Hg and held for 30 min with the payload power turned on. Thermocouples, for temperature measurement, were spaced along the length of the nose cone, and mounted in local heating areas of the instrumentation.

A second test at positive 35°C was performed using the same procedure (see the Appendix).

Payload operation was normal during both tests, and no large or damaging temperature rises were recorded, therefore inferring the payload may operate safely in a space environment.

4.23 Dynamic Balance

Two Pitot-Static nose cones have been examined for dynamic unbalance along the spin axis. The first, NASA 1419, was tested at GSFC while the second, NASA 14.21 was examined attached to its Apache motor, at the Wallops Island facility (see Fig. 56 and Fig. 57). In both cases, initial unbalance measurements were small or insignificant when compared to the rocket system, as was expected. The payload's basic geometry and symmetrically located internal instrumentation preclude the possibility of a serious unbalance existing.

Data taken from fourteen Pitot-Static Probe flights gives an arithmetic mean value of 9.1° for the included angle of the precession cone. The standard deviation is 5.2° with a minimum cone of 2.5° and a maximum cone of 20.3°.

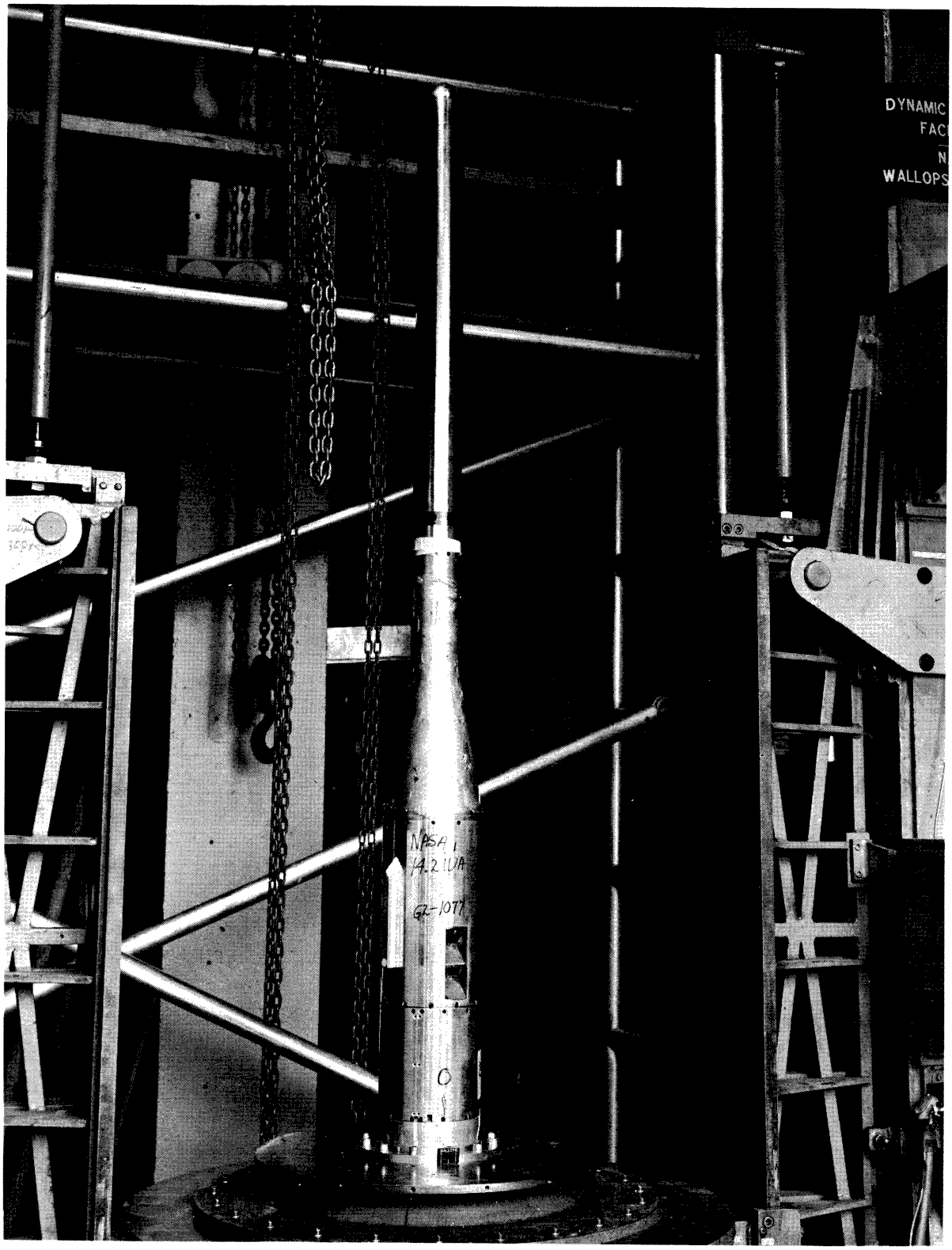

NASA W-63-330

Fig. 56. Dynamic balance of nose cone at Wallops Island.

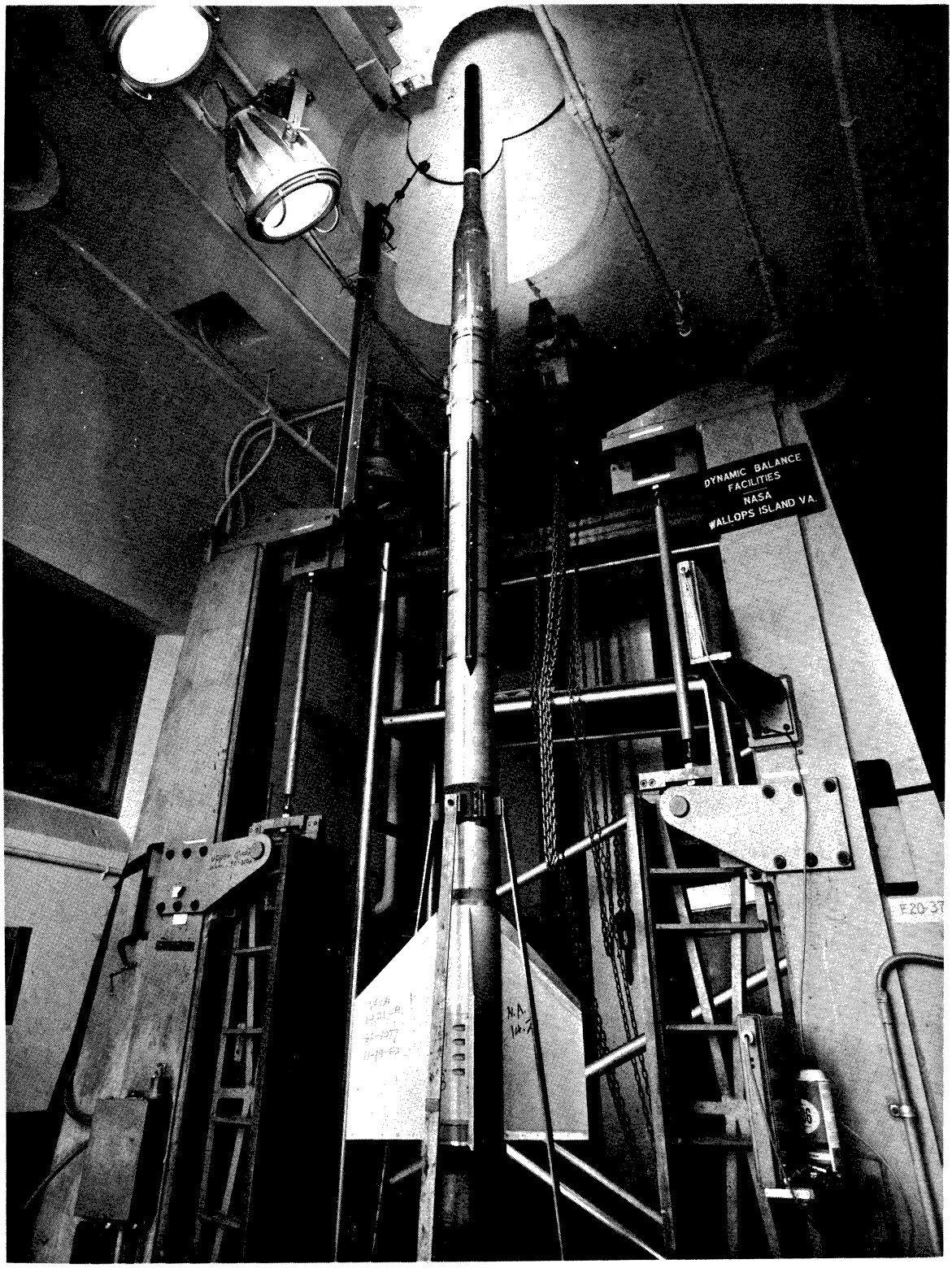

NASA W-63- 327

Fig. 57. Dynamic balance of nose cone and Apache at Wallops Island

5. SYSTEM PERFORMANCE

The engineering design of the Pitot-Static Probe payload is evaluated with respect to data accuracy and system reliability. Data accuracy is examined strictly from an instrumentation viewpoint with little regard to the absolute accuracy of the measurement. A complete systems error analysis,[15] is currently being studied, which will cover all aspects of the experiment, and should be available soon.

It is convient to consider aspect data separate from other data channels because in general, instrumentation effects on aspect accuracy can be ignored.

5.1 ASPECT DATA ACCURACY

Magnetometer data and solar aspect data are used primarily to determine the rocket angle of attack. Since the solar aspect information is in digital form, telemeter errors are negligible, and the accuracy of the angle of attack measurement is limited to the accuracy of the sensor itself, namely $\pm 1°$.

Stated without proof, the magnetometer system has been used to measure the angle of attack to within 5°. This figure being derived from comparisons of solar aspect data to magnetometer data in previous flights.

5.2 TELEMETERED DATA ACCURACY

Instrumentation parameters that effect data accuracy are found principally in the telemeter system and include both frequency response and noise in addition to absolute voltage errors. Although the subjects are interrelated, each will be treated separately so that the contribution of each to the total expected error may be realized.

5.21 Response

Multiplexed or commutated data are, by nature, effected by response because of the switching involved. The effect may be limited, however, by using proper data sampling and SCO bandwidths.

In this case, the commutator using a thirty channel IRIG format at 2.5 frames/sec, produces a data pulse width of approximately 8 msec. Naturally, the leading edge of the pulse is effected more by switching transcients, whereas, it is possible, given enough time, for the trailing edge to be at the correct level. Automatic decommutation equipment has the capability to

"throw out" unwanted portions of the pulse. In other words, the static portion of the pulse may be measured separately while ignoring the transients.

A SCO having a nominal intelligence frequency response of 1 kc (modulation index of five) will carry eight harmonics of the basic pulse frequency with negligible distortion.[9] Under these conditions over 75% of the pulse width remains at a constant level (assuming the data are constant) which by actual measurement has less than 0.1% error.

5.22 Noise

Sources of noise that can effect data accuracy emanate from the Densatrons as part of the output signal, or they are introduced in the modulated signal. Other noise sources likely to occur in the instrumentation, such as ripple, stray signal pickup, cross talk, and ground loop errors, are all minimized to levels far below those mentioned above.

5.221 Densatron Output Noise

Densatron noise outputs vary directly with the range of current being measured; this effect coupled with component variations produce unique noise characteristics in each unit. Table VI lists typical noise voltages found in Densatrons. Besides the converter switching spikes, the principal character of the noise is high frequency, random noise.

TABLE VI

DENSATRON AMPLIFIER NOISE CHARACTERISTICS

Current Range	Noise Level, mv Peak-to-Peak	
10^{-8}	2-5	Random noise
10^{-9}	2-5	Random noise
10^{-10}	2-5	Random noise
10^{-11}	7-10	Random noise plus 1/f noise
10^{-12}	40-60	Primarily 1/f noise. Level may increase as high as 100 mv after amplifier frequency compensation

Note 1: Converter switching spikes less than 1 μsec duration, 1 to 2 v magnitude are present on all ranges.

Note 2: Maximum sensitivities are 10^{-11} amp for ambient gage amplifier and 10^{-12} amp for ram gage amplifier.

The effect of the noise on data accuracy is measurably reduced by the automatic filtering and integration of the signal as it passes through telemeter and ground station circuits. To isolate and assess the actual data error due to noise is extremely difficult. However, experience has shown that noise errors on current ranges greater than 10^{-11} amp are indiscernable while the 10^{-12} amp range is probably faced with an error of $\pm 0.5\%$.

5.222 Telemeter System Noise

Noise generated in telemeter becomes appreciable as signal to noise (S/N) are reduced. Obviously, then signals must be kept large with respect to noise for optimum performance. There are three possible areas to consider in a FM/FM telemeter system, first the SCO bandwidths, second the RF carrier deviation, and third the RF signal level at the receiver.

The SCO bandwidths, according to IRIG standards,[13] are based on a modulation index of five to achieve the highest signal to noise ratio possible, and still provide adequate bandwidth within the subcarrier frequency spectrum.

As for RF carrier deviations, IRIG standards are again used which limit the maximum carrier deviation at $\pm$ 125 kc. Of course, the carrier deviation must be divided between each SCO in the system. By using subcarrier preemphasis,[10] with a minimum deviation of 5 kc for the low-frequency channels, S/N ratios are somewhat equal for each channel and yield comparable results. In practice final deviations are based on the outcome of experimental tests for removing cross modulation products that create unwanted disturbances in the signal.

Typical deviation values for a given payload appear below:

Channel	Cent. Freq.	Required Calculated Deviations	Actual Deviation	Actual Mod. Index
12	10.5 kc	10.9 kc	11 kc	1.045
A	22 kc	33.3 kc	34 kc	1.54
C	40 kc	80.8 kc	80 kc	2.0

The RF power requirements are covered specifically in an earlier section (see Section 2.41) that concludes that a signal strength deficiency does not exist, at least during the measurement portion of the flight.

From the standpoint of noise, data accuracy is not appreciably effected from any of the sources mentioned above—a possible exception being in the abnormal condition when low signals are received.

5.23 Voltage Errors

Because data acquisition by itself is a complex process which involves large amounts of equipment, accumulative errors can be large even though individual errors are small. Fortunately, major error sources are accounted for in the design by using in-flight voltage calibrations which automatically compensate for circuit and component drifts in both airborne and ground equipment.

As stated earlier, the calibration regulator supplies reference voltages for SCO calibrations that are accurate to $\pm 0.05\%$ under specified environmental changes. The SCO linearity specifications are $\pm 0.25\%$ of design bandwidth, however, in practice most of the units used are linear to $\pm 0.1\%$ or better. The accumulation of these errors yields a probable error not greater than $\pm 0.12\%$, which represents also a "worst case" error because, (1) the calibration regulator is usually more accurate than stated for the reason that environmental extremes are not experienced, and (2) linearity errors are greatly reduced because six calibration points are used.

Modulation and demodulation of the RF signal will not add appreciable error as long as two conditions are satisfied (1) a strong RF signal is received at the ground station, which is certainly true during the data portion of the flight, and (2) the modulation index is sufficient to capture significant data sidebands. The second condition is guaranteed in the design by using IRIG standards. The data error at this point which is due entirely to the payload is estimated at 0.12%.

Further demodulation and signal conditioning through the SPRL Data Conditioning System,[14] will add a theoretical error of 0.5%. Putting all of the errors together, we can conservatively estimate that from the SCO input to the digital output of the ground station a theoretical "worst case" error of 0.56% is possible although not expected.

The complete system has been tested in the laboratory with a resultant error of 0.3% which takes into account also, the errors generated by noise and response limitations for which no specific figures were given above.

Since a large percentage of the error is in the ground station, it is possible to reduce the error further by careful maintenance and calibration and/or future improvements in ground equipment.

5.24 Error Summary

Angle of attack measurements are accurate to $\pm 1°$ using the solar aspect system, and within 5° with the magnetometer system.

The payload has a theoretical telemetered data error of $\pm 0.12\%$ which increases to 0.56% in the ground station. The Densatron 10^{-12} amp current range will probably have a RMS error of around 0.75%, because of the high noise level on this range.

The instrumentation errors, as stated, are characteristic of past payloads, and in general are typical of the errors expected in future payloads until such time as system redesign is necessary.

5.3 RELIABILITY

System reliability is no better than the reliability of component parts, and/or the quality of workmanship that characterize the system. In an attempt to establish a high degree of reliability in the Pitot-Static Probe system, considerable emphasis is generated in the following areas of payload development, (1) design, (2) fabrication, (3) inspection, and (4) testing.

The design philosophy has been to use simple circuits, redundancy wherever economically feasible, provide adequate safety margins, and otherwise follow standards and specifications as set forth in appropriate NASA documents.[16,17]

Fabrication and inspection are supervised by personnel certified by a NASA quality assurance school. High reliability, quality components are used in circuits, and soldering standards and procedures are implemented as outlined in "Quality Requirements for Hand Soldering of Electrical Connections" NASA Quality Publication, 200-4.[16] The instrumentation are built to withstand shock and vibration using various potting compounds and cable lacing where necessary.

Testing is implemented at various stages of circuit and payload development, and individual performance tests of each circuit and subassembly is mandatory.

Vibration testing and approximately 25 hr of instrumentation tests and check out complete the testing, and provide a final degree of confidence in the payload.

Although the program outlined above is designed to provide a reliable payload the results can never really be proven except by actual launchings.

Perhaps then, the best definition of system reliability is found in the history of past flights. To date, the Pitot-Static Configuration has

been launched twenty-five times without evidence of any payload malfunction. On three occasions, however, pressure data were not obtained because of rocket malfunctions. The first loss of data occurred on NASA 14.29 which had no second stage ignition. The other two rockets "broke up" due to problems associated with the Apache. In each instance the payload instrumentation performed as expected and data undoubtably would have been acquired had the rockets functioned normally.

5.4 SUMMARY OF SYSTEM PERFORMANCE

Data quality has been examined with respect to frequency response, noise, and absolute voltage errors, with the result that a worst case error of $\pm 0.56\%$ is possible, however, certainly not expected. This error represents a fixed error due strictly to data conditioning processes in payload instrumentation and ground station equipment. It does not reflect the errors found in either theory, pressure calibrations, or the measurement technique all of which are covered in a separate report.[15]

Past Pitot-Static flights have proven the payloads capability to operate in a rocket environment. A program of quality control using appropriate NASA publications for guidelines and NASA certified personnel for inspection, has been implemented to enhance the payloads reliability. The results of the program can probably best be summarized by noting that none of the three failures recorded out of twenty-five flights are attributed to payload malfunction.

6. LAUNCH OPERATIONS

The final launch preparation of Pitot-Static Probe payload begins approximately three weeks prior to a scheduled launch. Each payload is completely assembled, checked out, and otherwise put in a flight condition before shipment to a launch site. Only a few operations, which cannot be done before hand, are required at the launch site. Advantages to this procedure are (1) the payload is assembled under laboratory controlled conditions and (2) range support requirements are minimized.

A typical time schedule of events preceding a launching is listed below.

TABLE VII

LAUNCH OPERATIONS TIME SCHEDULE

Launch Time	Function
L-21 Days	Payload fabrication and preliminary test completed.
L-19 Days	Final Densatron/gage assembly and preparation for calibration.
L-16 Days	Gage pressure calibrations completed.
L-16 Days	Densatrons installed in nose cone.
L-15 Days	Operational tests.
L-14 Days	Vibration test of complete payload except for DOVAP transponder.
L-14 Days	DOVAP section shipped to launch site.
L-13 Days	Operational tests after vibration.
L-13 Days	Gage pressure correlation tests.
L-12 Days	Payload shipped to launch site in evacuated vacuum shroud.
L- 8 Days	Payloads arrive at launch site.
L- 7 Days	Personnel arrive at launch site.
L- 6 Days	Payload operational tests including telemeter. Vacuum system assembled.
L- 5 Days	Vacuum pumping of nose cone begins and continues until launch day.
L- 3 Days	Magnetometer calibration tests.
L- 2 Days	Gage pressure correlation tests.
L- 1 Day	Complete horizontal test with payload and rocket assembled on launcher.
L- 3 Hours	Final assembly of payload to rocket on launcher.

TABLE VII (Concluded)

Launch Time	Function
L- 2 Hours	Vertical instrumentation test.
L-20 Minutes	Payload vacuum shroud removed.
L-17 Minutes	Start of launcher elevation.
L- 8 Minutes	DOVAP on external power.
L- 5 Minutes	Payload on external power.
L- 3 Minutes	Payload on internal power.
L- 2 Minutes	DOVAP on internal power.
L- 1 Minute	Payload in flight conditon.
L- 0	Rocket launched.
L + 390 Seconds	Approximate payload LOS

Note 1: The Densatron gage pressure calibrations are performed using the system shown in Fig. 58 and Fig. 59.

Note 2: The gage pressure correlation tests are performed with the payload completely assembled and the probe section surrounded by a vacuum shroud (Fig. 60).

Fig. 58. Pressure calibration system--front view of control panel.

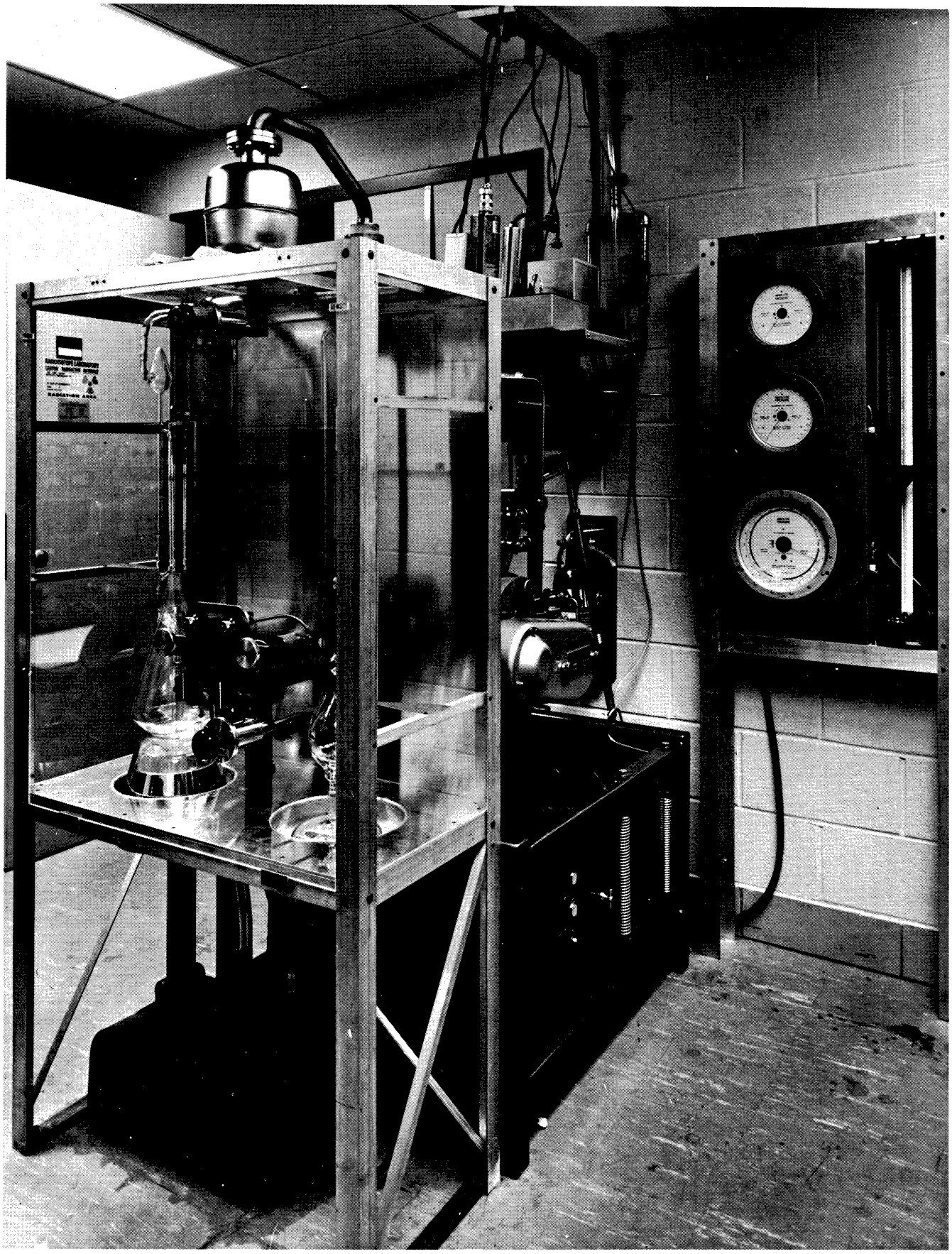

Fig. 59. Pressure calibration system—front view.

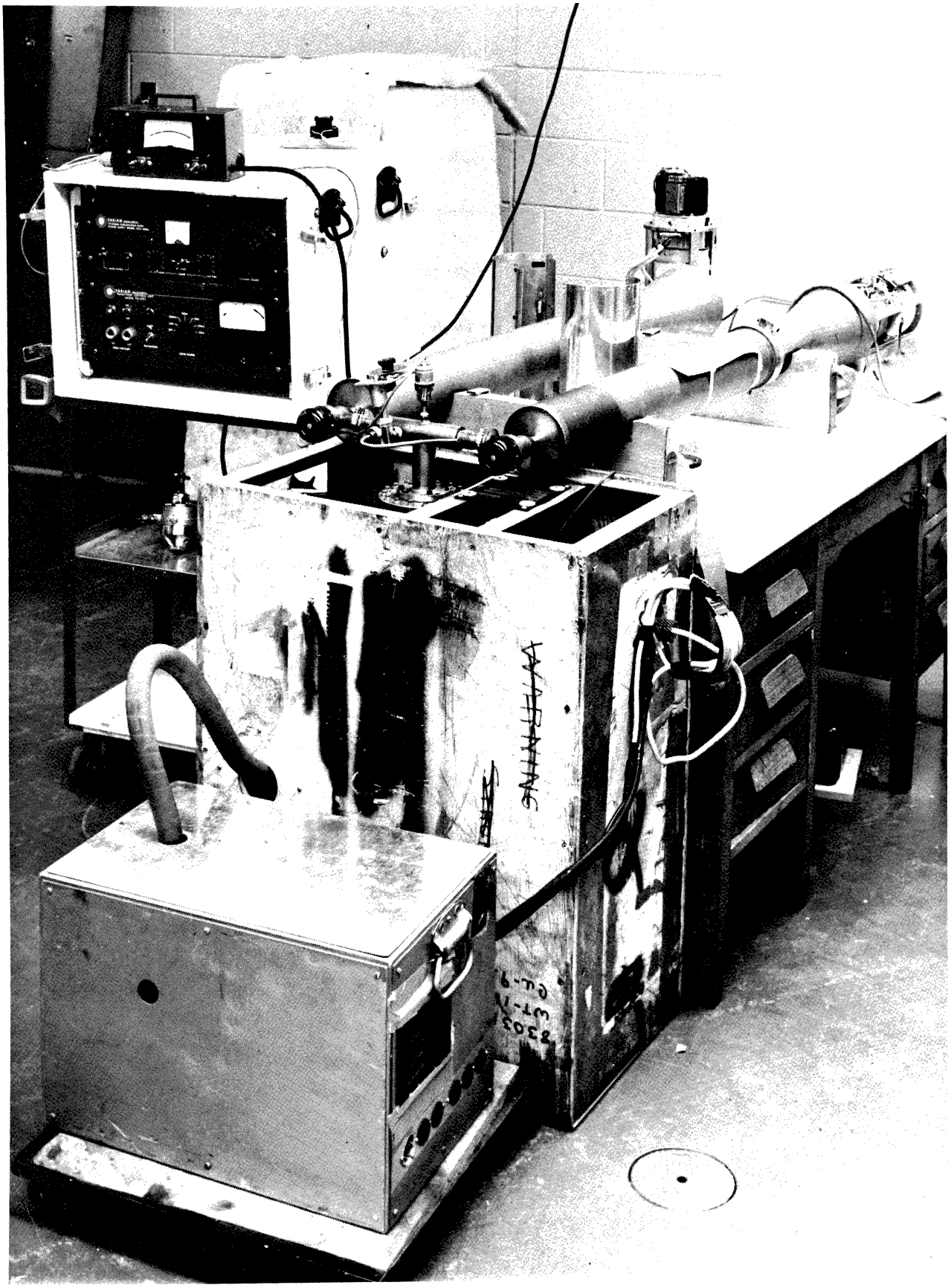

Fig. 60. Portable vacuum system.

Fig. 61. Vacuum control unit for portable vacuum system.

7. FUTURE CONSIDERATIONS

The basic philosophy governing the design of the Pitot-Static Probe system has been to constantly up-grade the experiments capabilities and accuracy without effecting its operational status. The payload, as it is described herein, represents the design as it stands to day which is the result of many incorporated changes since the programs inception. The subjects discussed below are physically realizable and undoubtedly will be great step forward in improving the scientific value of the experiment.

7.1 WIND MEASUREMENT

Standing foremost in scheduled changes for Pitot-Static Probe payloads is the addition of a wind measurement system capable of measuring atmospheric winds in the region between 90 km and 110 km. The system is now under development and should be completed by late 1967.

Included in the development is a specially designed hot filament pressure gage and amplifier combination. The measurement will be made using a single pressure port located immediately behind the ambient pressure ports that will give, because of the vehicle spinning, a wind modulated output.

Also added to the payload will be a despin module (Figs. 54 and 55) that uses a yo-yo despin technique,[18] to reduce the vehicle spin rate from a high of 10 rps to about 2 rps. Flight tests of the modules have been made on Pitot-Static Probe rockets NASA 14.168 and NASA 14.169.

Another instrument, associated with the wind measurement and currently in the development stage, is a moon sensor aspect system to be used for nighttime launchings. The expected completion date is late 1966.*

7.2 AMPLIFIER SYSTEM

Currently in the design stage is a new amplifier system for the radioactive ionization gages. The amplifier employs a new range switching concept that shortens amplifier recovery time between range changes. Additional current ranges will also be used to improve both resolution and accuracy of the measurement. The amplifier is scheduled for completion in early 1967.

---

*The first lunar sensor was successfully flight tested Feb. 1, 1967, on NASA 14.316.

7.3 IONIZATION GAGES

An attempt to extend the useful measurement range, both in lower and higher altitudes, will be made with a new gage configuration that uses americium as the radioactive source. The first flights with the new gage are scheduled for mid-1966. Overlapping ambient pressure measurements will be performed using an americium gage from 20 km to 55 km and a normal tritium source gage in the region between 40 km and 85 km. It is now expected that the americium source gage will eventually replace the tritium source gage altogether in the experiment.

It is also proposed, at this time, to develop a hot filament gage to be used primarily in the wind measurement. The advantages of this type of gage are improved sensitivity and much better electrical and chamber response. Preliminary work has already been completed.

8. APPENDIX

8.1 NOSE CONE HEATING

Temperature changes within the nose cone caused by aerodynamic heating have been measured by thermistor circuits similar to Fig. 19. The data are graphed in Fig. 62 to Fig. 69. The recorded temperatures appear normal for a Nike-Apache payload.[19]

Early measurements, such as those on AA6.340 and NASA 14.21, were limited in accuracy because of poor thermistor response and calibrations. Recorded temperatures are probably no better than $\pm 10°C$. The YSI thermistors used on NASA 14.251 and NASA 14.285 have a guaranteed 1% accuracy besides having a fast response. In these cases, the recorded temperatures are most likely within $\pm 2°C$ except in peak heating periods where response is again a limitation. Measurement resolution decreases with increasing temperatures; therefore, more accurate data can be expected at the lower recorded temperatures.

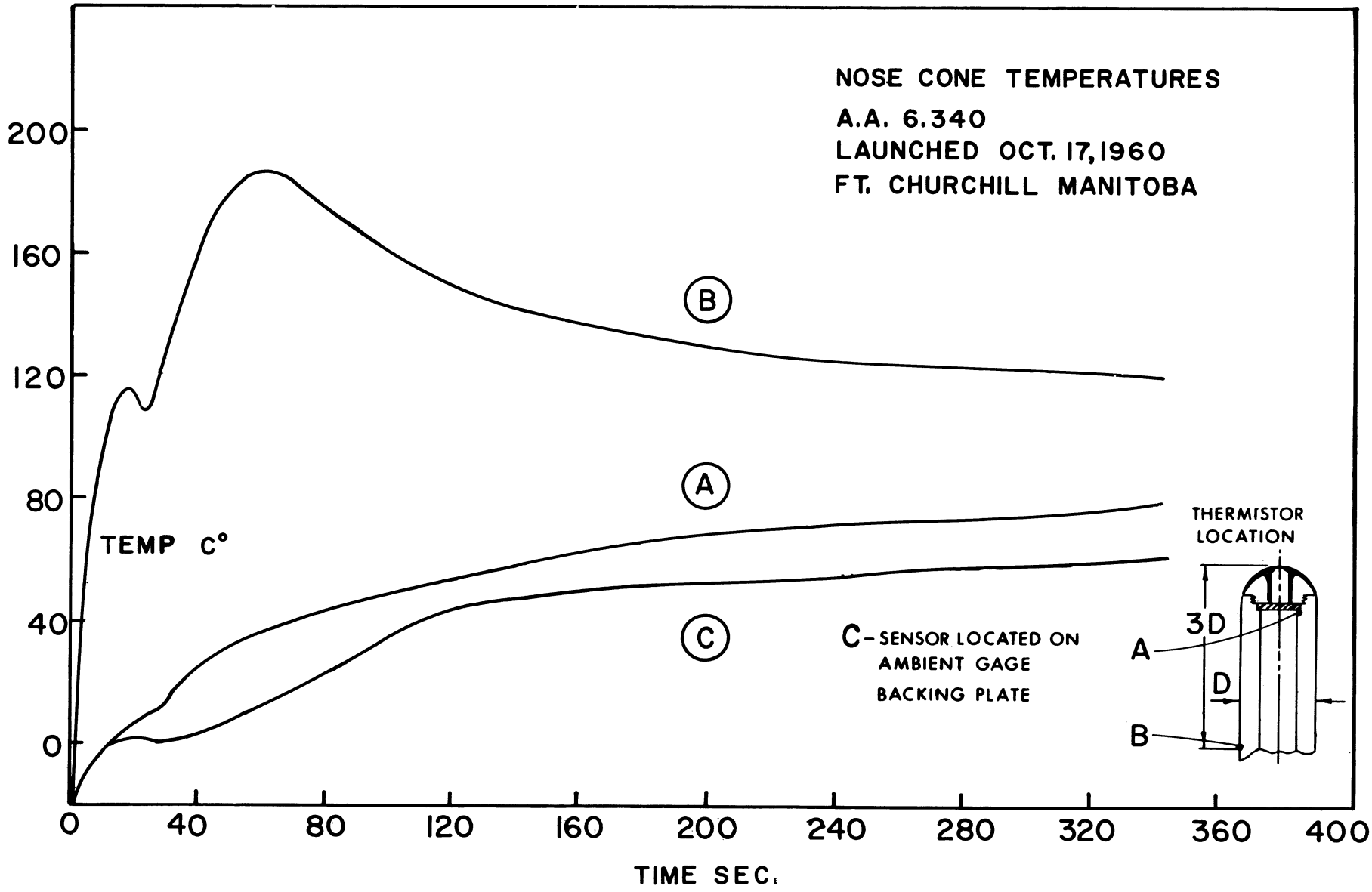
NOSE CONE TEMPERATURES
A.A. 6.340
LAUNCHED OCT. 17, 1960
FT. CHURCHILL MANITOBA
200
160
120
80
40
0
TEMP C°
B
A
C
C- SENSOR LOCATED ON AMBIENT GAGE BACKING PLATE
THERMISTOR LOCATION
3D
D
A
B
0
40
80
120
160
200
240
280
320
360
400
TIME SEC.

Fig. 62

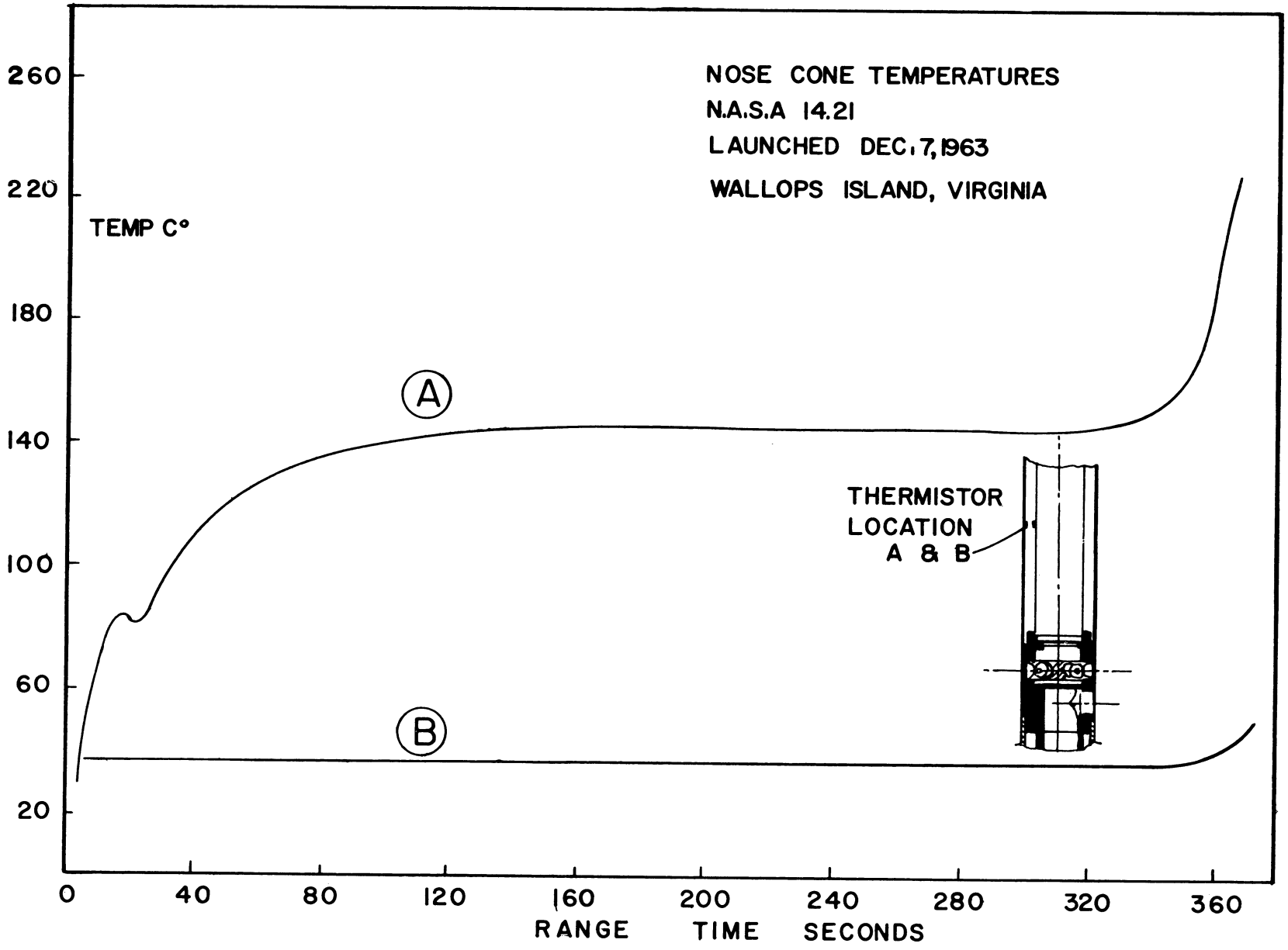
NOSE CONE TEMPERATURES
N.A.S.A 14.21
LAUNCHED DEC. 7, 1963
WALLOPS ISLAND, VIRGINIA
TEMP C°
260
220
180
140
100
60
20
A
B
THERMISTOR
LOCATION
A & B
0
40
80
120
160
200
240
280
320
360
RANGE TIME SECONDS

Fig. 63

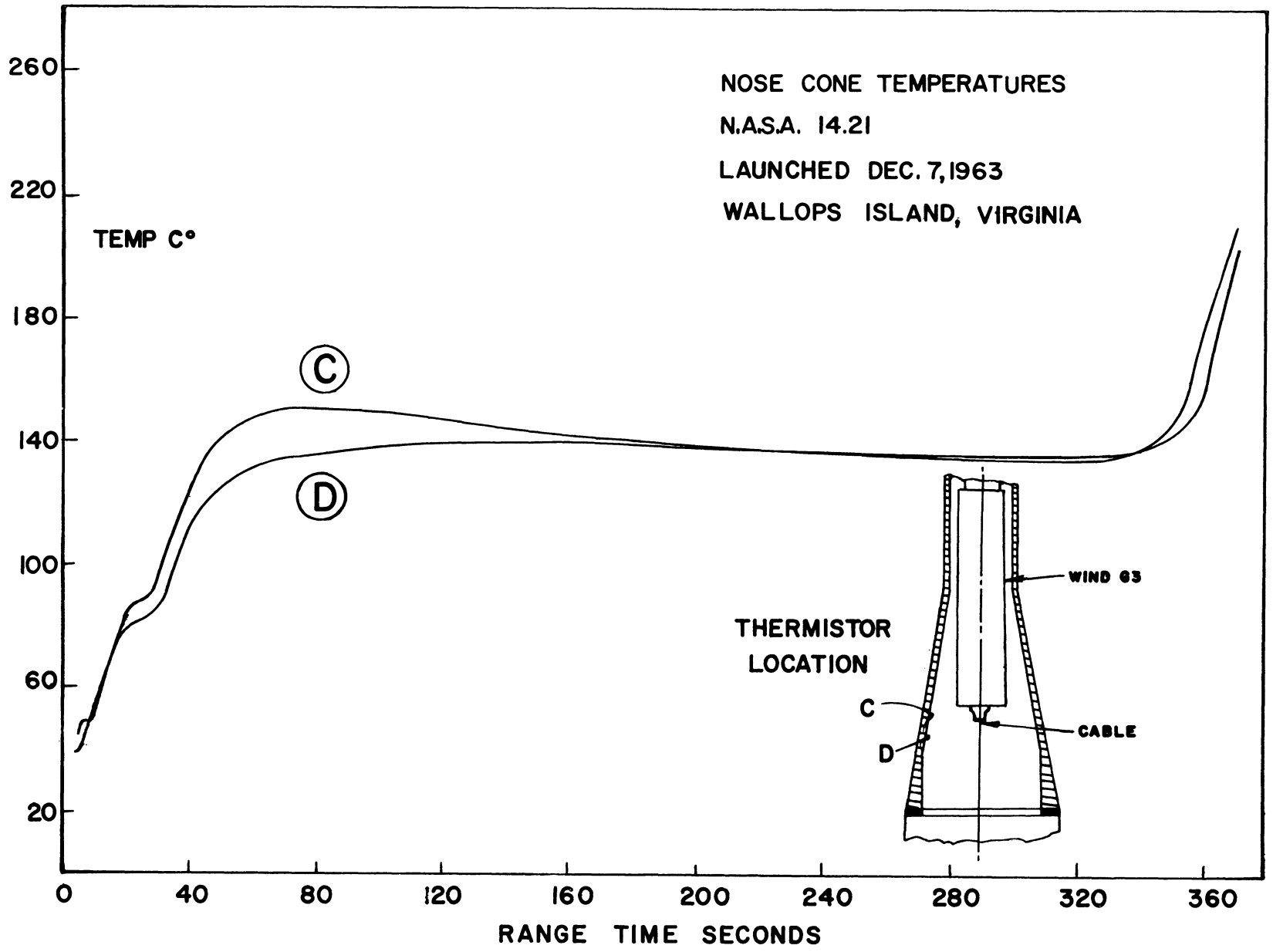
NOSE CONE TEMPERATURES
N.A.S.A. 14.21
LAUNCHED DEC. 7, 1963
WALLOPS ISLAND, VIRGINIA
TEMP C°
260
220
180
140
100
60
20
C
D
0
40
80
120
160
200
240
280
320
360
RANGE TIME SECONDS
THERMISTOR LOCATION
WIND 63
C
D
CABLE

Fig. 64

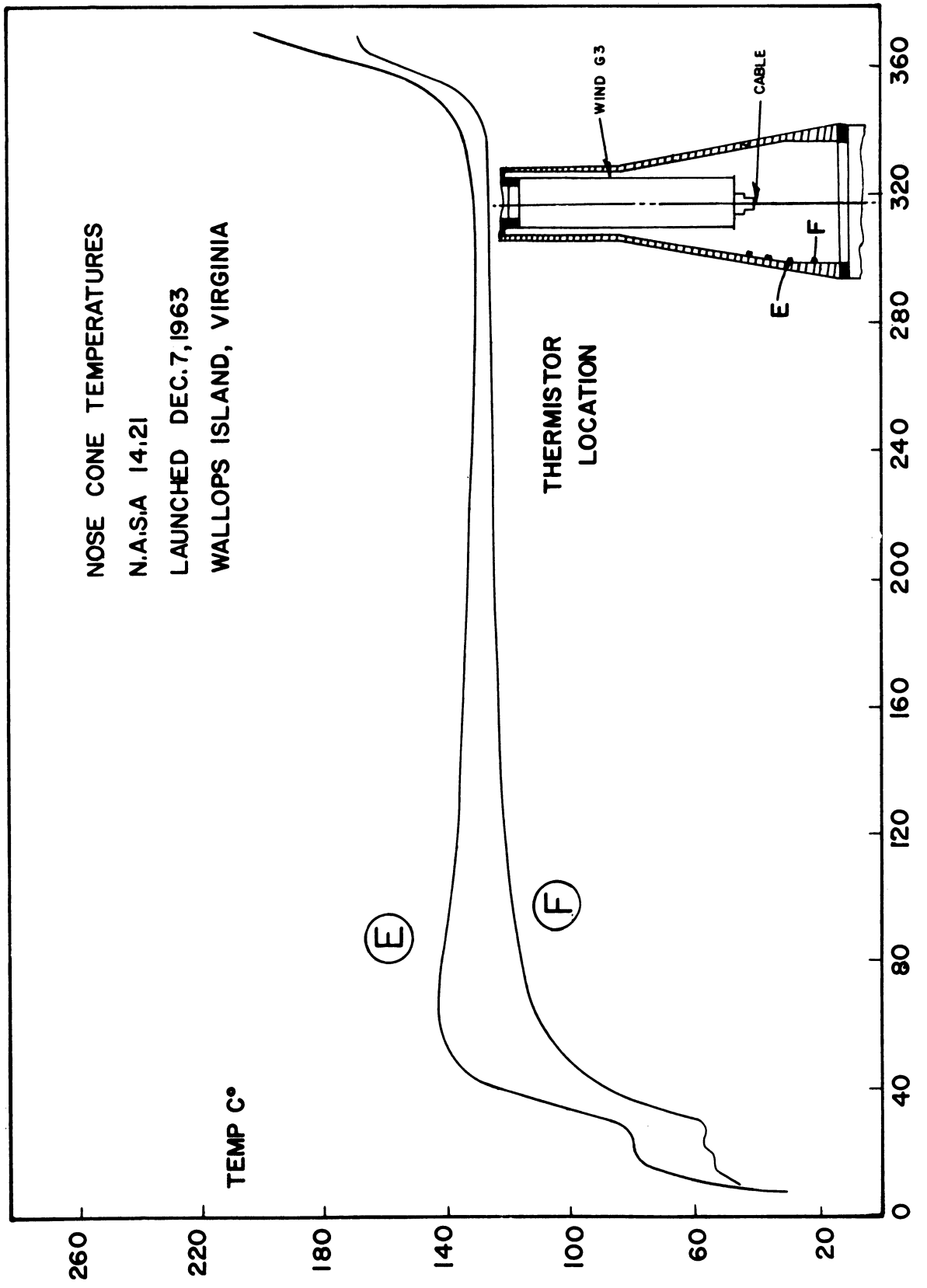
NOSE CONE TEMPERATURES
N.A.S.A 14.21
LAUNCHED DEC.7,1963
WALLOPS ISLAND, VIRGINIA
TEMP C°
RANGE TIME SECONDS
THERMISTOR LOCATION
WIND G3
CABLE
E
F
260
220
180
140
100
60
20
0
40
80
120
160
200
240
280
320
360

Fig. 65

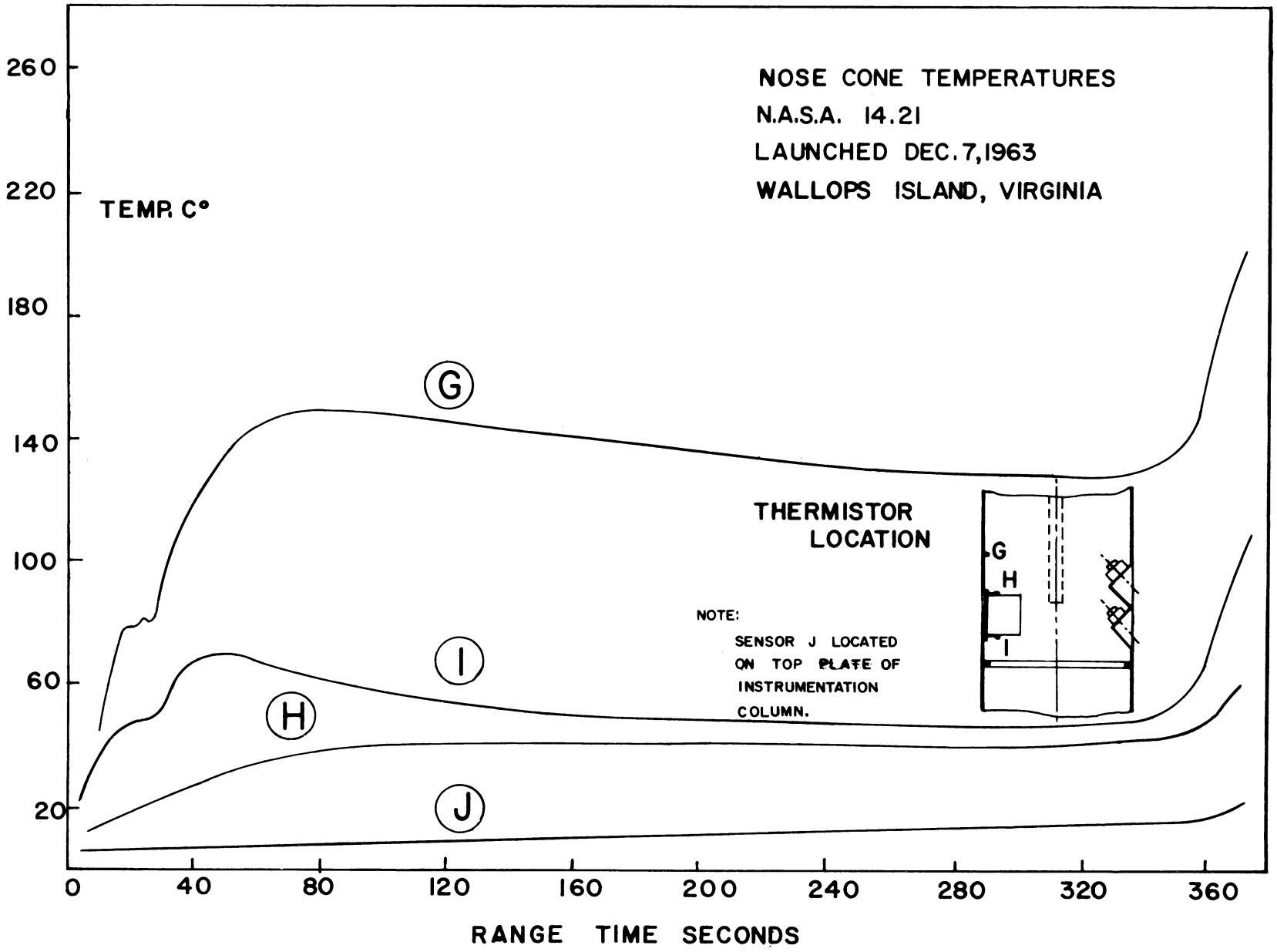
NOSE CONE TEMPERATURES
N.A.S.A. 14.21
LAUNCHED DEC. 7, 1963
WALLOPS ISLAND, VIRGINIA
TEMP. C°
260
220
180
140
100
60
20
0
40
80
120
160
200
240
280
320
360
RANGE TIME SECONDS
G
H
I
J
THERMISTOR LOCATION
NOTE:
SENSOR J LOCATED ON TOP PLATE OF INSTRUMENTATION COLUMN.

Fig. 66

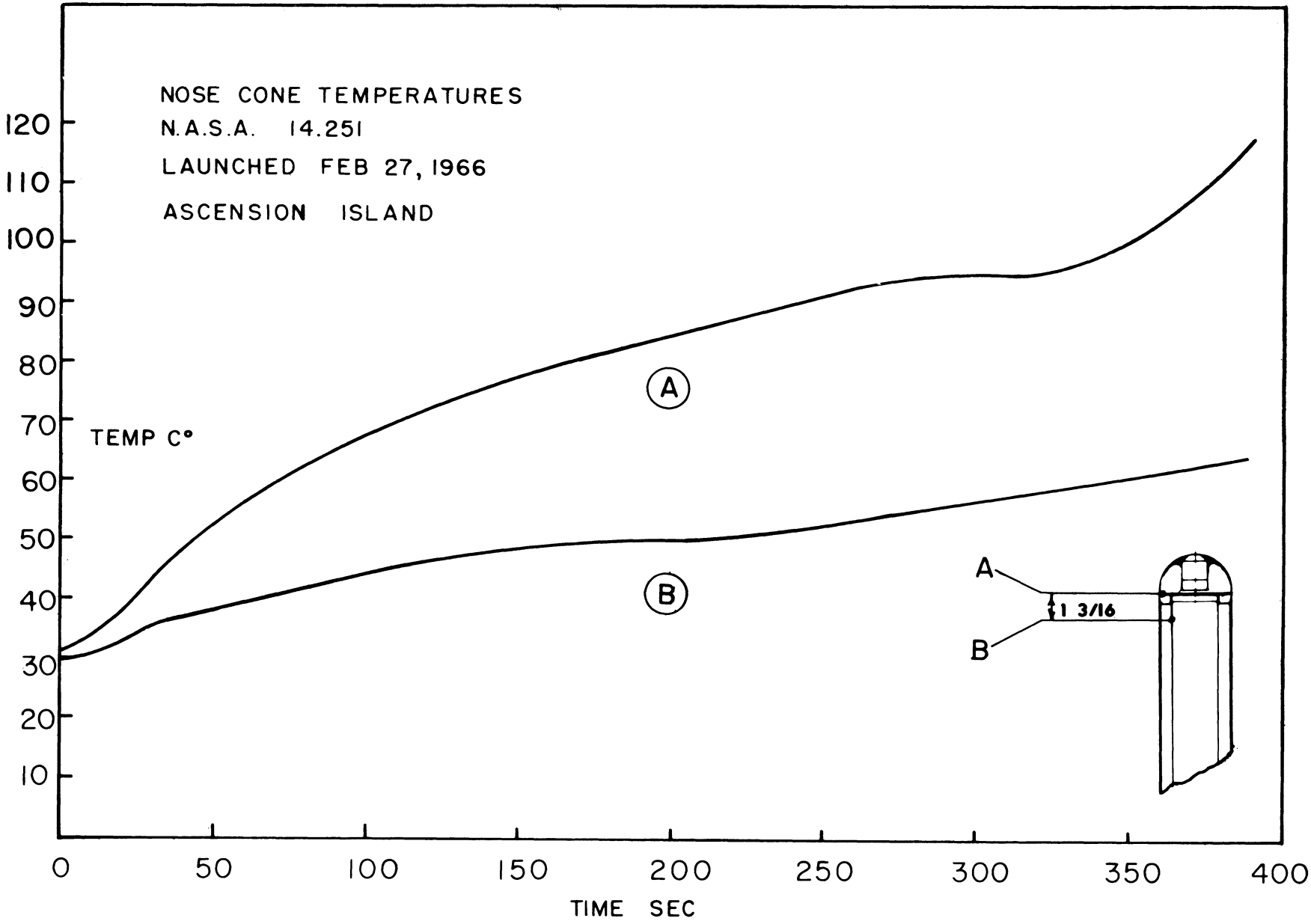
NOSE CONE TEMPERATURES
N.A.S.A. 14.251
LAUNCHED FEB 27, 1966
ASCENSION ISLAND
TEMP C°
TIME SEC
A
B
1 3/16
120
110
100
90
80
70
60
50
40
30
20
10
0
50
100
150
200
250
300
350
400

Fig. 67

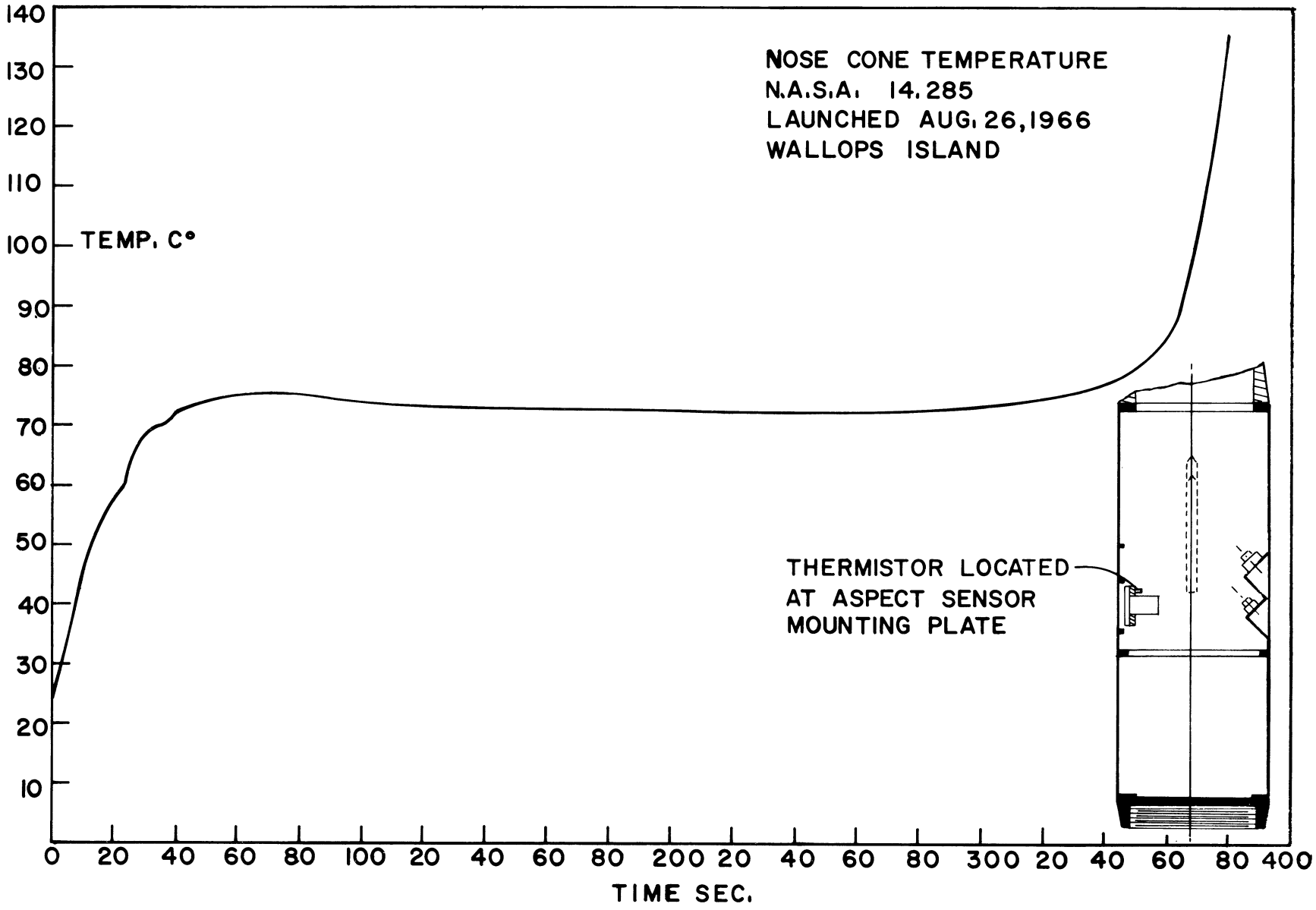
NOSE CONE TEMPERATURE
N.A.S.A. 14.285
LAUNCHED AUG. 26, 1966
WALLOPS ISLAND
TEMP. C°
140
130
120
110
100
90
80
70
60
50
40
30
20
10
0 20 40 60 80 100 20 40 60 80 200 20 40 60 80 300 20 40 60 80 400
TIME SEC.
THERMISTOR LOCATED
AT ASPECT SENSOR
MOUNTING PLATE

Fig. 68

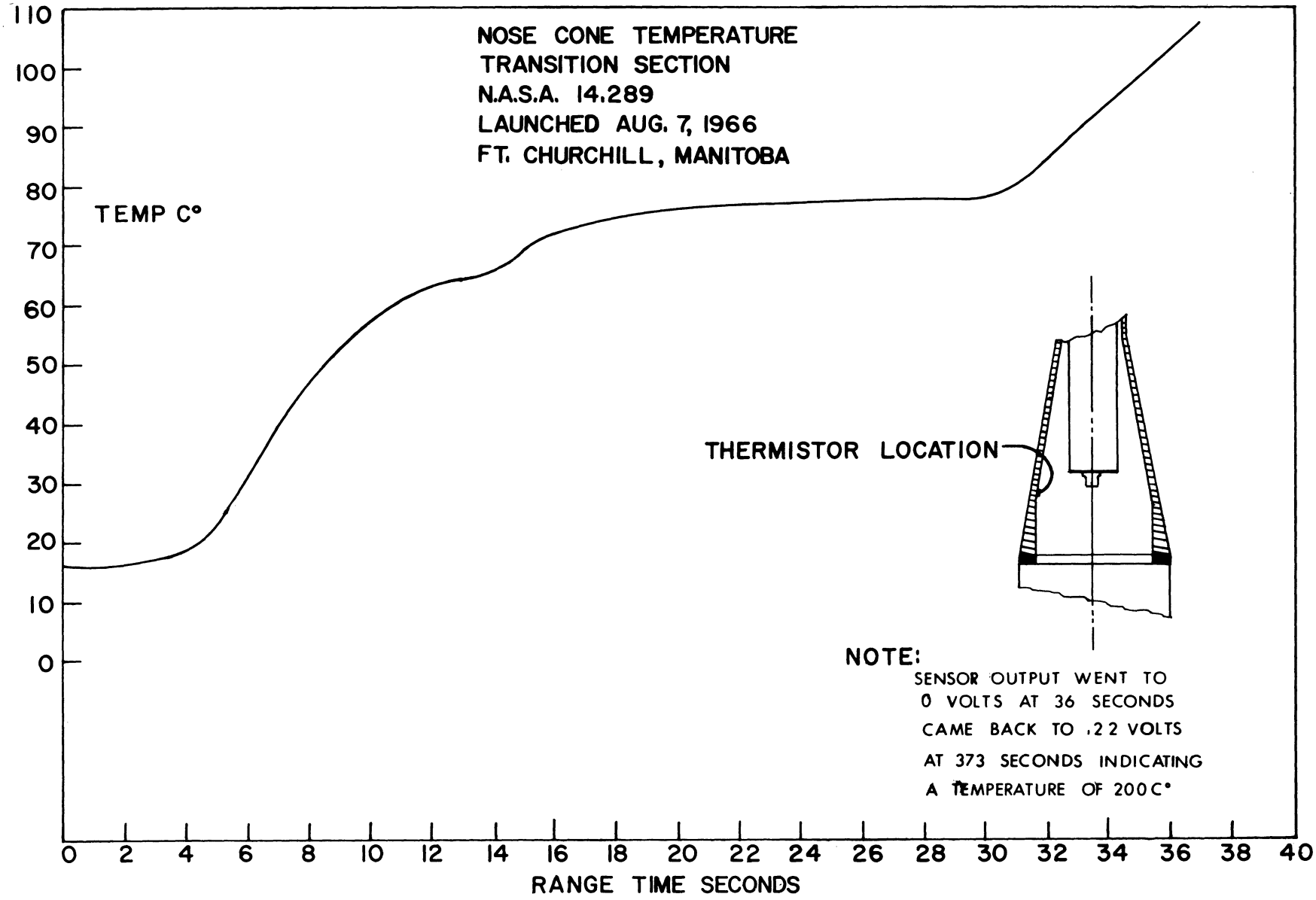
NOSE CONE TEMPERATURE
TRANSITION SECTION
N.A.S.A. 14.289
LAUNCHED AUG. 7, 1966
FT. CHURCHILL, MANITOBA
TEMP C°
110
100
90
80
70
60
50
40
30
20
10
0
THERMISTOR LOCATION
NOTE:
SENSOR OUTPUT WENT TO
0 VOLTS AT 36 SECONDS
CAME BACK TO .22 VOLTS
AT 373 SECONDS INDICATING
A TEMPERATURE OF 200C°
0 2 4 6 8 10 12 14 16 18 20 22 24 26 28 30 32 34 36 38 40
RANGE TIME SECONDS

Fig. 69

8.2 ENGINEERING HISTORY OF PITOT-STATIC PROBE LAUNCHINGS

Rocket Number:	AA6.340	NASA 14.19	NASA 14.20	NASA 14.21	NASA 14.22
Location:	Ft. Churchill	Wallops Island	Wallops Island	Wallops Island	Ascension
Date:	10-17-60	6-6-62	12-1-62	12-7-63	2-4-64
Time:	2104Z	2340Z	2034Z	1343Z	0135Z
Result:	Successful	Successful	Successful	Successful	Successful
Peak Altitude:	140 km	124 km	132 km	140 km	158 km
Measurements:	Ambient pressure Impact pressure Nose Cone Temp.	Ambient pressure Impact pressure Wind pressure	Ambient pressure Impact pressure Wind pressure	Ambient pressure Impact pressure Nose Cone Temp.	Ambient pressure Impact pressure
Instrumentation:	Densatron Model C Tritium Gages Bendix TM-System	Densatron Model C Tritium Gages Bendix TM-System	Densatron Model C Tritium Gages Bendix TM-System	Densatron Model E Tritium Gages Vector TM-System 2 watt 2.5 rps IRIG Commutator	Densatron Model F Tritium Gages Vector TM-System 2 watt 2.5 rps IRIG Commutator
Aspect:	None	Solar with earth cell	Solar with earth cell	Solar with earth cell	2 Axis Magnetometer
Comments:	Prototype Nose Cone Lost DOVAP Track at T+50 Seconds	Pump down Apparatus	Pump down Apparatus	Vacuum Shroud	Launched in Support of Project FIRE Vacuum Shroud

Rocket Number:	NASA 14.23	NASA 14.24	NASA 14.25	NASA 14.26	NASA 14.27
Location:	Ascension 8°S 15°W	Ascension	Ship 52°35'S 78°20'W	Ship 35°14'S 74°15'W	Ship 60°00'S 78°00'W
Date:	4-15-64	4-15-64	4-15-65	4-6-65	4-13-65
Time:	1556Z	0122Z	1600Z	1634Z	1600Z
Result:	Successful	Successful	Successful	Successful	Successful
Peak Altitude:	158 km	156 km	139 km	142 km	149 km
Measurements:	Ambient pressure Impact pressure	Ambient pressure Impact pressure	Ambient pressure Impact pressure	Ambient pressure Impact pressure	Ambient pressure Impact pressure
Instrumentation:	Densatron Model E Tritium Gages Vector TM-System 2 watt	Densatron Model D Tritium Gages Vector TM-System 2 watt	Densatron Model F Tritium Gages Vector TM-System 1/2 watt	Densatron Models E&F Tritium Gages Vector TM-System 1/2 watt	Densatron Model F Tritium Gages Vector TM-System 1/2 watt
Aspect:	Solar with earth	2 Axis Magnetometer	Solar with earth cell	Solar with earth cell	Solar with earth cell
Comments:	Launched in Support of Project FIRE Vacuum Shroud	Launched in Support of Project FIRE Vacuum Shroud	Vacuum Shroud	Vacuum Shroud	Vacuum Shroud

Rocket Number:	NASA 14.29	NASA 14.47	NASA 14.48	NASA 14.63	NASA 14.64
Location:	Ship - Wallops Island	Ascension	Ascension	Ship 44°23'S 77°47'W	Ship 0°00'S 84°8'W
Date:	11-19-64	5-22-65	5-22-65	4-9-65	3-8-65
Time:	1834Z	0202Z	1400Z	2026Z	1748Z
Result:	Failed	Successful	Successful	Successful	Successful
Peak Altitude:	13.8 km	158 km	158 km	147 km	143 km
Measurements:	Ambient pressure Impact pressure	Ambient pressure Impact pressure	Ambient pressure Impact pressure	Ambient pressure Impact pressure	Ambient pressure Impact pressure
Instrumentation:	Densatron Model F Tritium Gages Vector TM-System 1/2 watt	Densatron Model F Tritium Gages Vector TM-System 1/2 watt	Densatron Model E&F Tritium Gages Vector TM-System 1/2 watt	Densatron Model F Tritium Gages Vector TM-System 1/2 watt 2.5 rps IRIG Commutator	Densatron Model F Tritium Gages Vector TM-System 1/2 watt 2.5 rps IRIG Commutator
Aspect:	Solar with earth cell	2 Axis Magnetometer	Solar with earth cell	Solar with earth cell	Solar with earth cell
Comments:	Apache failed to ignite Instrumentation worked Vacuum Shroud No Data	Launched in Support of Project FIRE Vacuum Shroud	Launched in Support of Project FIRE Vacuum Shroud	Vacuum Shroud	Vacuum Shroud

Rocket Number:	NASA 14.65	NASA 14.66	NASA 14.67	NASA 14.168	NASA 14.169
Location:	Ship 0°52'S 84°9'W	Ship 24°5'S 76°5'W	Ship 60°00'S 78°00'W	Ft. Chruchill	Ft. Churchill
Date:	3-9-65	4-4-65	4-13-65	11-9-65	11-10-65
Time:	0626Z	1606Z	0405Z	1840Z	1630Z
Result:	Successful	Sucessful	Successful	Successful	Failed
Peak Altitude:	145 km	140 km	151 km	N/A	N/A
Measurements:	Ambient pressure Impact pressure	Ambient pressure Impact pressure	Ambient pressure Imapct pressure	Ambient pressure Impact pressure	Ambient pressure Impact pressure
Instrumentation:	Densatron Model F Tritium Gages Vector TM-System 1/2 watt 2.5 rps IRIG Commutator	Densatron Model F Tritium Gages Vector TM-System 1/2 watt 2.5 rps IRIG Commutator	Densatron Model F Tritium Gages Vector TM-System 1/2 watt 2.5 rps IRIG Commutator	Densatron Model F Tritium Gages Vector TM-System 1/2 watt 2.5 rps IRIG Commutator	Densatorn Model F Tritium Gages Vector TM-System 1/2 watt 2.5 rps IRIG Commutator Thermistor Pressure gage
Aspect:	2 Axis Magnetometer	Solar with earth cell	2 Axis Magnetometer	Solar with earth cell 1 Axis Magnetometer	2 Axis Magnetometer
Comments:	Vacuum Shroud	Vacuum Shroud	Vacuum Shroud	Despin Launched with NASA 18.03 Vacuum Shroud	Apache head-cap failure Despin Launched with NASA 18.02 Vacuum Shroud No Data

Rocket Number:	NASA 14.251	NASA 14.252	NASA 14.285	NASA 14.286	NASA 14.289
Location:	Ascension	Ascension	Wallops Island	Wallops Island	Ft. Churchill
Date:	2-27-66	2-27-66	8-26-66	8-26-66	8-7-66
Time	1657Z		1911Z	0423Z	1949Z
Result:	Successful	Failed	Successful	Successful	Successful
Peak Altitude:	131.2 km	N/A	149 km	150.5 km	N/A
Measurements:	Ambient pressure Impact pressure Nose Cone Temp.	Ambient pressure Impact pressure	Dual Ambient pressure Impact pressure Nose Cone Temp.	Dual Ambient pressure Impact pressure	Dual Ambient pressure Impact pressure
Instrumentation:	Densatron Model F Tritium Gages Vector TM-System 1/2 watt 2.5 rps IRIG Commutator	Densatron Model F Tritium Gages Vector TM-System 1/2 watt 2.5 rps IRIG Commutator	Densatron Model F Americium & Tritium Gages Vector TM-System 1/2 watt 5 rps IRIG Commutator	Densatron Model F Americium & Tritium Gages Vector TM-System 1/2 watt 5 rps IRIG Commutator	Densatron Model F Americium & Tritium Gages Vector TM-System 1/2 watt 5 rps IRIG Commutator
Aspect:	Solar with earth cell	2 Axis Magnetometer	Solar with earth cell & Magnetometer	2 Axis Magnetometer	1 Axis Magnetometer
Comments:	Support of Apollo Reentry Exper. No. 26 24 hr after reentry Nose Cone Temp. Vacuum Shroud	Apache headcap failure Program Back-up vehicle for Apollo support Vacuum Shroud No Data	COSMET-NAM program Nose Cone Temp. Vacuum Shroud **New Apache Headcap Design**	COSMET-NAM program **New Apache Headcap Design**	New Apache head-cap design Nose Cone Temp. Vacuum Shroud

Rocket Number:	NASA 14.315	NASA 14.316	NASA 14.317	NASA 14.318	NASA 14.319
Location:	Ft. Churchill	Ft. Churchill	Ft. Churchill	Ft. Churchill	Ft. Churchill
Date:	2-1-67	2-1-67	2-1-67	2-1-67	1-31-67
Time:	0109Z	0826Z	0346Z	0538Z	2317Z
Result:	Failed	Successful	Failed	Successful	Successful
Peak Altitude:	N/A	160 km (Radar)	161.5 km (Radar)	164.4 km (Radar)	N/A
Measurements:	Dual Impact pressure Ambient pressure	Dual Impact pressure Ambient pressure Nose Cone Temp.	Dual Impact pressure Ambient pressure Nose Cone Temp.	Dual Impact pressure Ambient pressure	Dual Impact pressure Ambient pressure
Instrumentation:	Densatron Model F Hot Filament & Americium Gages 2.5 rps Commutator	Densatron Model F Hot Filament & Americium Gages 2.5 rps Commutator	Densatron Model F Hot Filament & Americium Gages 2.5 rps Commutator	Densatron Model F Hot Filament & Americium Gages 2.5 rps Commutator	Densatron Model F Hot Filament & Americium Gages 2.5 rps Commutator
Aspect:	1 Axis Magnetometer	1 Axis Magnetometer Lunar Sensor	1 Axis Magnetometer	1 Axis Magnetometer	1 Axis Magnetometer
Comments:	Launched 2nd in series of 6 Rocket Failed Vacuum Shroud	Launched 5th in series of 6 Vacuum Shroud	Launched 3rd in series of 6 Commutator failure Data may be recoverable	Launched 4th in series of 6 Vacuum Shroud	Launched 1st in series of 6 Vacuum Shroud

Rocket Number:	NASA 14.322
Location:	Ft. Churchill
Date:	2-1-67
Time:	1158Z
Result:	Successful
Peak Altitude:	N/A
Measurements:	Dual Impact pressure Ambient Pressure
Instrumentation:	Densatron Model F Hot Filament & Americium Gages 2.5 IRIG Commutator
Aspect:	1 Axis Magnetometer Solar Sensor
Comments:	Launched 6th in series of 6 Vacuum Shroud

8.3 EQUIPMENT SPECIFICATIONS

8.31 Transmitter

TRANSISTORIZED CRYSTAL-CONTROLLED TRANSMITTER model TRPT-501

- **Output: 0.5 watt.**
- **Frequency Range: 215 to 260 MHz.**
- **Weight: 9 ounces.**

Model TRPT-501 is an all-silicon, transistorized, phase-modulated telemetry transmitter capable of transmitting the intelligence from any telemetry subcarrier system in the 215 to 260 MHz telemetry band. The unit has a power output of 0.5 watt. It is mechanically rugged and ultra-stable over wide temperature ranges. The transmitter is capable of supplying maximum power output with the use of available transistors in the telemetry band.

ELECTRICAL SPECIFICATIONS

POWER OUTPUT: 0.5 watt nominal.

OUTPUT IMPEDANCE: 50 ohms nominal.

FREQUENCY RANGE: 215 to 260 MHz.

TUNE UP TOLERANCE: ±0.005%.

CARRIER DEVIATION: ±150 kHz maximum; ±125 kHz nominal.

TYPE OF MODULATION: Phase.

INPUT IMPEDANCE: 5 kilohms minimum.

MODULATION CHARACTERISTICS: See modulation chart.

MODULATION SENSITIVITY: 0.2 volt rms for a modulation index of 1 measured at 1 kHz.

MODULATION FREQUENCY RANGE: 100 Hz to 200 kHz.

MODULATION DISTORTION: Less than 1.5% for the following modulation index:

Frequency	Index
400 Hz to 5.4 kHz	4
7.35 kHz to 22 kHz	2
30 kHz to 70 kHz	1

POWER REQUIREMENTS: +28 volts dc ±10% at 150 ma.

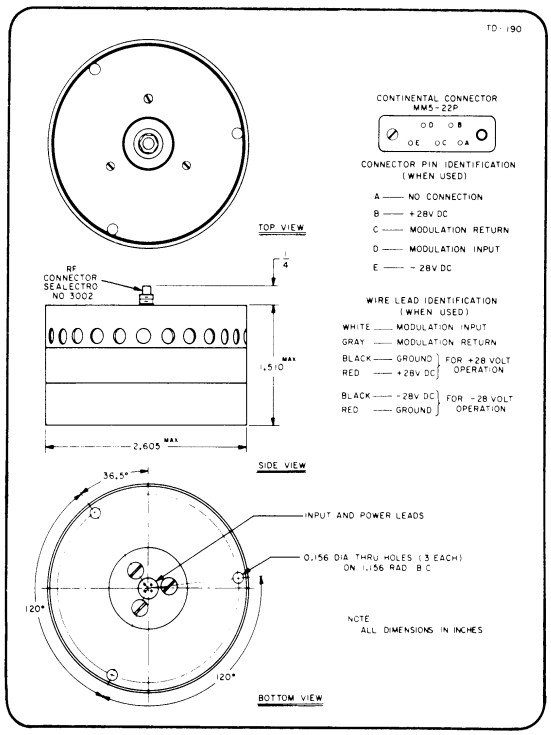

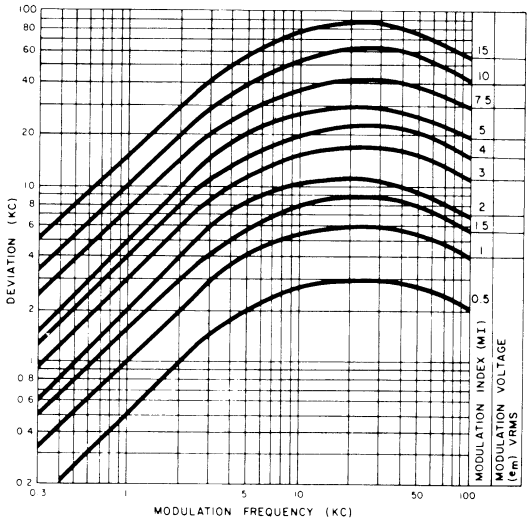

MECHANICAL SPECIFICATIONS

SIZE:	Cylindrical: 2.6 inches diameter x 1.5 inches long. Square: 2.6 inches x 2.6 inches x 1.5 inches.
WEIGHT:	Approximately 9 ounces.
MOUNTING:	Any flat surface by use of three through bolts.
CONNECTORS:	See outline drawing.
CONTROLS:	Eight screwdriver adjustments accessible by removing nameplate.

ENVIRONMENTAL SPECIFICATIONS

The unit will maintain the following performance characteristics:

FREQUENCY STABILITY:	±0.005%.
DISTORTION:	Less than 3%.
POWER OUTPUT:	±1.5 db.
FM NOISE:	Less than 2% per channel.

when subjected to any of the environments listed below:

TEMPERATURE:	−20°C to +80°C.
HUMIDITY:	90% relative humidity to 50°C.
ALTITUDE:	Sea level to vacuum.
VIBRATION:	From 5 to 30 Hz at 0.2 inch double amplitude. From 30 to 2000 Hz at 25 g. Four 15 minute sweeps in each of the major axes.
SHOCK:	200 g for 11 milliseconds. 3 shocks in each major axis.
ACCELERATION:	100 g for 1 minute in any axis.

ORDERING INFORMATION

WHEN ORDERING SPECIFY:	Model TRPT-501	Frequency	Shape

8.32 Mixer Amplifier

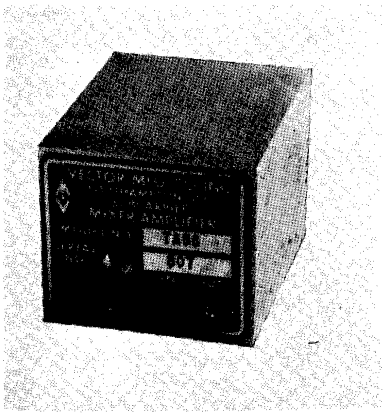

SUBMINIATURE TRANSISTORIZED
MIXER AMPLIFIER
TYPE TA-58

GENERAL DESCRIPTION:

The subminiature transistorized mixed amplifier is a high-gain, feed-back audio amplifier. It is used for summing the outputs of subcarrier oscillators.

The unit has been designed for use in airborne equipment such as guided missiles and other similar equipment. It meets all applicable military specifications.

The unit is characterized by extreme ruggedness. The supporting framework is light but sturdy and transistors and other component parts have been anchored securely to withstand existing environmental conditions such as; shock, vibration, acceleration, temperature, and humidity.

Selection of materials, finishes, and relative position of components have been based upon effective heat transfer characteristics and anti-corrosive properties.

I. PERFORMANCE CHARACTERISTICS:

GAIN:	Adjustable to approximately 20 x by means of two resistors mounted beneath the rack chassis.
FREQUENCY RESPONSE:	Less than ±0.25 db from 100 to 100,000 cps.
INPUT IMPEDANCE:	10 kilohms.
OUTPUT IMPEDANCE:	Less than 5000 ohms.
INPUT SIGNAL:	100 millivolts min.
OUTPUT SIGNAL:	2.0 volts rms.
HARMONIC DISTORTION:	Less than 0.5% at 1.5 volts rms output.
NOISE:	Equivalent noise input 30 microvolts.
STABILITY:	±10% variation in supply voltage will cause no change in unit gain.
POWER REQUIREMENTS:	+28 volts dc at 10 ma.

II. ENVIRONMENTAL CHARACTERISTICS:

ACCELERATION:	Capable of withstanding at least 200 g.
SHOCK:	Capable of withstanding at least 200 g.
VIBRATION:	Capable of withstanding 25 g in each major axis from 55 to 2000 cps.
TEMPERATURE:	Operating range from −55°C to +125°C.

III. PHYSICAL CHARACTERISTICS:

SIZE:	Space requirements have been given utmost consideration resulting in an extremely compact unit. Overall dimensions: 7/8″ x 1-1/6″ x 1-3/8″, excluding connector and potentiometers. The outline drawing is included in the bulletin.
WEIGHT:	The total weight is approximately 1½ ounces.

IV. INSTALLATION AND OPERATION:

MOUNTING: Mounting against flat surface with one screw extending through the unit.

CONNECTOR: De-Jur connector.

TEST POINTS: Two test points available for input and output voltage measurements.

V. SPECIAL REQUIREMENTS:

All of the above specifications may be modified to suit specific installations and systems.

VECTOR MANUFACTURING COMPANY, INC.

TECHNICAL DATA	DWG. NO. TD-178
UNIT TA-58	DATE 7-9-62

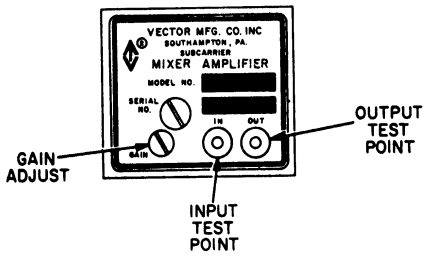

TOP VIEW

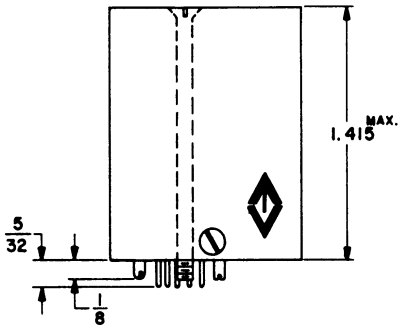

SIDE VIEW

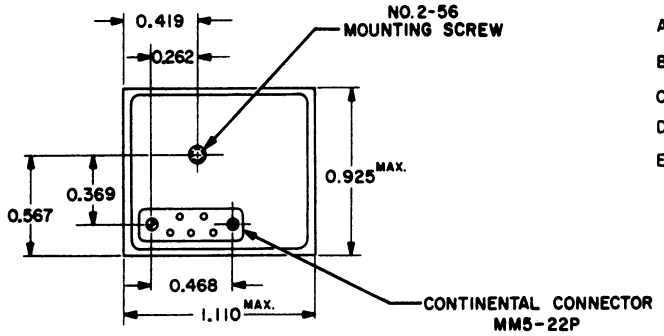

BOTTOM VIEW

CONTINENTAL CONNECTOR
MM5-22P

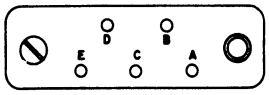

PIN CONNECTIONS

SERIES A

- A ——— NO CONNECTION
- B ——— +28V DC
- C ——— SIG OUTPUT
- D ——— SIG INPUT
- E ——— GROUND (SIG, PWR & CHASSIS)

SERIES B

- A ——— CHASSIS GROUND
- B ——— +28V DC
- C ——— SIG OUTPUT
- D ——— SIG INPUT
- E ——— GROUND (SIG & PWR)

MIXER AMPLIFIER, TA-58, OUTLINE DRAWING AND PIN CONNECTIONS.

8.33 Voltage Controlled Oscillator

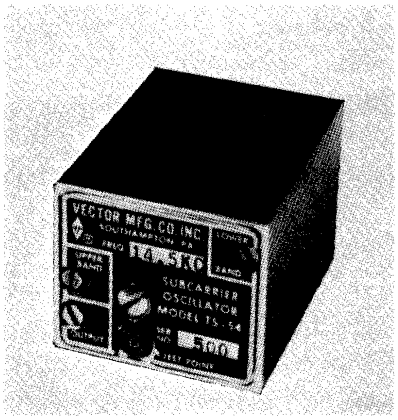

TRANSISTORIZED
VOLTAGE CONTROLLED
SUBCARRIER OSCILLATOR

Type TS-54

GENERAL DESCRIPTION:

The TS-54 Subcarrier Oscillator is a transistorized, voltage controlled oscillator designed for telemetry applications. The oscillator converts intelligence in the forms of varying dc voltages into frequency modulated subcarrier signals for further transmission by wire or radio to distant receiving stations. The major functional sections contained in the TS-54 are a voltage regulator, a compensated amplifier, a free-running multivibrator, and an output filter.

The oscillator has been designed for use in aircraft, missile, re-entry vehicle, and satellite programs and meets all applicable military specifications, and is available in all standard IRIG channels. The oscillator is also characterized by extreme ruggedness due to the supporting framework being light but sturdy, and the transistors and other components having been anchored securely to withstand environmental conditions such as shock, vibration, and acceleration.

Selection of materials, finishes and relative position of components have been based upon affective heat transfer characteristics and anti-corrosive properties.

I. PERFORMANCE CHARACTERISTICS:

INPUT IMPEDANCE:	1 megohm ±20% or 500 kilohms min. available.
INPUT VOLTAGE:	0 to 5 v, ±2.5 v, 0 to 3 v or ±1.5 v.
OUTPUT IMPEDANCE:	47 kilohms.
OUTPUT VOLTAGE:	0.85v p-p with a 10 kilohm load. 0 to 2 volts rms at test point.
MODULATION SENSITIVITY:	0 to 5 volts dc for ±7.5% or ±15% deviation. ±2.5 volts dc for ±7.5% or 15% deviation. 0 to 3 volts dc for ±7.5% deviation. ±1.5 volts dc for ±7.5% deviation. Special units available with ±40% deviation.
DRIFT:	Within ±0.25% of design bandwidth for a period of 8 hours at ambient temperature following a warm-up period of 15 minutes.
DISTORTION:	At center frequency the total harmonic distortion of output is less than 0.75%.
LINEARITY:	Less than ±0.25% of design bandwidth from best straight line. This linearity is maintained at temperatures from −20°C to +80°C.
STABILITY:	A change in supply voltage of ±10% will vary the center frequency less than ±0.5% of design bandwidth at temperatures from −20°C to +80°C.
INTELLIGENCE FREQUENCY RESPONSE:	For modulation index of 5.0 or greater, the intelligence frequency response is within 0.1 db of the dc response.
AMPLITUDE MODULATION:	Less than ±5%.
SENSITIVITY TO SOURCE IMPEDANCE CHANGE:	Changing the source impedance from zero to infinity varies the frequency less than 1.0% of design bandwidth.
SENSITIVITY TO OUTPUT IMPEDANCE CHANGE:	10 to 1 change in the load impedance will cause less than 1% change in output frequency.
INTELLIGENCE FREQUENCY COMPONENT IN OUTPUT:	Harmonics of intelligence frequency are suppressed 40 db below output signal.
POWER REQUIREMENTS:	28 volts dc ±10% at 15 ma.

II. PHYSICAL CHARACTERISTICS:

SIZE:	Overall dimensions: 7/8" D x 1-1/16" W x 1 3/8" H, excluding connector.
WEIGHT:	1.75 oz.
SPECIAL FEATURE:	This unit is completely encapsulated.

III. ENVIRONMENTAL CHARACTERISTICS:

TEMPERATURE:	The operating range is from −55°C to +125°C. At any information input, the output frequency is stable within ±1% of design bandwidth (based on best reference) for a temperature change of 0°C to +80°C; likewise, the output frequency is stable within ±2% of dbw (based on best reference) for a temperature change of −20°C to +80°C. Special units are available with stability of ±1% of dbw (based on best reference) for a temperature change from −20°C to +80°C.
HUMIDITY:	When exposed to a relative humidity of 95% for 2 hours at +50°C center frequency is stable within ±1% of design bandwidth.

ALTITUDE: With constant temperature and at any altitude from sea level up, center frequency is stable within $\pm 0.5\%$ of design bandwidth.

VIBRATION: Center frequency is stable within $\pm 0.5\%$ of design bandwidth when subjected to 30 g rms vibration from 55 to 2000 cps in each major axis.

SHOCK: After a shock of 200 g of 10 millisecond duration in the direction of each major axis, center frequency is stable within $\pm 0.5\%$ of design bandwidth.

ACCELERATION: Under constant acceleration of 100 g in each direction of each major axis, center frequency is stable to within $\pm 1\%$ of dbw.

IV. INSTALLATION AND OPERATION:

MOUNTING: Against a flat surface with one captive screw extending through the unit.

CONNECTION: Continental Type MM5-22P connector is used for input and output signal and power supply connections.

CONTROLS: OUTPUT — Provides adjusting the TS-54 output voltage level.

LOWER BAND—Provides adjustment of the lower frequency deviation limit.

UPPER BAND—Provides adjustment of the upper frequency deviation limit.

TEST POINT: Enables monitoring output voltage and frequency.

V. SPECIAL REQUIREMENTS AND OPTIONAL FEATURES:

All of the above specifications can be modified to suit specific installations and systems. Because of the extremely high stability of the TS-54 oscillator, special units are available without the deviation limit and output potentiometers. These oscillators are adjusted at the factory to the customers specifications.

VI. ORDERING INFORMATION:

To order specify; Model TS-54 Frequency, Deviation, and Input signal voltage and polarity.

Patent Pending

Specifications are subject to change without notice.
Verification of specifications will be given with each order.

VECTOR MANUFACTURING COMPANY, INC.

TECHNICAL DATA	DWG. NO. TD-126
UNIT TS-54	DATE 4-4-62

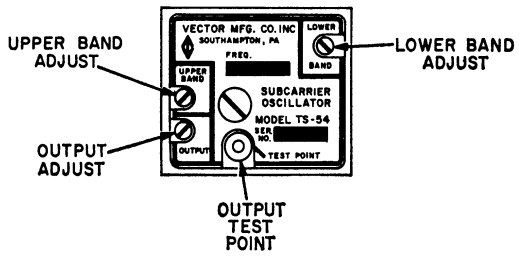

TOP VIEW

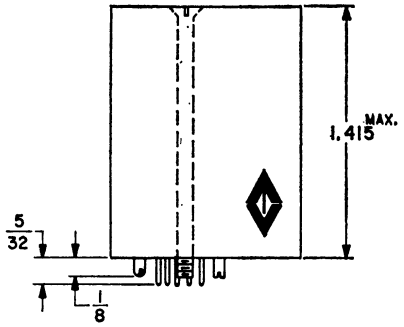

SIDE VIEW

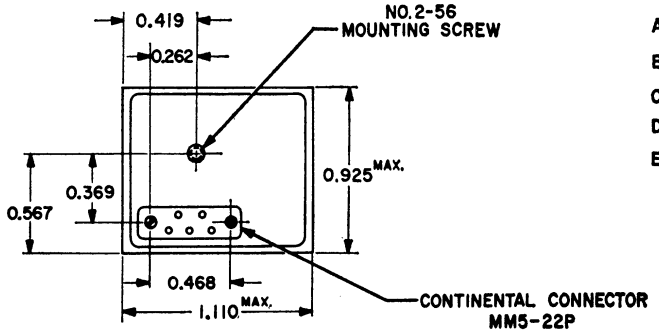

BOTTOM VIEW

CONTINENTAL CONNECTOR
MM5-22P

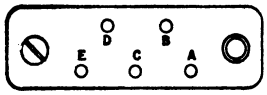

PIN CONNECTIONS

SERIES A

- A ——— +28V DC
- B ——— NO CONNECTION
- C ——— SIG OUTPUT
- D ——— SIG INPUT
- E ——— GROUND (SIG, PWR & CHASSIS)

SERIES B

- A ——— +28V DC
- B ——— CHASSIS GROUND
- C ——— SIG OUTPUT
- D ——— SIG INPUT
- E ——— GROUND (SIG & PWR)

8.34 Magnetometer Calibration

HELIFLUX®
MAGNETIC ASPECT SENSOR
TYPE RAM- 53 CX

CALIBRATION DATA

Y Axis

SERIAL NO 2

FIELD IN MILLIGAUSS	OUTPUT SIGNAL IN VOLTS D C	
600	4.975	
550	4.792	
500	4.615	
450	4.412	
400	4.209	
350	3.980	
300	3.753	
250	3.508	
200	3.301	
150	3.080	
100	2.874	
50	2.691	
0	2.500	(BIAS LEVEL)
-50	2.312	
-100	2.131	
-150	1.922	
-200	1.709	
-250	1.502	
-300	1.264	
-350	1.025	
-400	.811	
-450	.588	
-500	.393	
-550	.204	
-600	.018	

DIRECTION OF MAGNETIC FIELD FOR VOLTAGE SIGNALS ABOVE BIAS LEVEL

NOTE:
CALIBRATION MADE WITH A 100K OHM RESISTOR FROM SIGNAL OUTPUT TO NEGATIVE TERMINAL OF BATTERY SOURCE, AND A 100K OHM RESISTOR FROM BIAS OUTPUT TO NEGATIVE TERMINAL OF BATTERY SOURCE

SCHONSTEDT INSTRUMENT COMPANY
SILVER SPRING, MARYLAND

CALIBRATION MADE WITH BATTERY SUPPLY OF 28,0 VOLTS DATE Dec. 17, 1963

11262

8.35 Aspect Sensor and Shift Register

SHIFT REGISTER

MODEL 235

The Model 235 Shift Register works with one Model 135 or Model 131B Aspect Sensor for spinning vehicles.

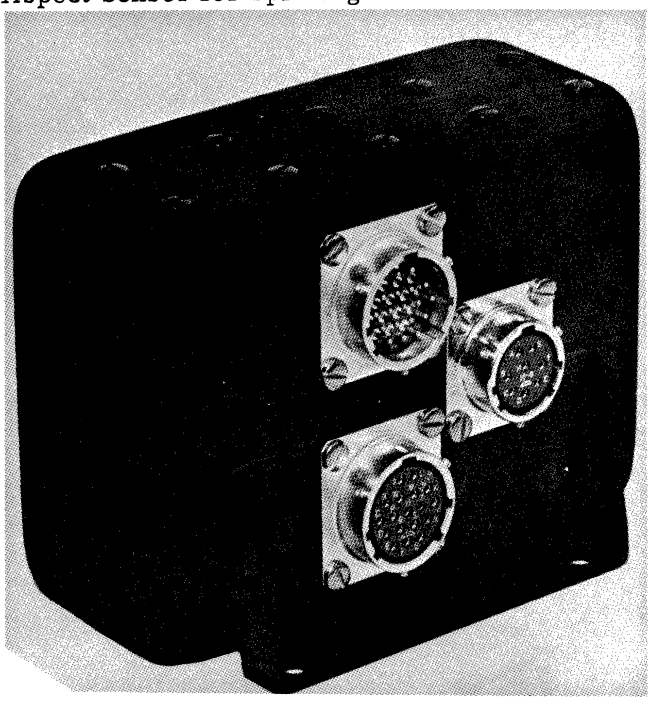

SPECIFICATIONS

INPUT:

Power:	+26 to +40 VDC, 0.5 watt Solar aspect bits shifted in in parallel upon signal from command eye.

OUTPUT:

Format:	Serial seven bit Gray coded word indicating angle plus end of word bit, 50% duty cycle. Earth output superposed as shift in reference levels.

Voltage levels into 10 K ohms:

	Earth telescope activated	Earth telescope not activated
Reference	1.25 ±.1 v	3.9 ±.1 v
"zero"	0.25 ±.1 v	2.9 ±.1 v
"one"	2.25 ±.1 v	4.9 ±.1 v

Shift out rate: 1 to 1000 bits per second selectable by changing capacitor. Internal oscillator may be disconnected and external shift out pulses used with characteristics as follows:

amplitude:	+5 v
pulse width:	5 us
rise time:	5 us
P rf:	10 Kc

SIZE: 2" x 3 1/4" x 4 5/8"

WEIGHT: 15 1/2 oz.

CONSTRUCTION: Printed circuit boards

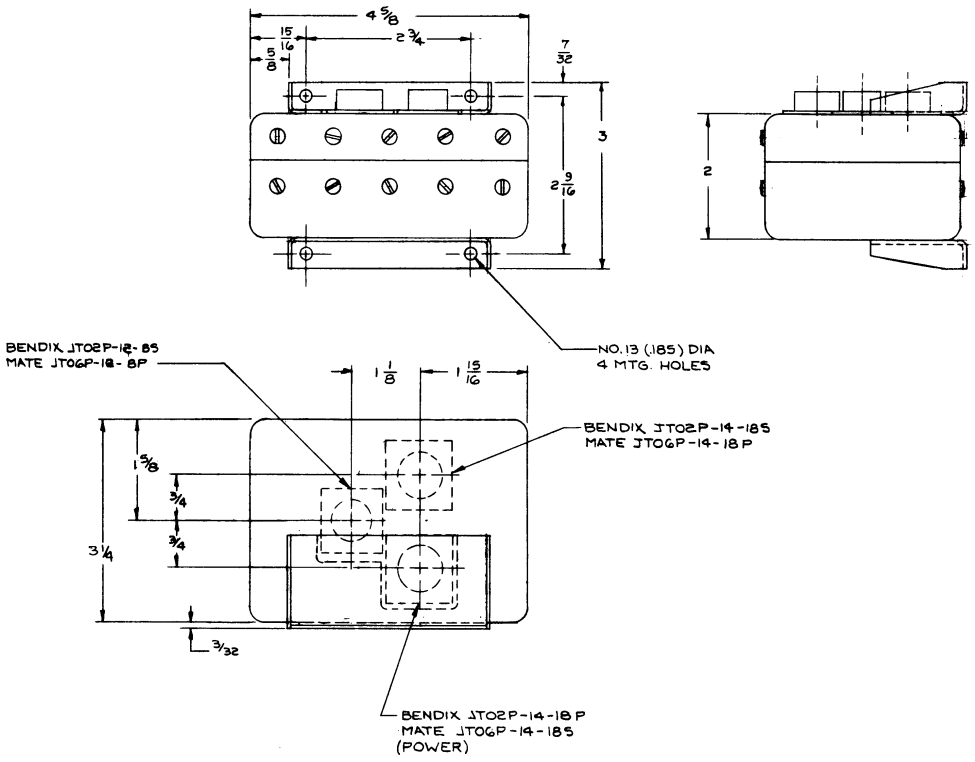

ASPECT SENSOR

MODEL 135

The Model 135 Aspect Sensor is used on spinning vehicles. The sensor combines a Model 131B sensor with the addition of a telescope which senses the presence of the earth in its field of view. The telescope utilizes a silicon solar cell as the photodetector.

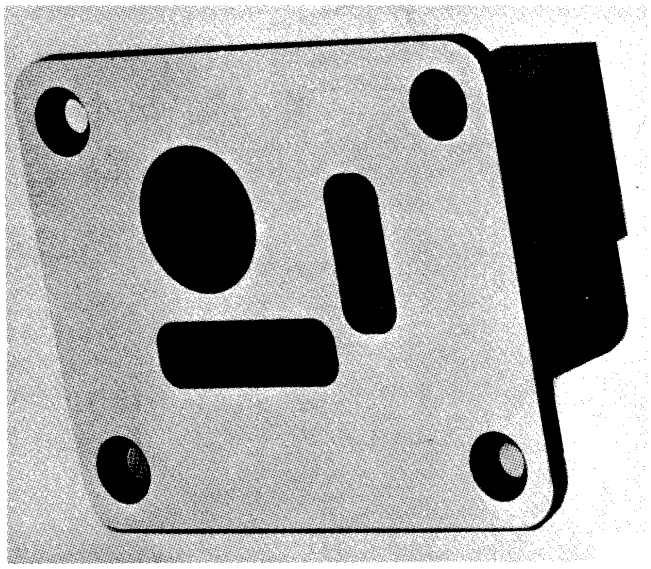

SPECIFICATIONS

SOLAR ASPECT SENSOR

Field of view:	$\pm 64^{\circ}$
Angular resolution:	1°
Accuracy at transition:	$\pm .25^{\circ}$

EARTH TELESCOPE

Field of view:	$1^{\circ} \pm .25^{\circ}$ conical field of view.
SIZE:	1 15/16" x 2 7/16" x 1 11/16"
WEIGHT:	4 oz.
SPIN RATE:	12 rps or less

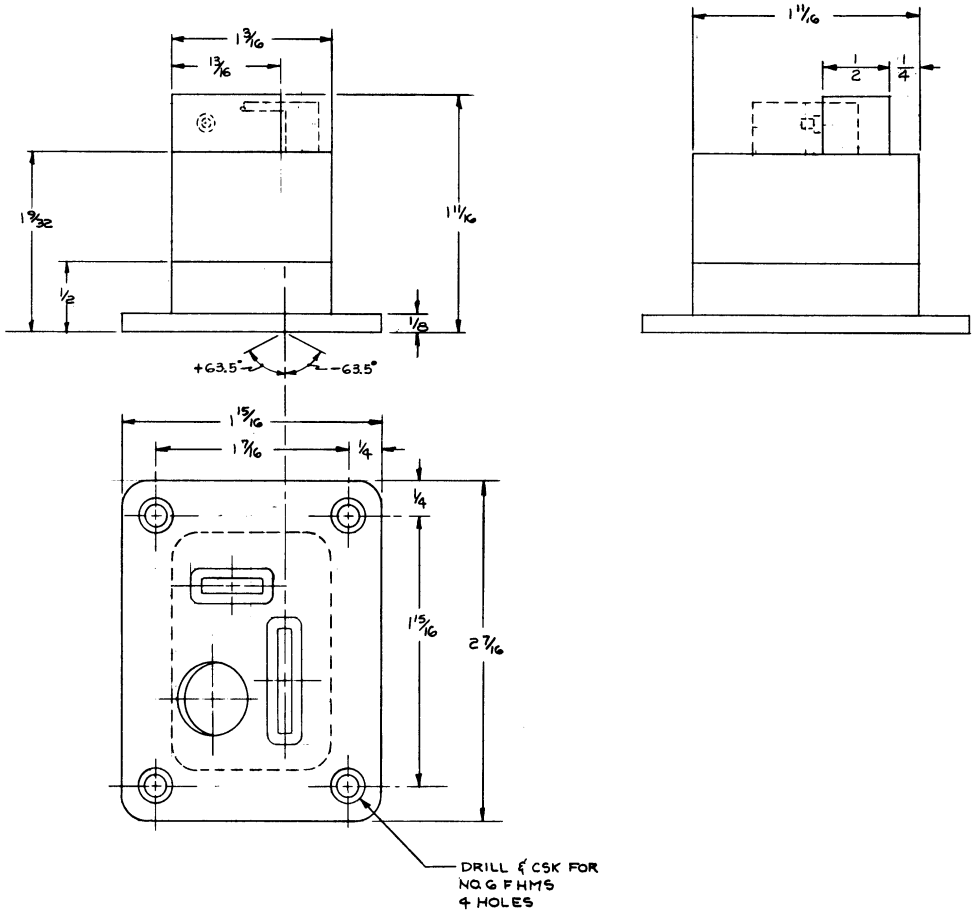
1 3/16
1 3/16
1 3/32
1 11/16
1/2
1/8
+63.5°
-63.5°
1 15/16
1 7/16
1/4
1/4
1 5/16
2 7/16
DRILL & CSK FOR
NO. 6 F HMS
4 HOLES
1 11/16
1/2
1/4

8.4 THERMAL VACUUM TEST

MEMORANDUM
REPORT NO. 322-5-62
May 16, 1962

TO : Test and Evaluation Division Files

FROM : Thermal-Vacuum Test Section
Thermodynamics Branch

SUBJECT: Nike-Apache Neutral Particle Pitot - Static Experiment (NASA - 14.19 UA), Results of Thermal-Vacuum Tests

INTRODUCTION

Flight Objectives:

The flight objectives of the Pitot - Static Experiment are as follows:

1. To measure atmospheric pressure, temperature and density in the region of 30 - 120 KM altitude.

2. Measurement of high altitude atmospheric winds.

3. Test of the interferometer Dovap system as a means of gathering trajectory data for the Pitot - Static probe experiment.

4. Test of the optical aspect system.

Environment:

Sounding rockets launched during the month of May at Wallops Island are subject to 95% probability of launch temperature extremes of 0°C to 35°C. Since aerodynamic heating is not a factor because of short flight time launch temperature extremes were used for test parameters.

Atmospheric pressure during the planned experimental flight varies from sea level ambient to 2.1×10^{-5} mm Hg at an altitude of 120 KM.

Payload Personnel:

Payload functional tests were conducted by the following University of Michigan Engineers:

J. C. Maurer - System Engineer
G. F. Rupert - Instrumentation Engineer
J. J. Horvath - Project Engineer

PROCEDURE

The thermal-vacuum tests were performed at GSFC on 5 May and 6 May 1962 in the Stokes 8' x 8' Vacuum Chamber. The following procedure was observed:

1. Initial check-out of experiment in thermal-vacuum chamber at ambient conditions.

2. Evacuate chamber to approximately 40 microns and backfill with dry nitrogen.

3. Reduce chamber temperature to 0°C ±2C and stabilize.

4. Energize experiment and evacuate chamber to less than 2×10^{-5} mm Hg.

5. Payload personnel to perform functional tests coincident with chamber evacuation.

6. This phase of test to continue for not less than 30 minutes from start of evacuation.

7. Return to atmospheric pressure.

8. Repeat steps 3 through 7 using a temperature of 35°C ±2C in step 3.

RESULTS

Run #1 - Five hours were required to reduce the payload temperature to 0°C and stabilize. Chamber evacuation was started at 1630 hours (5/4/62) and continued for 35 minutes, reaching a final pressure of 1.8×10^{-5} mm Hg. Payload engineers performed functional tests at ten minute intervals during evacuation. All test objectives were met and the payload functioned without incident.

Run #2 - Payload temperature was increased to +35°C and stabilized at atmospheric pressure. Chamber evacuation was started at 2348 hours (5/4/62) and continued for 32 minutes reaching a final pressure of 5.6×10^{-5} mm Hg. Payload engineers performed functional tests at ten minute intervals during evacuation. Tests were performed without incident.

CONCLUSIONS

The Pitot - Static Probe experiment was subjected to thermal-vacuum environmental testing which was in acceptable agreement with proposed flight conditions and met all performance requirements.

It was noted on run #2 that the minimum chamber pressure recorded was 5.6×10^{-5} mm Hg, which is in excess of the 2×10^{-5} mm Hg specified under "Procedure." In view of the final low pressure of run #1 (1.8×10^{-5} mm Hg) and the uninterrupted performance of the payload it is felt the pressure differential of run #2 is not of sufficient magnitude to invalidate the test results.

W. W. AUER
Thermal-Vacuum Test Section

WWA:kmf

Distribution List:

Director's Reading File
Office of Technical Services
Thermodynamics Branch (3)
Thermal-Vacuum Test Section (2)
Systems Evaluation Branch (2)
GSFC Coordinator (W. S. Smith)
GSFC Project Manager (N. W. Spencer)

TABLE I

Temperature History of Payload Test @ 0° ±2°C
(Temperatures in °C)

Time	1615	1630	1635	1640	1645	1650	1655	1700	1705
TC #1	1.0	1.5	1.0	0	-0.2	-1.0	-0.5	-0.8	-0.5
TC #2	1.0	1.5	1.0	0	-0.2	-1.0	-0.5	-0.8	-0.5
TC #3	1.0	1.0	1.0	0.2	0	0	0	0	0.5
TC #4	0	0.5	1.0	2.0	2.0	2.0	4.0	4.0	5.0
TC #5	1.0	1.0	0.2	-0.2	-1.0	-1.0	-1.0	-1.0	-1.0
TC #6	1.0	1.0	-1.5	-3.7	-3.8	-3.8	-3.0	-2.8	-2.5
TC #7	0.2	0.5	-2.2	-3.8	-4.0	-4.0	-3.8	-3.2	-3.0
TC #8	1.0	1.0	0.2	-0.5	-0.5	-1.0	-0.5	-0.5	-0.5
TC #9	0	0.5	4.0	11.0	7.2	5.0	7.0	13.0	11.0
TC #10	0	0.5	-3.5	-4.5	-3.8	-3.0	-2.0	-1.5	-1.0
TC #11 (Chamber Wall)	0	0.2	0.2	-0.5	-1.0	-1.0	-1.0	-1.2	-1.0
TC #12 (Chamber Ambient)	1.5	1.5	-22.5	-11.0	-3.8	-1.5	-0.5	0	0.1
Pressure (mm Hg)	640	640	100	14	2.2	0.240	6.5×10^{-3}	7.0×10^{-4}	1.8×10^{-5}
	Payload Temperature Stabilized	Payload On (1630) Start Evacuation			Payload Off (1641)		Payload On (1653)	Payload Off (1700)	

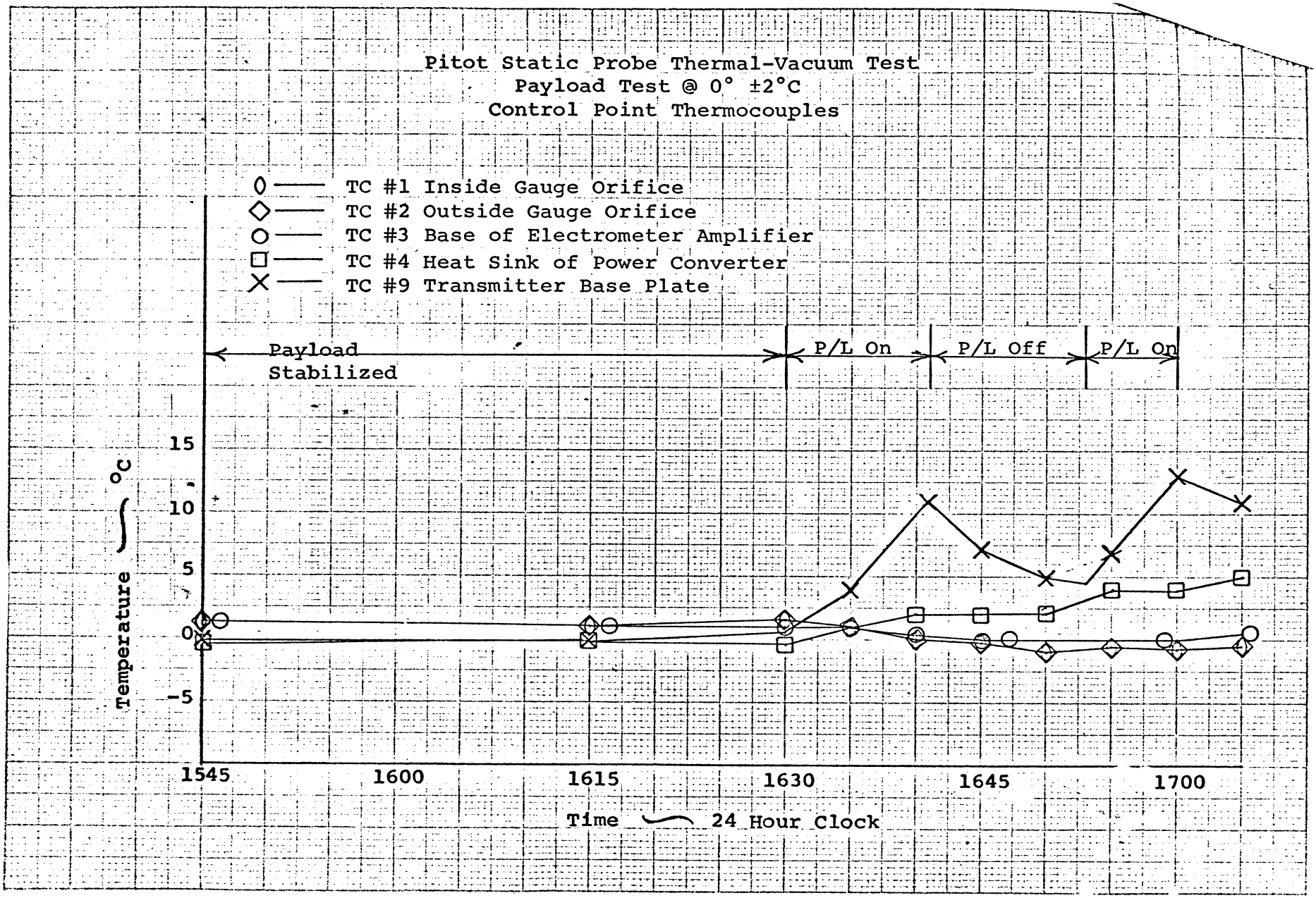
Pitot Static Probe Thermal-Vacuum Test
Payload Test @ 0° ±2°C
Control Point Thermocouples
TC #1 Inside Gauge Orifice
TC #2 Outside Gauge Orifice
TC #3 Base of Electrometer Amplifier
TC #4 Heat Sink of Power Converter
TC #9 Transmitter Base Plate
Payload Stabilized
P/L On
P/L Off
P/L On
Temperature °C
15
10
5
0
-5
1545
1600
1615
1630
1645
1700
Time 24 Hour Clock

TABLE II

Temperature History of Payload Test @ 35° ±2°C
(Temperatures in °C)

Time	2330	2345	2350	2355	2400	0005	0010	0015	0020
TC #1	34.5	34.5	35.0	34.0	34.0	34.0	34.0	34.0	34.0
TC #2	34.5	34.5	34.0	34.0	34.0	34.0	34.0	34.0	34.0
TC #3	35.0	35.0	35.0	35.0	35.0	34.8	35.0	35.0	35.0
TC #4	34.5	34.5	35.5	37.0	37.0	37.2	39.5	41.0	40.5
TC #5	35.0	35.0	34.5	34.0	34.0	34.0	34.0	34.0	34.0
TC #6	34.5	34.5	32.5	30.5	30.5	31.0	32.0	32.5	32.5
TC #7	34.5	34.5	32.5	31.0	30.5	31.0	31.5	32.0	32.2
TC #8	34.5	34.7	34.0	34.0	34.0	34.0	34.0	34.0	34.0
TC #9	35.0	34.0	37.0	44.0	43.0	39.8	43.5	50.0	50.8
TC #10	34.5	34.5	32.0	30.5	31.5	32.5	33.2	34.0	34.5
TC #11 (Chamber Wall)	35.5	36.0	36.0	36.0	36.0	36.0	36.0	36.0	36.0
TC #12 (Chamber Ambient)	34.5	34.5	5.2	22.5	31.2	34.0	34.2	34.5	34.5
Pressure (mm Hg)	640	640	120	12	1.2	0.09	9.2×10^{-3}	9.0×10^{-5}	5.6×10^{-5}
		Payload Temperature Stabilized	Payload On (2348) Start Evacuation		Payload Off (2358)		Payload On (0010)		Payload Off (0020)

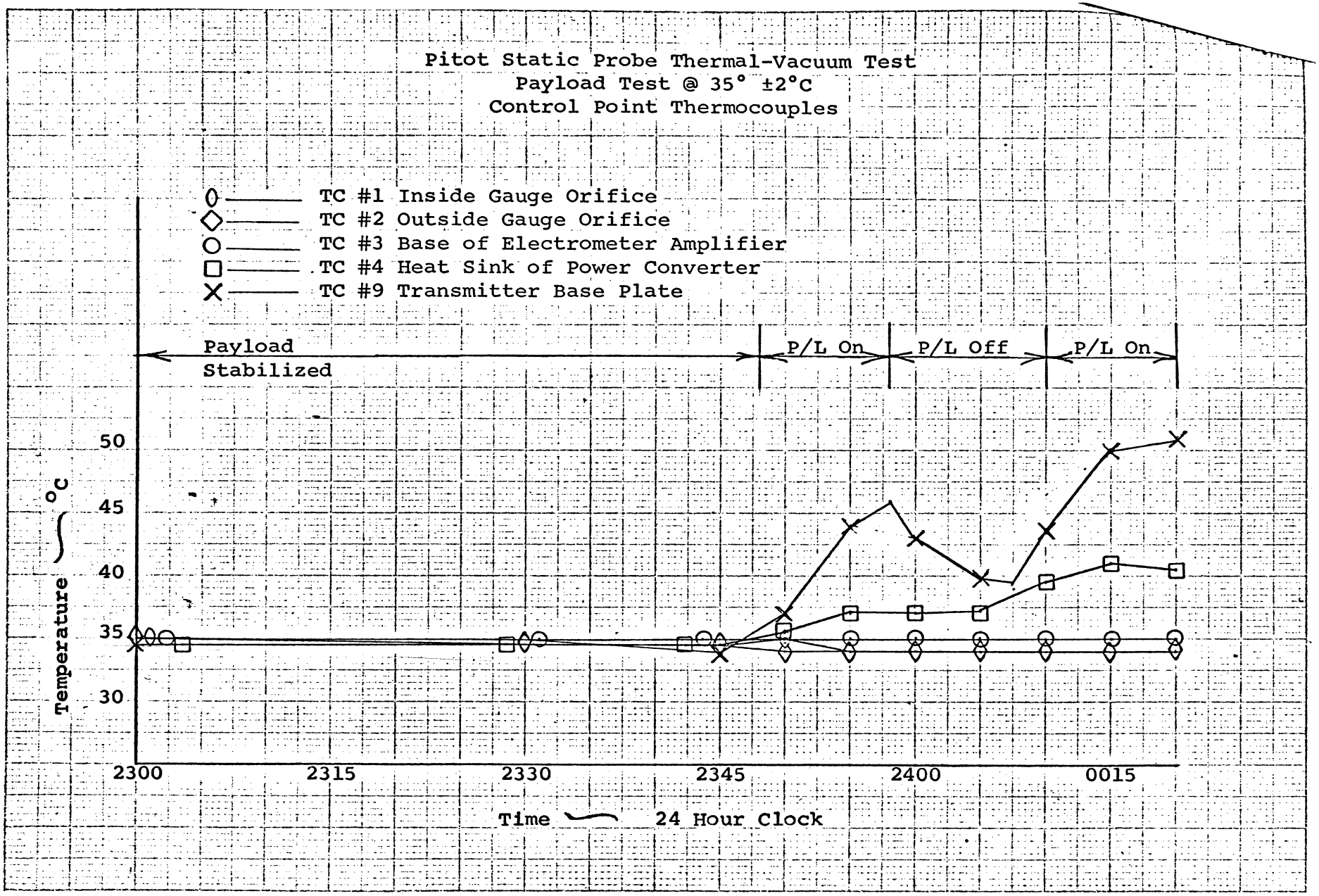
Pitot Static Probe Thermal-Vacuum Test
Payload Test @ 35° ±2°C
Control Point Thermocouples
TC #1 Inside Gauge Orifice
TC #2 Outside Gauge Orifice
TC #3 Base of Electrometer Amplifier
TC #4 Heat Sink of Power Converter
TC #9 Transmitter Base Plate
Payload Stabilized
P/L On
P/L Off
P/L On
Temperature °C
50
45
40
35
30
2300
2315
2330
2345
2400
0015
Time — 24 Hour Clock

Nike-Apache Pitot-Static Probe
(NASA 14.19 UA)
Thermo Couple Locations

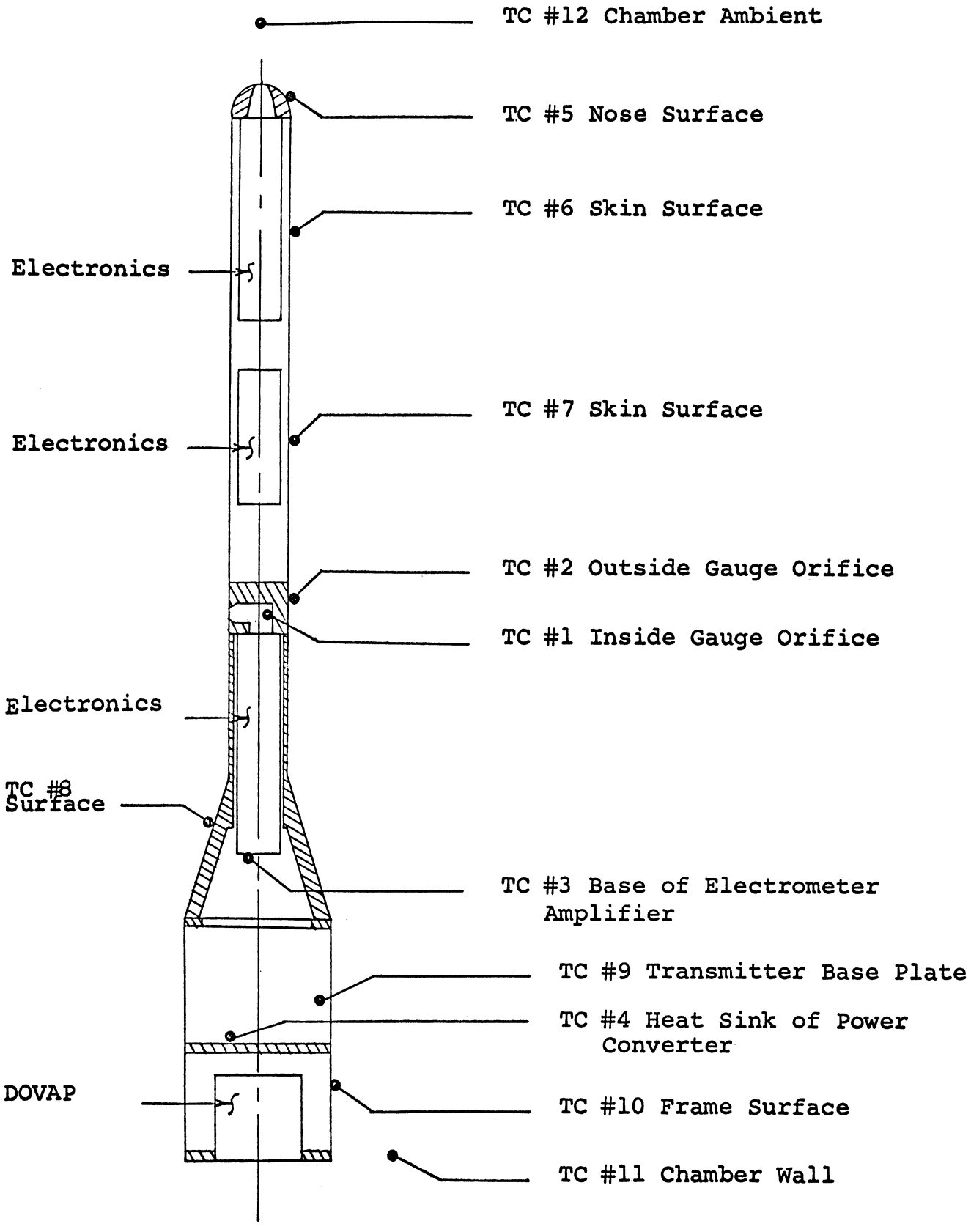

NOT TO SCALE

9. REFERENCES

1. Ainsworth, J. E., D. F. Fox, and H. E. LaGow, "Upper Atmosphere Structure Measurement made with the Pitot-Static Tube," Jour. Geophysical Research 66(10), 3191-3211, 1961.

2. Spencer, N. W., and R. L. Boggess, "A Radioactive Ionization Gage Pressure Measurement System," Jour. Am. Rocket Soc., January 29, 1959.

3. Horvath, J. J., R. W. Simmons, and L. H. Brace, "Theory and Implementation of the Pitot-Static Technique for Upper Atmosphereic Measurements," Univ. of Michigan ORA Report 03554, 04673-1-S, March 1962.

4. Hines, P. B., "DOVAP Systems and Data Reduction Methods," New Mexico State University, Physical Science Lab., Univ. Park, N. M., January 31, 1962.

5. Seddon, C. J., "Preliminary Report on the Single-Station Doppler Interferometer Rocket Tracking Technique," NASA Technical Note D1344, January 1963.

6. Spafford, M., R. Wiack, and R. Woodman, "The Rocket Interferometer Tracking (RIT) System," NASA Technical Note D2682, March 1965.

7. El-Moslimany, M. A., "Thoretical and Experimental Investigation of Radioactive Ionization Gauges," The University of Michigan Research Institute 2096, 2406, 2597, 03554-1-S, May 1960.

8. Burr-Brown, "Handbook of Operational Amplifier Applications," Burr-Brown Research Corporation, 1963.

9. Peaks, H. J., "Some Basic Considerations of Telemetry System Design," NASA Technical Note D355, June 1960.

10. Sliltz, H. L., et al., "Aerospace Telemetry," Vol. II, Prentice Hall Inc., Englewood Cliffs, N. J., 1966.

11. Keenan, B. M., "Design and Performance of the Models 2.003, 2.004, 2.005 and 2.009 Telemetry Quadraloop Antennas," Physical Science Laboratory, New Mexico State University, Scientific Report No. 1, December 1, 1961.

12. Thoikol Chemical Corporation; Astro-Met Division; "Aeroelastic Flight Loads on a Pitot-Static Probe Payload," July 29, 1966.

13. IRIG Document No. 106-60, "Telemetry Standards Revised June 1962," August 1962. Defense Documentation Center AD284370.

REFERENCES (Concluded)

14. Caldwell, J., "The Space Physics Research Laboratory Data Conditioning System," Univ. of Michigan ORA Report 05776-1-E, January 1966.

15. Horvath, J. J., Report of Pitot-Static Probe system error analysis to be published in 1967.

16. NASA Quality Publication NPC 200-4 "Quality Requirements for Hand Soldering of Electrical Connections," August 1964.

17. Gay Jr., J. A., "Reliable Electrical Connections," Third Edition, NASA Technology Handbook SP .5002, December 1963.

18. Fedor, J. V., "Theory and Design Curves for A Yo-Yo Despin Mechanism for Satellites," NASA TN D-708, August 1961.

19. Sterhardt, J. A., "Environmental Test of Nike Apache Rocket NASA 14.111 GT." Goddard Space Flight Center technical report No. X-671-65-236, June 1965.

20. Vector Division of United Aircraft Corporation "Transistorized Crystal Controlled Transmitter, Type TRPT-501," Vector Technical Bulletin No. 5033.

21. Vector Division of United Aircraft Corporation "Subminiature Transistorized Mixer Amplifier; Type TA-58," Vector Technical Bulletin 2041.

22. Vector Manufacturing "Transistorized Voltage Controlled Subcarrier Oscillator, Type TS-54," Vector Technical Bulletin 1021, October 1962.

23. Adcole Corporation "Aspect Sensor, Model 135," Specification Sheet.

24. Adcole Corporation "Shift Register, Model 235," Specification Sheet.